# $CO_2$ MEASURED IN THE GAS PHASE AS AN INDICATOR OF BIOFILM METABOLISM

**by**

Marthinus Kroukamp

B.Eng (Chemical), University of Stellenbosch, 1998

M.Sc (Biochemistry), University of Stellenbosch, 2004

A dissertation

presented to Ryerson University

in partial fulfilment of the requirements for the degree of

Doctor of Philosophy in the program of Civil Engineering

Toronto, Ontario, Canada, 2010

# Declaration

I hereby declare that I am the sole author of this thesis or dissertation. I authorize Ryerson University to lend this thesis or dissertation to other institutions or individuals for the purpose of scholarly research.

_____ _____

Signature Date

I further authorize Ryerson University to reproduce this thesis or dissertation by photocopying or by other means, in total or in part, at the request of other institutions or individuals for the purpose of scholarly research.

_____ _____

Signature Date

# $CO_2$ MEASURED IN THE GAS PHASE AS AN INDICATOR OF BIOFILM METABOLISM



Doctor of Philosophy

Civil Engineering

Ryerson University, Toronto

## ABSTRACT

The behaviour of microorganisms in biofilms is uniquely dependent on their location within the biofilm-matrix and the dynamic interplay between the countless microenvironments that is in constant flux because of physicochemical and inter-cell exchanges. To study microorganisms in the biofilm environment, the above mentioned heterogeneity forces any researcher to either focus on micro-niches (whose data may or may not be suitable for extrapolation to infer information about the whole) or stand back and study a global biofilm parameter (as a sum-total of micro-behaviours but losing informa-

tion about the diversity). Either way, the positional dependence of behaviour arguably favours in situ studies with the least amount of disruption whether physical or the addition of chemicals. A simple technology was developed to measure in situ biofilm $CO_2$ production as an indication of overall metabolism, in real-time and non-destructively. The first system developed was a carbon dioxide evolution measurement system (CEMS) with biofilms growing on the inside of a $CO_2$ and $O_2$ permeable silicone tube with quantification of microbially produced $CO_2$ transferred across the tube wall could. The concept of measuring biofilm $CO_2$ was subsequently expanded to accommodate any biofilm reactor by measuring $CO_2$ in the reactor effluent. By monitoring $CO_2$ the advantage is that both aerobic and anaerobic metabolism can be tracked with any combination of microbial community members with varying growth conditions such as temperature and nutrient composition. It furthermore allows the setup of carbon balances over a reactor system to address fundamental biofilm aspects such as percentages of inflowing nutrients used for respiration or quantification of "missing" carbon fractions. The ability to measure metabolism in real-time provides insight into both steady state and transient biofilm responses to changes in their environment while the non-destructive nature of the technique gives the opportunity to determine the possibility of adaptive behaviour in the same biofilm after repeated exposure. Practical applicability of these measurement systems has been demonstrated in a wide range of biofilm related phenomena such as the areas of biofilm architecture, biofilm development and biofilm resilience after physical and antimicrobial attacks.

# Acknowledgements

I wish to extend my sincerest gratitude to my supervisor, Dr. Gideon M. Wolfaardt who took a significant risk in accepting me as a graduate student. Thank you for creating an environment where it was acceptable to explore and fail on the way to acquire understanding. Your continued interest and excitement about the project was enough to encourage when everything went slow.

I would like to thank Dr Martina Hausner and Dr Steven N. Liss for valuable advice and support throughout the duration of the project.

Financial support that was provided by NSERC, MITACS and a Ryerson Graduate Scholarship is gratefully acknowledged.

Romeo Dumitrache is a jovial colleague whose humour and persistence ensured that the $\mu_{\text{max biofilm}}$ and antimicrobial experiments were completed enjoyably and on time.

Elanna Bester, fearless fellow expatriate and fellow graduate student, is worthy of special gratitude for countless discussions, a perpetual smile and exemplary reliability.

I would like to thank Lee Boonzaaier, the best of friends, who fought a similar battle on a different shore for continued interest and support.

Finally, I would like to express my appreciation and thanks toward my wife, Susan, and parents who carried the burden with me. Thank you for all your patience, support and understanding.

For my wife and parents

# Contents

# List of Figures

# List of Symbols and Abbreviations

| | |
|---|---|
| $\Delta l$ | thickness of the membrane (m) |
| $\mu_{\max}$ | specific growth rate ($h^{-1}$) |
| $\sigma_1$ | partitioning coefficient (–) |
| $A_0$ | surface area of the bacteria at time = 0 |
| $C$ | concentration of antibiotic inside the cell , see equation (5.1), page 105 |
| $c$ | concentration (mol· $m^{-3}$) |
| $c_l^*$ | concentration of gas in the liquid phase that is in equilibrium with the gas phase ($\mu$mol of gas·$liter^{-1}$ liquid medium) |
| $C_1^{in}$ | solute concentration in the adjacent phase in equilibrium (eq) with the solute concentration at the membrane surface (mol· $m^{-3}$) |
| $c_m$ | concentration at the membrane surface (mol· $m^{-3}$) |
| $C_1$ | liquid phase $CO_2$ concentration (mol· $m^{-3}$) |
| $c_{FC,in}$ | $CO_2$ concentration in the sterile liquid medium entering the flow cell ($\mu$mol of $CO_2$ · $liter^{-1}$ of liquid medium) |

| | |
|---|---|
| $c_{FC,o}$ | $CO_2$ concentration exiting the flow cell and serves as the feed to the CMR ($\mu$mol of $CO_2 \cdot$ liter$^{-1}$ of liquid medium) |
| $c_{l,CMR}$ | dissolved gas concentration in the liquid phase in the CMR ($\mu$mol of gas$\cdot$ liter$^{-1}$ of liquid medium) |
| $c_{m1}$, $c_{m2}$ | concentrations of the species crossing the membrane at the membrane surfaces on either side (mol$\cdot$ m$^{-3}$) |
| $D$ | diffusion coefficient (m$^2\cdot$ s$^{-1}$) |
| $d_0$ | outer diameter of the silicone tube (m) |
| $F_{g,CMR,in}$ | total gas volumetric flow rate into the CMR (liters of gas$\cdot$h$^{-1}$) |
| $F_{g,CMR,out}$ | total gas volumetric flow rate out of the CMR (liters of gas$\cdot$h$^{-1}$) |
| $F_g$ | gas flow rate (liter $\cdot$ h$^{-1}$) |
| $F_{l,CMR,in}$ | liquid flow rate into the CMR (liters of liquid medium $\cdot$h$^{-1}$) |
| $F_{l,CMR,out}$ | liquid flow rate out of the CMR (liters of liquid medium$\cdot$h$^{-1}$) |
| $F_{l,FC,in}$ | liquid flow rate into the flow cell (liter $\cdot$ h$^{-1}$) |
| $F_{l,FC,out}$ | liquid flow rate out of the flow cell (liter $\cdot$ h$^{-1}$) |
| $H$ | Henry's law constant relating equilibrium values ($\sigma_1/\sigma_2$) , see equation (2.6), page 31 |
| $H$ | dimensionless Henry's law coefficient (liter of liquid$\cdot$liter$^{-1}$ of gas) , see equation (3.8), page 58 |
| $J$ | flux of antibiotic into the cell , see equation (5.1), page 105 |

| | |
|---|---|
| $J$ | flux of the compound crossing the membrane (mol $\cdot$ $s^{-1}$ $\cdot$ $m^{-2}$) , see equation (2.1), page 27 |
| $J_{ave}$ | average flux (mol $\cdot$ $m^{-2}$ $\cdot$ $s^{-1}$) |
| $k_1$ and $k_2$ | mass transfer coefficients (m$\cdot$ $s^{-1}$) |
| $K_L$ | overall transfer coefficient (m$\cdot$ $s^{-1}$) |
| $K_z$ | local transfer coefficient (m$\cdot$ $s^{-1}$) |
| $K_1$ | relates the equilibrium of dissolved $CO_2$ and the bicarbonate ion |
| $k_l a$ | volumetric transfer coefficient ($h^{-1}$) |
| $L$ | length of the tube (m) |
| $m_t$ | number of the moles of $CO_2$ in the system at time *t* |
| $P$ | pressure in the CMR (kPa) , see equation (3.5), page 57 |
| $Q_2$ | volumetric flow rate of the gas ($m^3$/s) |
| $R$ | universal gas constant (liter$\cdot$ kPa$\cdot K^{-1}\cdot mol^{-1}$) |
| $T$ | temperature of the gas in the CMR (in K) |
| $V_0 e^{\mu t}$ | cell volume at time $t$ |
| $V_0$ | volume of the bacteria at time = 0 |
| $V_g$ | headspace volume of CMR (liter) |
| $V_l$ | liquid volume in the CMR (liter) |
| $x$ | length (m) |

| | |
|---|---|
| $x_{g,CMR,in}$ | $CO_2$ concentration of gas flowing into the CMR (ppm; $\mu$l of $CO_2$ ·liter$^{-1}$ of total gas) |
| $x_{g,CMR}$ | $CO_2$ concentration in the gas phase in the CMR (ppm; $\mu$l of $CO_2 \cdot$ liter$^{-1}$ of total gas) |
| $X_{t2}$ | $CO_2$ production at time, $t_2$ |
| *gfp* | green fluorescent protein |
| CEMS | carbon dioxide evolution measurement system |
| $CER_{CMR}$ | gas produced in the CMR system ($\mu$mol of $CO_2 \cdot h^{-1}$) |
| $CER_{FC}$ | $CO_2$ production rate ($\mu$mol of $CO_2 \cdot h^{-1}$) of all microbial cells within the flow cell |
| CF | cystic fibrosis |
| CLSM | confocal laser scanning microscopy |
| CMR | carbon dioxide measurement reactor |
| CTC | 5-cyano-2,3-ditolyl tetrazolium chloride |
| DAPI | 4',6-diamidino-2-phenylindole |
| EPS | extracellular polymeric substances |
| FISH | fluorescence in situ hybridization |
| INT | *p*-iodonitrotetrazolium violet |
| MBEC | minimum biofilm eradication concentration |
| MIC | minimum inhibitory concentration |

| | |
|---|---|
| TOC | total organic carbon |
| TSB | Tryptic Soy Broth |
| XTT | 2,3-bis[2-methyloxy-4-nitro-5-sulfophenyl]- 2$H$-tetrazolium-5-carboxanilide |

# Chapter 1

# Introduction

# 1. Introduction

## 1.1. Biofilms are temporally and spatially heterogeneous

The dictum: "know thyself know thy enemy" has been attributed to an ancient Chinese general, Sun Tzu. In the case of microbial biofilm related infections and diseases, humankind is still in the process of getting to know their enemy. If the previous statement sounds melodramatic, it might be worthwhile to consider that even in the twenty first century, there are still about 80 000 diabetes related (due to faulty wound healing, ischemia and foot ulcers) amputations[1] performed in the United States each year. It is estimated that 60 – 80 % of all human infectious diseases are chronic (including chronic wounds) (Costerton et al., 1995; Davies, 2003). The primary reason that chronic wounds do not heal properly has been attributed to the biofilm phenotype of microbial infections (Bjarnsholt et al., 2008; James et al., 2008). Coupled to the physical crippling effects caused by biofilm infections, humans suffer on various secondary levels such as clinical depression (Ismail et al., 2007) and loss of quality of life. Bacterial biofilms are also a main contributing factor to persistent colonization of hospital surfaces and remain viable candidates as agents in nosocomial infections (Richards and Melander, 2009) resulting in costs in excess of a billion pounds in the United Kingdom (Smith and Hunter, 2008) or a billion dollars in the United States of America (Trampuz and Widmer, 2004).

[1] it is furthermore estimated that around 80 % of amputees does not survive 5 years after the loss of limbs

Biofilms have also been used for exploits beneficial to humankind. The harnessing of beneficial biofilm traits remains an attractive investment in existing technologies such as waste gas treatment (Kumar et al., 2008; Mudliar et al., 2010) or wastewater treatment (McAdam and Judd, 2006; Sun et al., 2010) and also emerging technologies like cellulosic bioethanol conversion (Carere et al., 2008; Wang and Chen, 2009), or use in biotransformations (Qureshi et al., 2005; Gross et al., 2007; Rosche et al., 2009) for instance enzyme production (Govender et al., 2010).

Depending on the circumstances, microorganisms present themselves exhibiting many different forms and regardless whether they are considered an ally or an enemy, they cannot be ignored. The aeons old interaction between humans and microorganisms impacted humans long before the existence of any knowledge of the microbial world's almost inexhaustible diversity and omnipresence. It is therefore not surprising that humans react towards biofilms no differently than expected when compared to the response when being faced by a threat to public security or the response to the opportunity to earn revenue from a natural resource .

The biofilm mode of growth has been described as the dominant form of microbial existence (Monds and O'Toole, 2009); which appears to be realistic since an estimated 99.9 % of organisms can be found in biofilms (James et al., 2008; Costerton et al., 1995; Fux et al., 2005). Even pure-culture biofilms are characterized by extreme heterogeneity with regards to architecture (Werner et al., 2004; Klayman et al., 2008) and physico-chemical properties (Xu et al., 1998), resulting in numerous micro-environments where microorganisms, even while in close proximity (Stewart et al., 1995), will display vast differences in physiological behaviour like differential protein synthesis (Werner et al., 2004; Rani et al., 2007), gene expression (Rani et al., 2007; Lenz et al., 2008), metabolism (Huang et al., 1995; Rani et al., 2007) and growth rates (Wentland et al., 1996; McKay et al., 1997). The latter is not surprising when considering that even batch cultures of individual *Es-*

*cherichia coli* clones had growth rates that differed substantially (Sufya et al., 2003) with doubling times varying between 24 and 500 minutes.

The efficiency of microorganisms living in biofilms can be inferred from the wide variety of environments that can be successfully colonized. Many environments commonly found on our planet are inherently hostile to life. Microorganisms need, for example, to overcome the challenges of osmoregulation in salt marshes, to be adapted for protection against protein denaturation in hot springs or to maintain membrane fluidity in arctic conditions. Microorganisms inhabiting more temperate niches are not guaranteed an easy existence and are still faced with the obstacles of adapting to environmental changes like variations in temperature and pH, toxic substances, starvation, high solute concentration, desiccation, competition from other microorganisms or host immune defence mechanisms and even predators.

Among the possibilities of general adaptive behaviour are the regulated changes in metabolic pathway fluxes and activities, variable morphology, the establishment of symbiotic interactions with other microorganisms (often in biofilms with the concomitant excretion of extracellular polymeric substances (EPS)). Many authors venture to claim that most microorganisms in their natural habitat actually occur in what Jefferson (2004) eloquently describes as a: "sessile, exopolymer-enshrouded community referred to as a biofilm". Biofilms are most often heterogenous communities (multi-species or even multi-kingdom) of microorganisms, attached to a solid surface and covered with a slimy layer of EPS, which exhibit complex three dimensional structures with channels and pores interspaced throughout the biofilm matrix (Picioreanu et al., 2000). Specific mention needs to be made of the complete heterogenous nature of biofilms. The variables that exist around and within a biofilm, for example, constituent organisms, flow patterns surrounding the biofilm, spatial variations in nutrient availability and diffusion gradients will all contribute to the immense complexity. The biofilm structure is dependent on a combi-

nation of intrinsic factors such as the genotype of the cells and the extrinsic factors that will include the complete surrounding physico-chemical environment (Wimpenny et al., 2000). It is thus conceivable that biofilm matrices formed even by identical organisms will vary considerably in composition and physical properties (Allison, 2003). Much has been written about the advantages (and disadvantages) afforded to microorganisms when co-habiting with other microorganisms in biofilms. One of the favourable aspects to a microorganism living in a biofilm would be a matter of defence. Organisms within biofilms can withstand nutrient deprivation, pH changes, desiccation, shear forces, oxygen radicals, disinfectants, and antibiotics better than their planktonic counterparts. Biofilms are also more resistant to phagocytosis. Furthermore, there are various benefits to be gained by microorganisms from the communal nature of a biofilm (Stoodley et al., 2002), including the division of the metabolic burden making commensalism a widespread occurrence in biofilms[2] (Shapiro, 1998; Tolker-Nielsen and Molin, 2000). Horizontal gene transfer within biofilms may also benefit the organism through the exchange of antibiotic resistant determinants (Hausner and Wuertz, 1999). Altruistic behaviour among biofilm community members may also benefit the rest of the community although this has not been proven experimentally. Possible disadvantages to biofilm life from the microorganism's perspective are nutrient limitations in the deeper layers of the biofilm, excessive excretion products or competition for physical space.

The complexity within biofilms warrants studying the multitude of facets about them in the hope that every bit of knowledge gained might cause the biofilm microorganisms to relinquish the secrets they possessed due to their hitherto enigmatic existence.

[2]not to the exclusion of other symbiotic relationships such as competition, mutualism and parasitism Hansen et al. (2007a,b)

## 1.2. Biofilm heterogeneity complicates the determination and interpretation of phenomenological (e.g. metabolism) data

Questions about microbial biofilm existence can be asked on many levels. At the base level there is the question: "what is happening in this micro-environment?". This question corresponds to phenomenological[3] data obtained from biofilms.

Phenomenological studies of biofilms are divided into 3 main areas:

- gaining insight into biofilm architecture, cellular morphology and cell-cell aggregation and clustering (usually by means of various microscopic techniques)
- determining behavioural response to a set of environmental conditions for example motility, metabolic tempo (substrate consumption rate) and different metabolic rates at different temperatures or
- studying the physiological state of the cells for example chemical composition, gene expression and translation.

Knowledge gained from studying microorganisms in the biofilm mode of growth (especially in situ) have proved to be more challenging to interpret than information gained from studying planktonic (suspended) cultures for the following reasons.

Planktonic reactors supporting suspended microbial growth (for instance, batch reactors and continuously stirred tank reactors) mostly contain organisms that exist in a relatively similar physico-chemical and physiological state. General phenotypic responses

[3]phenomenological data describes the phenotypical (or measurable attributes) information of biofilms which is equivalent to the "form" of biofilms in the context when "form and function" of biofilms are mentioned. Function on the other hand implies a specific purpose for the phenotype or form according to Monds and O'Toole (2009). For example the phenotype of increased resistance to antimicrobials compared to planktonic cells has the function of species survival. These authors furthermore encourage researchers to push beyond phenomenological descriptions (answering "what" questions) to research that will link phenotype to function (answering "why" questions) but this falls outside the scope of this document.

can therefore easily be interpreted in terms of group behaviour with the added advantage that general reactor behaviour can be inferred from studying either a small or large fraction of the microbial subpopulation as the majority of microorganisms display an averaged growth characteristic that is assumed to be representative of the majority of constituent microorganisms. This has the benefit that a certain global function can be interpreted from the physiological state of any subpopulation.

The biofilm researcher however is forced to deal with the challenge that studying a subpopulation might not be sufficient to explain the overall phenotype observed (partly due to the phenotypic heterogeneity like metabolic rate or gene expression that occurs even a few microns apart) (Stewart et al., 1995). In the same way, only studying overall behaviour will be a gross underestimation of the complexities and intricacies involved in the biofilm lifestyle.

To demonstrate the complexity involved in elucidating a function of biofilms as established from studying phenotypes, increased antimicrobial resistance as compared to their logarithmic phase[4] planktonic counterparts (up to 1000 times more resistant e.g. (Olson et al., 2002)), will be used as an example. The biofilm mode of life affords an environment to its resident microorganisms that makes it extremely suitable for survival (for example how they feature as reservoirs for pathogens (Parsek and Singh, 2003; Hota et al., 2009) and they are notoriously hard to eradicate and more resistant to cleaning and antimicrobial strategies) and proliferation (Bester et al., 2009).

Stewart (2002) mentioned that poor antibiotic penetration and diffusion, nutrient limitation, adaptive stress response, persister cells and slow growth could all be involved in a concerted interplay to cause the biofilm microorganisms to be better protected against antimicrobial onslaughts. Echoing the previous thought and taking into account that metal resistance and antibiotic resistance have been linked, Harrison (2008) came to similar con-

[4]according to (Spoering and Lewis, 2001), stationary phase planktonic cells display similar resistance to 4 different kinds of antibiotics than biofilm cells

**Table 1.1.** Comparison of mechanisms of antimicrobial and metal resistance in biofilms

| Stewart (2002) (antibiotic resistance) | Harrison (2008) (metal resistance) |
|---|---|
| poor antibiotic penetration and diffusion | immobilization of antimicrobial compounds by adsorption to biomass |
| nutrient limitation (coupled to slow growth) | chemical and metabolic gradients in the biofilm introduced by structured population growth, |
| adaptive stress response | adaptive responses of the biofilm that may change the physiology of some cells to a resistant or tolerant state |
| persister cells | metabolically quiescent cells, termed persister cells, which do not grow, yet do not die on exposure to metal ions |
| | cell-cell signalling events via small messenger molecules that contribute to the biofilm lifestyle |
| | genetic rearrangements or mutations that produce variant phenotypes in the population |

clusions than Stewart and postulated that biofilm antimicrobial resistance against metals is due to multiple factors. The findings of the two aforementioned studies are summarized in Table 1.1.

It is clear from the above two studies that numerous factors influence antimicrobial resistance (often simultaneously) in biofilms but that it is difficult to delineate the exact cause and weighted influence of the contributing factors to the resistance. Instances of above points can be demonstrated in terms of a specific example of *Pseudomonas aeruginosa*[5] and the aminoglycoside antibiotic tobramycin[6], to narrow down the focus:

- Tobramycin is a positively charged aminoglycoside and has been purported to adhere to the predominantly negative charges of the phosphate groups in the EPS

[5] the majority of cystic fibrosis patients suffer from chronic respiratory infection caused by *Pseudomonas aeruginosa* (Döring et al., 2000)

[6] one of the most popular treatment strategies in cystic fibrosis (Banerjee and Stableforth, 2000; Moreau-Marquis et al., 2009)

(Fux et al., 2005), as well as alginate[7] (Hentzer et al., 2001) which retards penetration into the biofilm (or periplasmic glucans that physically interact with the tobramycin (Mah et al., 2003)) as compared to molecules whose movement (Stewart, 2003) in the biofilm is only hindered by steric interactions.

- nutrients can affect the biofilm in terms of growth rate, oxygen concentration and virulence (Høiby et al., 2010). Slow growth rate within biofilms has been shown to enhance antimicrobial resistance (Brown et al., 1988; Roberts and Stewart, 2004). Non-growing zones in a biofilm are better protected against an antimicrobial onslaught when compared to biofilms growing at a uniform rate (Xu et al., 2000). Oxygen penetration into a biofilm has been shown to have a more pronounced effect on biofilm susceptibility to tobramycin than antimicrobial penetration (Walters et al., 2003); an observation that has also been confirmed by other studies (Hassett et al., 2002; Borriello et al., 2004; Hill et al., 2005; Field et al., 2005). Iron depletion on its own (Anwar et al., 1989; Cai et al., 2009) has also been shown to enhance antimicrobial resistance and enhanced virulence when coupled with low oxygen concentrations (Kim et al., 2003).

- biofilms have been known to have enhanced capacity to launch adaptive stress responses against antimicrobial attacks for example stimulated catalase production (Elkins et al., 1999) when exposed to hydrogen peroxide, increased beta-lactamase activity (Bagge et al., 2000) and the transcribing of genes for an efflux pump when treated with tobramycin (Whiteley et al., 2001; Zhang and Mah, 2008). Szomolay et al. (2005) also shows that biofilm cells experience a delayed exposure to antibiotics and would be more suited to survive when the time scale for adaptation is faster than the time scale for disinfection.

[7] anionic polysaccharide produced by *P. aeruginosa* (May et al., 1991)

- persister cells (cells that neither grow nor die in the presence of antimicrobials) are believed to occur in much higher numbers in biofilms than in planktonic populations (Stewart, 2002). These persister cells are postulated to be neither defective cells, nor cells created in response to antibiotics but that their production depends on growth stage and that they are specialist survivor cells (Keren et al., 2004a).

- quorum sensing mutants of *P. aeruginosa* PA01 were susceptible to kanamycin at much lower concentration than the wild type (Shih and Huang, 2002).

- cells in biofilms are prone to high rates of conjugation (Hausner and Wuertz, 1999) and stochastic gene expression and genotypic variation that is enhanced by selection within the biofilm (Stewart and Franklin, 2008). This genetic transfer might in principle be responsible for an increase in transfer of antibiotic resistance genes. Boles et al. (2004) introduced the term "insurance effects" of biofilm associated *P. aeruginosa* as it undergoes extensive self generated diversification to safeguard the community against possible environmental adverse conditions.

From the above list it is clear that various experimental techniques are necessary to shed light on the proposed mechanisms of increased biofilm antimicrobial resistance and that complementary approaches would be more successful in reaching solutions given the complexity and intricacy of the problem. The aim of this document, however, is not to systematically and exhaustively mention all the experimental techniques involved in phenomenological studies of biofilms but rather focus on one of the areas namely the inquiry into biofilm metabolism.

## 1.3. Literature overview of techniques to determine biofilm metabolism

Depending on the nature of the different measuring techniques, the biofilm metabolism has either been determined for local conditions or global conditions. Microscopy and micro-electrodes (typically measuring dissolved oxygen concentration) are capable of measuring local conditions. For microscopic images the field of view will vary roughly from 0.2 $mm^2$ at 20 times magnification to 0.008 $mm^2$ at 100 times magnification. Measuring of limiting nutrient concentrations, total bioluminescence and spectrophotometric on the other hand will be an example of global metabolic rate. The usefulness of whether a researcher determines local or global metabolic rates will depend on the specific questions asked. For example, addressing more fundamental concerns, measuring local rates in a micro-colony might show that the metabolic rates in biofilms are stratified in response to the nutrient gradients that exist within the three dimensional architecture with microorganisms on the outer layers displaying faster metabolism and growth (Werner et al., 2004). In the same experiment, measuring global rates may shed light on the fraction of active cells when more applied knowledge is required.

In the following paragraph examples will be given of the most popular methods for determining metabolic rates[8] in biofilms. The main strategies are to demonstrate that a measurable metabolic process is active. Such measurable metabolic processes include the measurement of enzyme activity, substrate consumption and catabolite formation or instances of ATP dependent bioluminescence that requires energy regeneration processes in the cell to be active. Examples of measurement of enzyme activity include:

[8]note that measurements of microbial growth rate will not be included in this list or discussion. Metabolic rates have been used to determine growth rates in biofilms but mostly it has been accomplished by measuring an increase in biochemical components (e.g. cell numbers, protein concentration, weight, infrared bands of attenuated total reflectance-Fourier transform infrared (ATR-FTIR) corresponding to proteins, polysaccharides, and nucleic acids)

- Determination of phosphotransacetylase activity by spectrophotometrically following the formation of acetyl-coenzyme A (Eschbach et al., 2004).

- Alkaline phosphatase activity with a fluorogenic stain and measured with epi-fluorescent microscopy with frozen cross sections to demonstrate spatial variability (Huang et al., 1995; Xu et al., 1998) or other fluorogenic substrates in micro-titer readers with fluorometer (Augustin et al., 2004)

- Measurement of dehydrogenase activity, fluorescein diacetate hydrolysis and the reduction of dimethyl sulfoxide (Riis et al., 1998)

- measurement of hydrolysis of tetrazolium salts like *p*-iodonitrotetrazolium violet (INT), sodium 3'-[1-(phenylamino)-carbonyl]-3,4-tetrazolium]-bis(4-methoxy-6-nitro) benzenesulfonic acid hydrate (XTT) and 5-cyano-2,3-ditolyl tetrazolium chloride (CTC) have been used for the detection of dehydrogenase activity by reduction of tetrazolium salts to formazan as a measure of the total respiratory or electron transport systems activity of the microorganisms (Huang et al., 1995; Ragusa et al., 2004)

Substrate utilization have been measured as indicators of cellular metabolism like the uptake of radio labeled carbon (Fletcher, 1986) or oxygen uptake rate measured with dissolved oxygen probes (Simões et al., 2005) or micro-electrodes (Wäsche et al., 2000), or metabolic end products measured with HPLC (Eschbach et al., 2004).

Examples of luminescence measurements include:

- Light output measured with a luminometer of a self-bioluminescent *P. aeruginosa* strain (Marques et al., 2005)

- Reporter systems where a luciferase gene was chromosomally integrated under the control of the *Streptococcus mutans* lactate dehydrogenase promoter (Merritt et al., 2005)

- Protein synthetic activity with green fluorescent gene reporter constructs (Sternberg et al., 1999; Werner et al., 2004) as a reporter of gene expression

In the measurement of biofilm metabolism there are desirable experimental qualities that may serve as criteria to determine whether the measurements are done on a local or global scale; for instance the ability to monitor the metabolism in realtime, the ability to measure the metabolism non destructively in situ and lastly to have access to a broad method applicable to various growth conditions (e.g. aerobic and anaerobic systems) and microorganisms.

The tracking of enzyme activities has some drawbacks like the toxic nature of some cleavage products[9], difficulty to monitor light intensity quantitatively in a continuous manner and the killing of cells with prolonged exposure to fluorescent light sources. Furthermore, enzymatic activity can continue even in cell free extracts[10] and the enzymes of lysed cells may therefore mask the true activity of intact biofilm cells. On the contrary, cells injured by antibiotics (with the possibility of subsequent recovery) may keep on displaying enzymatic activity and will therefore be a better indicator of antimicrobial effectiveness than methods relying solely on the viability tests of heterotrophic plate counts (Stewart et al., 1994; McFeters et al., 1995).

Bioluminescence assays have been used for realtime measurement of antimicrobial treatment strategies (Marques et al., 2005) but a hinderance to the general applicability of these systems is that they are microorganism specific in the sense that either self-bioluminescence or genetic manipulation (insertion of fluorescent protein genes) is required (Werner et al., 2004; Merritt et al., 2005).

The measurement of catabolic products as an indication of metabolic rate is often hard to do in realtime and it is furthermore organism and substrate specific. The measurement

[9]Results of some studies indicated that the tetrazolium salts INT, XTT and CTC have been used in concentrations that were toxic to groundwater bacteria (Hatzinger et al., 2003)

[10]an observation that resulted in a Nobel Prize for Eduard Bucher in 1907

of oxygen uptake rate has been widely used with success both with dissolved oxygen probes for a global scale and with micro oxygen sensors for a local perspective. However, the approach is limited to aerobic systems.

The measurement of carbon dioxide as an indication of microbial activity has a long history in the monitoring of microbial reactor systems and has been used in upflow biofilm type reactors. Advantages of carbon dioxide measurements are that it is applicable to both aerobic and anaerobic metabolism and it is not substrate or organism specific. A possible reason for hesitation in using carbon dioxide as monitoring compound is its variability in solubility with changes in temperature and pH. In this study, carbon dioxide measurements in the gaseous phase was implemented in quantitatively monitoring in situ whole biofilm metabolism (global scale) non-destructively and in realtime.

## 1.4. Formulation of objectives for a new method to study biofilm metabolism

The overall goal of this study was to develop a system based on carbon dioxide measurements that would be a reliable indicator of biofilm metabolism and be amenable to expose various fundamental biofilm related metabolic behaviours. The experiments were done in two different reactor configurations developed specific for this study, each with benefits in addressing different types of questions.

The first reactor configuration exploited the high permeability of silicone to gases like oxygen and carbon dioxide. The growth reactor was a silicone tube (already used previously to cultivate biofilms (Sauer et al., 2002)) encased in a gas impermeable Tygon tubing where carbon dioxide produced by the microorganisms growing in the tube reactor could be transferred across the tube wall and measured in the gas phase by an infrared carbon dioxide gas analyzer. Different experiments were performed to calibrate the measured

results and to test the validity of the results in terms of known microbial physiological behaviour (discussed in more detail in Chapter 2).

Once it was realized that the carbon dioxide results indeed made physiological sense, the measurement system was expanded to a downstream carbon dioxide measurement unit that could, in principle, measure the metabolic rate of any upstream biofilm reactor. The downstream measurement reactor was a simple continuously stirred reactor configuration from where the dissolved carbon dioxide was stripped by a purging gas and again measured in the gas phase. Operating the downstream reactor under different liquid and gas flow regimes, different types of information could be gained from the upstream biofilm reactor (Chapter 3).

The working hypothesis of this study was that $CO_2$ measurements in the off-gas is a reliable and robust way to track global in situ biofilm metabolism.

The specific goals for this study were to:

- Develop and build a device (carbon dioxide evolution measurement system or CEMS) that would allow the $CO_2$ measurement from a biofilm grown in a flow system and to monitor the $CO_2$ production in real-time
- To calibrate the device and to determine if the $CO_2$ data makes physiological sense in terms of known microbial metabolism models
- To use the CEMS to test its applicability to determine
  - biofilm development and specific biofilm development rates
  - antimicrobial resistance of biofilms in
    - aerobic and
    - micro-aerophilic conditions
  - carbon channeling

- To extend the silicone tube based system to a more generally applicable system (carbon dioxide measurement reactor or CMR) that would measure downstream $CO_2$ of any biofilm flow reactor
- To demonstrate the applicability of the CMR to interpret physiological behaviour such as the relative metabolic contributions of different layers in the biofilm

## 1.5. Implementation of the new biofilm metabolism measurement method

### 1.5.1. Development and calibration: Outline of Chapter 2

The first goal was to design a carbon dioxide evolution measurement system (CEMS) to track metabolic responses in biofilms and to determine if the gaseous $CO_2$ measurements had the ability to relay physiologically interpretable information. In short, the CEMS consists of a tubular biofilm reactor with gas permeable silicone walls. The $CO_2$ crossing over the silicone membrane can be measured in the gas phase with a $CO_2$ analyzer which provided an online measurement system to track in situ biofilm metabolic behaviour in real time. The $CO_2$ produced by microorganisms occurs in the dissolved state and from there dissociates into the different available solutions it comes into contact with (liquid growth media, silicone membrane and gas); environmental conditions such as pH, temperature and solutes influence these equilibriums. These physical relationships and constants were reconciled to the reactor and measurement system design in order to make physiological sense of the measured data. For example, measurement regimes such as open or closed loop gas phase configurations had to be evaluated for suitability given the biological constraints of microbial metabolic capacity under the specific growth conditions. The $CO_2$ transfer in the CEMS was calibrated with sterile dissolved $CO_2$ solutions and transfer

models were developed for the nonporous (dense-polymer) silicone membrane to mathematically relate the dissolved $CO_2$ in the CEMS to the gaseous $CO_2$ measured by the analyzer. Subsequently, the metabolic response of mature pure culture biofilms was investigated under different environmental conditions including variations in temperature and limiting nutrient concentration. The metabolic responses of the biofilm cells were congruent with metabolic models (i.e. Arrhenius and square root relationship for microorganisms growing at suboptimal in temperature models and the metabolic response (as described by Gillooly et al. (2001) in relation to limiting nutrient concentration) in each case which strengthened the confidence in the method to monitor biofilm metabolic behaviour. In addition to the ability to monitor biofilm metabolic responses, the CEMS allowed the determination of a carbon balance over the biofilm reactor.

### 1.5.2. Extending the concept to more general applicability: Outline of Chapter 3

Although the CEMS is a useful tool in monitoring in situ biofilm respiration rates, a limitation was the necessity for the biofilms to be cultivated inside the silicone tube. Using $CO_2$ to measure biofilm respiration rate would be more broadly applicable if different surface attachment areas could be used and compared. With above considerations in mind, the concept of measuring biofilm $CO_2$ as an indication of biofilm metabolism was expanded to use downstream measurement of $CO_2$ produced by an upstream biofilm grown on any type of surface. The basic idea was that dissolved $CO_2$ in the liquid phase would transfer to the gas phase for measurement by the infrared $CO_2$ analyzer. Requirements for downstream plumbing to be gas impermeable have no influence on the biofilm reactor so in principle any surface or biofilm reactor configuration can be studied. In this particular part of the research a carbon dioxide measurement reactor (CMR) was designed and based on gas transfer in a chemostat to capture dissolved $CO_2$ concentrations of biofilm

reactor effluent.

Initially, whole biofilm metabolic activity was measured as steady state values. However, the downstream steady state measurements of whole biofilm metabolism was actually a combination of attached (adhered and slime layer cells) and free floating planktonic cells. The question therefore arose: what was the $CO_2$ contribution of the planktonic cells to the overall steady state value and the need to separate the $CO_2$ contribution of the attached and planktonic cells presented itself.

Furthermore, the concept of biofilms occurring in stratified layers with different metabolic activities (Coufort et al., 2007; Derlon et al., 2008; Mangalappalli-Illathu et al., 2009) has emerged. The CMR proved to be a diverse tool to study $CO_2$ concentrations under different configurations and flow regimes. Steady state liquid and gas flow configurations were used to measure total biofilm (base layer, slime layer and planktonic cells) $CO_2$ production. With the CMR operated as a batch system, the $CO_2$ contribution of the slime layer and the planktonic cells could be determined (which was found to have a negligible influence on the total $CO_2$ readings). It was thus possible to demonstrate the different metabolic activities of the different layers on a per cell basis and even the metabolic behaviour post separation of the base biofilm and the shear-susceptible layer. Microscopy was combined with the CMR studies to compare the visual observations with metabolic response.

### 1.5.3. Applying the original device to study biofilm development: Outline of Chapter 4

While most of the measurements done with CEMS in the work described in Chapter 2 were discrete data points obtained by steady state measurements, the configuration lent itself to acquisition and interpretation of dynamic (time dependent) data as well. The CEMS was used to study whole biofilm development in terms of lag phase, maximum

biofilm growth rate and stationary phases using different inocula and with the biofilms grown under different nutrient conditions.

Traditional methods to study biofilm growth suffered from some drawbacks. A few methods only measured total biomass increase (including EPS) with no way to distinguish between living and dead organic matter like quartz crystal microbalances (Tam et al., 2007), large area photometry (Bester et al., 2005; Milferstedt et al., 2006), electrical capacitance (Maurício et al., 2006), fiber optical devices (Tamachkiarow and Flemming, 2003), differential turbidity measurement devices (Klahre and Flemming, 2000), microfluidic biochips (Richter et al., 2007), optical coherence tomography (Haisch and Niessner, 2007), pressure drop or friction resistance (Lee et al., 1998), heat transfer resistance (Ludensky, 1998), nuclear magnetic resonance (Seymour et al., 2004), attenuated total reflectance-Fourier transform infrared spectroscopy (Delille et al., 2007), and photoacoustic spectroscopy (Schmid et al., 2004). Furthermore, some techniques are destructive for instance the physical removal of biofilm from coupons or fluorescent dyes used for microscopy that kill the cells. And lastly, some techniques are only measuring local growth like micro-sensors and microscopic techniques.

The term "biofilm growth rate" is not completely analogous to microbial planktonic growth rates as determined for example in batch shake flasks as, although the increase in biofilm cells could be considered a batch system, there are outside influences like erosion and immigration (Caldwell et al., 1981) that contribute to the net increase in cell numbers which then would not reflect a true growth rate in biofilms. Previous studies have shown that cells in biofilm can grow slower, faster or at the same rate as planktonic cells (Rice et al., 2000).

By tracking the net biofilm growth rate in realtime it was possible to witness sloughing events and rapid growth recovery especially at different (higher) nutrient concentrations. It was also possible to evaluate and compare the tempo of biofilm formation (duration of

lag phase) and the efficiency of nutrient utilization (value of steady state metabolism) of different pure and mixed culture biofilms under different growth conditions.

Experimenters often lament the heterogeneity of biofilms that impede the ability to study them (Lewandowski et al., 2004) but our studies showed that the source of the inoculum had a pronounced effect on the reproducibility of biofilm formation and that biofilm effluent cells and planktonic cells in the exponential phase used as inoculum lead to biofilms that demonstrated remarkable conformity with regards to developmental behaviour.

Finally the validity of this newly developed method of $CO_2$ measurements as an indicator of biofilm growth during early biofilm development was confirmed with protein concentration measurements.

### 1.5.4. Antimicrobials: Outline of Chapter 5

The real-time, non-destructive nature of the CEMS measurements (coupled to the ability to determine both aerobic and anaerobic metabolic rates) makes this an ideal system to study antimicrobial resistance in biofilms. The real-time capabilities allows the tracking of both transient and steady state responses to different durations and doses of antimicrobial exposure. The non-destructive characteristic provides the opportunity to repeatedly treat the same biofilm with antimicrobials to determine possible adaptive behaviour over time. Furthermore, the release of viable cells to the effluent could be correlated to in situ biofilm metabolism.

*P. aeruginosa* PA01 biofilms were grown under both aerobic and anaerobic conditions with the anaerobic biofilms demonstrating similar development rates than aerobic conditions but higher metabolic steady state values. This observation is contrary to reports in literature that states that low oxygen penetration into biofilms lead to slower growth and increased antimicrobial resistance. The biofilms were treated with tobramycin and the

anaerobic biofilms were more severely affected in both the magnitude and duration of metabolic rate reduction which is confirming reports that faster growing microorganisms are more affected by antibiotics (that normally target macromolecular synthesis).

# Chapter 2*

# $CO_2$ production as an indicator of biofilm metabolism

*This chapter has been published as: Kroukamp, O. and Wolfaardt, G.M., $CO_2$ production as an indicator of biofilm metabolism *Applied and Environmental Microbiology*, 2009, **75**, 4391–4397
(Writing was completed in consultation with the co-authors.)

# 2. $CO_2$ production as an indicator of biofilm metabolism

## 2.1. Abstract

Biofilms are important in aquatic nutrient cycling and microbial proliferation. In these structures, nutrients like carbon are channeled into the production of extracellular polymeric substances or cell division; both are vital for microbial survival and propagation. The aim of this study was to assess carbon channeling into cellular or noncellular fractions in biofilms. Growing in tubular reactors, biofilms of our model strain *Pseudomonas* sp. strain CT07 produced cells to the planktonic phase from the early stages of biofilm development, reaching pseudo steady state with a consistent yield of $\sim 10^7$ cells·cm$^{-2}$·h$^{-1}$ within 72 h. Total direct counts and image analysis showed that most of the converted carbon occurred in the noncellular fraction, with the released and sessile cells accounting for <10% and <2% of inflowing carbon, respectively. A $CO_2$ evolution measurement system (CEMS) that monitored $CO_2$ in the gas phase was developed to perform a complete carbon balance across the biofilm. The measurement system was able to determine whole-biofilm $CO_2$ production rates in real time and showed that gaseous $CO_2$ production accounted for 25% of inflowing carbon. In addition, the CEMS made it possible to measure biofilm response to changing environmental conditions; changes in temper-

ature or inflowing carbon concentration were followed by a rapid response in biofilm metabolism and the establishment of new steady-state conditions.

## 2.2. Introduction

Notable advances have been made in the study of biofilms since the early recognition (for examples, see references (Marshall et al., 1971; Geesey et al., 1978)) of this form of microbial existence. Following these earlier studies of selective adherence of bacteria to surfaces was the development of continuous flow cells, as well as computer assisted and scanning confocal laser microscopy that enabled the improved description of bacterial behaviour at surfaces (for an example, see reference (Lawrence et al., 1995)), and we now know that biofilms are organized aggregates of extracellular polymeric substance (EPS)-enclosed cells that differ substantially from suspended cells (Stoodley et al., 2002). Observing biofilm phenotypic responses may provide insight to guide researchers in conducting directed experiments to unravel underlying fundamental mechanisms; however, we still lack methods to measure and monitor biofilm function. Flemming (2003) grouped industrial biofilm monitoring systems into the following three categories: (i) systems detecting the increase and decrease of materials accumulating on a surface without differentiating biomass from other components, (ii) those that can distinguish between biotic and abiotic material, and (iii) those that provide detailed chemical information of biofilms. Janknecht and Melo (2003) categorized online biofilm monitoring techniques in a similar way when comparing applications in industrial systems but added a category for monitoring metabolic activity (a category that Flemming (2003) hinted at with the proposal of a technique that can distinguish between living and dead organisms on a surface). In brief, a nonexhaustive list of techniques that deal only with online monitoring increase (whether of biotic or abiotic origin) and the decrease of biofilms includes quartz

crystal microbalances (Tam et al., 2007), large area photometry (Bester et al., 2005; Milferstedt et al., 2006), electrical capacitance (Maurício et al., 2006), fiber optical devices (Tamachkiarow and Flemming, 2003), differential turbidity measurement devices (Klahre and Flemming, 2000), microfluidic biochips (Richter et al., 2007), optical coherence tomography (Haisch and Niessner, 2007), pressure drop or friction resistance (Lee et al., 1998), and heat transfer resistance (Ludensky, 1998). Techniques that provide information about the physical structure and chemical properties of biofilms are nuclear magnetic resonance (Seymour et al., 2004), attenuated total reflectance-Fourier transform infrared spectroscopy (Delille et al., 2007), and photoacoustic spectroscopy (Schmid et al., 2004). Some biofilm monitoring techniques provide information about metabolic activity in biofilms, such as those using electrochemical devices like dissolved oxygen and redox probes (Lee et al., 2007), microbiologically influenced corrosion monitoring (Mollica and Cristiani, 2003), nuclear magnetic resonance (Wolf et al., 2002), measurement of substrate consumption (Tanji et al., 2007; Kappelhof et al., 2003) or metabolic products (Vanhooren et al., 2000), bioluminescence assays, and fluorometry (Wolf et al., 2002). The objective of the study was to develop a real-time monitoring system to measure gaseous $CO_2$ production as an indicator of biofilm metabolism and to use the system to determine the biofilm response to environmental conditions and to measure carbon channeling in biofilms.

## 2.3. Materials and Methods

### 2.3.1. Culture media and growth conditions.

Pure culture biofilms of *Pseudomonas* sp. strain CT07 *gfp* (Bester et al., 2005) and *Pseudomonas aeruginosa* PA01 *gfp* were grown in silicone tubes (Sauer et al., 2002). The silicone tubes were inoculated with 200 to 500 $\mu$l from an overnight culture (the same medium was used as that described below except 5 mM of sodium citrate was used instead of 1

mM) with the pump turned off for 30 min to 1 h to allow initial adhesion to the tube walls. Sterile defined growth medium [a final concentration of 1.51 mM $(NH_4)_2SO_4$, 3.37 mM $Na_2HPO_4$, 2.20 mM $KH_2PO_4$, 179 mM NaCl, 0.1 mM $MgCl_2 \cdot 6H_2O$, 0.01 mM $CaCl_2 \cdot 2H_2O$, 0.001 mM $FeCl_3$] with either 1 mM sodium citrate or 3 mM glucose as the sole carbon source was continuously supplied by a Watson Marlow 205U peristaltic pump at 15 ml/h (unless specified otherwise). Medium retention time was 12 minutes for this reactor size and flow rate.

### 2.3.2. CEMS and measurements

A carbon dioxide evolution measurement system (CEMS) was constructed, which is essentially a silicone tube biofilm reactor (inside diameter, 0.16 cm; outside diameter, 0.24 cm; length, 150 cm; VWR International, Mississauga, ON, Canada) encased in a sealed Tygon tube (inside diameter, 0.48 cm; outside diameter, 0.79 cm; formulation R-3603; VWR International, Mississauga, ON, Canada) with the annular space being connected to a $CO_2$ analyzer. Silicone tubing has a relatively high permeability to both $CO_2$ and $O_2$ compared to that of Tygon tubing; approximately 50 times and 200 times higher for $CO_2$ and $O_2$, respectively, according to permeability coefficients provided by the manufacturer. Given a higher gaseous $CO_2$ concentration on the inside of the lumen of the silicone tube due to biofilm metabolic activity, it can be assumed that a fraction will cross the silicone tube wall to the annular space where it can be measured. The annular space of the carbon dioxide exchange system (CEMS) was connected to an absolute, nondispersive, infrared LI-820 $CO_2$ gas analyzer (LI-COR Biosciences, NE), and compressed air was used as the sweeper gas. The steady-state $CO_2$ concentration in the compressed air was measured and subtracted from the steady-state $CO_2$ originating from the CEMS. Gas flow rates were determined by volumetric displacement and a thermal gas mass flow meter (Aalborg, NY). Although the use of silicone for carbon dioxide transfer has been applied to measure mi-

crobial metabolic activity in water research and fermentations, such an approach has to our knowledge not been applied in biofilm studies. For example, Visser et al. (2002) and Aboka et al. (2006) measured the transfer of $O_2$ and $CO_2$ across silicone membranes to monitor respiration of *Saccharomyces cerevisiae* isolates grown in a chemostat, and Dahod (1993) used submerged silicone tubes in a fermentor to measure respiration rates of industrial *Streptomyces* organisms on a pilot plant scale.

### 2.3.3. Theory

During development of the CEMS, it was clear that it would be useful to have a mathematical relationship that determines what fraction of $CO_2$ will cross the silicone membrane under certain experimental conditions. In this way, it would be necessary to measure only the $CO_2$ concentration on one side while being able to relate it to the $CO_2$ concentration on the other side of the membrane.

### 2.3.4. Gas transport across silicone membranes.

Gas mass transfer across a membrane is often described in terms of Fick's law of diffusion (for examples, see references (Mulder, 1996), and (Hoffman, 2003)) as follows:

$$J = -D\frac{dc}{dx} = \frac{D}{\Delta l}\left(c_{m1} - c_{m2}\right) \tag{2.1}$$

where $c$ describes the concentrations (mol$\cdot$ m$^{-3}$), $x$ is the length (m), $J$ is the flux of the compound crossing the membrane (mol $\cdot$ s$^{-1}$ $\cdot$ m$^{-2}$), $D$ is the diffusion coefficient (m$^2\cdot$ s$^{-1}$), $\Delta l$ is the thickness of the membrane, and $c_{m1}$ and $c_{m2}$ (mol$\cdot$ m$^{-3}$) are the concentrations of the species crossing the membrane at the membrane surfaces on either side.

Silicone membranes can be described as nonporous (dense-polymer) membranes like

the kind used for pervaporation, perstraction, or gas separations as opposed to porous membranes used in microfiltration or ultrafiltration (Mulder, 1996). In addition to diffusion, the partitioning of the solute between the membrane and adjacent solution plays an important role in the transport. The partitioning of solute between the adjacent solution and the membrane surface is linearly related via a partitioning coefficient analogous to a Henry's law constant of the form $\sigma_1 = c_m(eq)/C_1^{in}(eq)$ and $\sigma_2 = c_m(eq)/C_2^{out}(eq)$ where $\sigma_1$ is the partitioning coefficient (sometimes called a solubility coefficient, but it serves the same purpose of relating the surface membrane concentration to the adjacent phase concentration), and $C_1^{in}$ is the solute concentration in the adjacent phase in equilibrium (eq) with the solute concentration at the membrane surface ($c_m$). If the adjacent or bulk solutions are the same (e.g., aqueous), $\sigma_1 = \sigma_2 = \sigma$ and equation 2.1 can be written as

$$J = \frac{D}{\Delta l}\left(\sigma C_1^{in} - \sigma C_2^{out}\right) = \frac{\sigma D}{\Delta l}\left(C_1^{in} - C_2^{out}\right) \tag{2.2}$$

Note that the partitioning coefficient can be written in many forms, depending on the driving force (partial pressure or concentration difference across the membrane). It can be dimensionless or can relate partial pressure to concentration or vice versa, so attention has to be given to the appropriate units. Under certain conditions with specific membrane polymers and permeants, the permeability coefficient, $P$, can be given as the product of the diffusion constant, $D$, and the partitioning coefficient, $\sigma$. The partition coefficient serves as an indicator of the ability of the membrane to allow transport of certain molecules. Again, the units of $P$ may vary widely depending on the driving force (Yasuda, 1975).

Depending on the nature (e.g., the size of the molecule) of the solute and membrane properties, diffusion or solubility of the solute in the membrane ($\sigma$) will contribute in different amounts to the overall mass transfer. In the case of carbon dioxide transfer through rubber or silicone, solubility plays by far the most important role in gas transport

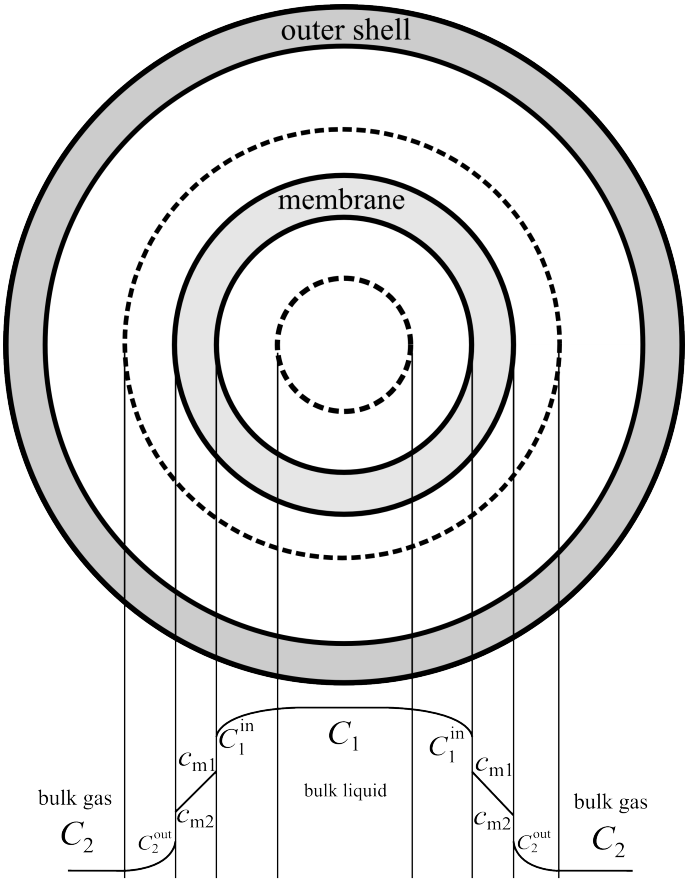


**Fig. 2.1.** Cross section to illustrate radial transfer of $CO_2$ from the liquid bulk phase to the gas bulk phase in the CEMS. Adapted from reference (Dindore et al., 2004) with permission from Elsevier

(Mulder, 1996).

### 2.3.5. Gas transport across a silicone tube wall in the CEMS

The permeability of silicone rubber membranes to $O_2$ and $CO_2$ has long been known and is implied in liquid-gas contact applications, such as a membrane gills for submarines and underwater stations (Robb, 1968) or gas exchange in blood (Spaeth and S.K.Friedlander, 1967). However, when the two phases adjacent to the membrane are not the same, equation 2.2 does not accurately describe the mass transfer anymore. The different phases will pose different mass transfer resistances on either side of the membrane, and the partition-

ing coefficients may vary (see references (Jenkins and Krishnan, 2004), (Mavroudi et al., 2006), (Zhang et al., 2008) for examples). If the solutions adjacent to the membrane are not the same (e.g., aqueous and gas) (Côté et al., 1989), $\sigma_1 = \sigma_2$ and equation 2.1 becomes as follows:

$$J = \frac{D}{\Delta l}\left(\sigma_1 C_1^{in} - \sigma_2 C_2^{out}\right) \tag{2.3}$$

The concentrations for $C_1^{in}$ and $C_2^{out}$ are usually not the same as the concentrations in the bulk solutions, $C_1$ and $C_2$. For a steady-state flux of solute from bulk solution 1 to bulk solution 2, the fluxes can be expressed as follows: $J = k_1(C_1 - C_1^{in}) = D/\Delta l(\sigma_1 C_1^{in} - \sigma_2 C_2^{out}) = k_2(C_2^{out} - C_2)$ where $k_1$ and $k_2$ are mass transfer coefficients (m$\cdot$ s$^{-1}$) (Sirkar, 1992). The relationship described above can be simplified as follows:

$$J = \frac{1}{\frac{\sigma_1}{k_1} + \frac{\Delta l}{D} + \frac{\sigma_2}{k_2}}\left(\sigma_1 C_1 - \sigma_2 C_2\right) = \frac{1}{\frac{\sigma_1}{k_1\sigma_2} + \frac{\Delta l}{D\sigma_2} + \frac{1}{k_2}}\left(\frac{\sigma_1}{\sigma_2}C_1 - C_2\right) \tag{2.4}$$

If the bulk solution on side 1 is water and the bulk solution on side 2 is air, based on equation 2.4, a local transfer coefficient ($K_z$) can be written as $1/K_z = \sigma_1/k_1\sigma_2 + \Delta l/D\sigma_2 + 1/k_2$ and equation 2.4 can be rewritten as follows:

$$J = K_z\left(\frac{\sigma_1}{\sigma_2}C_1 - C_2\right) \tag{2.5}$$

Equation 2.5 describes the radial transfer from the liquid bulk phase to the gas bulk phase (Figure 2.1). To determine the overall transfer coefficient ($K_L$) of the CEMS, a mass balance can be written across an infinitely thin slice of the CEMS and integrated along the length of the tube, similar to treatment carried out by Dindore et al. (2004). The average flux over the entire length of the tube can be shown by the following equation:

$$J_{ave} = \frac{Q_2 \left( HC_1 - HC_1 e^{-\frac{\pi d_0 K_L}{Q_2} L} \right)}{\pi L d_0} \tag{2.6}$$

where $J_{ave}$ is the average flux (mol $\cdot$ m$^{-2}$ $\cdot$ s$^{-1}$), $Q_2$ is the volumetric flow rate of the gas (m$^3$/s), $H$ is a Henry's law constant relating equilibrium values ($\sigma_1/\sigma_2$), $L$ is the length of the tube (m), and $d_0$ is the outer diameter of the silicone tube (m). Note that in the derivation of equation 2.6, it is assumed that the concentration on the liquid side remains constant throughout the length of the reactor tube (see the supplemental material). With equation 2.6, it is therefore possible to determine the overall transfer coefficient for the CEMS, $K_L$, with known liquid phase $CO_2$ concentrations ($C_1$) by measuring the $CO_2$ flux appearing in the gas phase. Once calibrated for a particular membrane configuration, the gas phase results can be used to calculate the $C_1$ for other experimental conditions. In an experimental configuration where microbes grow in a biofilm on the inside wall of the silicone tube, they will excrete their $CO_2$ into their surroundings. The $CO_2$ from microbial respiration is transferred across cell membranes in a dissolved form or aqueous $CO_2$ (Jones and Greenfield, 1982). Aqueous $CO_2$ can either be converted to a gaseous form or remain dissolved and even be transformed into bicarbonate and carbonate ions as schematically represented by Zeng (1995).

$$\begin{array}{ccccc} \mathrm{CO_2^{(measured)}} & & \mathrm{CO_2^{(in\ vivo)}} & & \\ \uparrow & & \downarrow & & \\ \mathrm{CO_2}(g) & \leftrightharpoons & \mathrm{CO_2}(aq) & \leftrightharpoons \mathrm{H_2CO_3} \leftrightharpoons \mathrm{HCO_3^-} + H^+ \leftrightharpoons \mathrm{CO_3^{2-}} + 2H^+ \end{array} \tag{2.7}$$

The ratio of the dissolved forms of $CO_2$ is dependent on pH, temperature, and ion activity (Frahm et al., 2002). At a pH of 4 to 7, the carbonate ion concentration is negligible.

### 2.3.6. Linearity of dissolved carbon dioxide.

A dilution series of dissolved $CO_2$ was used to correlate the amount of $CO_2$ in the liquid phase transferred by the CEMS to the gas phase. A saturated solution of $CO_2$ in Milli-Q water was made by stirring pieces of "dry ice" (solid $CO_2$) until the pH stabilized at room temperature. This saturated solution was used to make a dilution series of 1% to 4% (vol/vol) dissolved $CO_2$ and sealed in serum vials with butyl rubber stoppers. Steady-state $CO_2$ concentrations in the off-gas were measured with increasingly dissolved $CO_2$ samples.

### 2.3.7. Effect of temperature on biofilm respiration/metabolism

To test the sensitivity of biofilm respiration to temperature changes, the CEMS was submerged in a cooling water bath overnight at 15 °C and subsequently subjected to changes in temperature between 27 °C and 10 °C and $CO_2$ concentrations in the off-gas measured. To ensure an even distribution of temperature, the carrier gas and growth medium were controlled in the same water bath as the CEMS.

### 2.3.8. Effect of citrate or glucose concentration

In each replicate experiment, biofilms were grown for 8 days in the CEMS at citrate and glucose concentrations of 1 mM and 3 mM, respectively, at room temperature before the influent concentrations were randomly varied between 0.125 mM and 5 mM and the $CO_2$ concentrations were measured in the off-gas. The validity of the biofilm response to different citrate or glucose concentrations in a carbon-limited environment was tested with the following relationship described by Gillooly et al. (2001): metabolic rate $\propto$ (concentration of reactants)(fluxes of reactants)(kinetic energy of the system). For the conditions where only the concentrations of the carbon source were varied, the last two terms can be

considered constant.

### 2.3.9. Determination of cell numbers and carbon in cellular and noncellular fractions

Cell numbers in the effluent and biofilm were determined by heterotrophic plate counts and total direct cell counts. In brief, cell suspensions were vortexed and diluted in 0.9% saline and stained with 4',6-diamidino-2-phenylindole (DAPI). The suspension was filtered onto a 0.22 m black polycarbonate filter, and the cell numbers were determined by epifluorescence microscopy. Images were recorded with a Leica DM5000 B epifluorescence microscope and a Leica DFC350 FX camera, and cell sizes were determined on a PC computer using the Microsoft Windows version of the public domain NIH Image program from the U.S. National Institutes of Health (available at http://rsb.info.nih.gov/nih-image/). Digital image processing was done as described by Massana et al. (1997), which involved the application of a series of Gauss, Laplace, and median filters with manual thresholding steps in between. Both cell numbers and cell dimensions could be determined from the processed images. The pseudomonad cells were rod shaped, and cellular volumes were determined by using the following equation: $V = [w^2(\pi/4)](l - w) + [w^3(\pi/6)]$, where $w$ and $l$ are the width and length of the cell, respectively. Values for $w$ and $l$ were determined from the digitally processed images, and the average two-dimensional cell area determined by the equation was 0.98 $\pm$ 0.12 $\mu$m$^2$, which is very similar to values of 0.86 $\pm$ 0.12 $\mu$m$^2$ for *Pseudomonas fluorescens* as determined by Mueller (1996). *Pseudomonas* sp. strain CT07 is closely related to *P. fluorescens* (Bester et al., 2005). Posch et al. (2001) described an allometric conversion formula to relate cellular volume to cellular carbon based on images obtained for a specific dye. For DAPI-stained images, the conversion is given by the following equation: cellular carbon = 218 $\times V^{0.86}$, with the cellular carbon measured in femtograms of carbon and $V$ in micrometers cubed.

### 2.3.10. Determination of unused citrate exiting the reactor in the liquid phase

Unused citrate exiting the reactor was determined with an enzymatic analysis kit from Enzytec (Scil Diagnostics GmbH, Germany).

### 2.3.11. Carbon balance

For the carbon balance, both effluent liquid samples and off-gas samples were taken at 24-h intervals and measured for carbon content. These discrete concentration values were used together with the flow rates to calculate the cumulative carbon exiting the CEMS. The total carbon in the effluent was measured with a catalytic combustion, nondispersive infrared total carbon analyzer (TOC-$V_{CSH/CSN}$; Shimadzu, Kyoto, Japan), while the $CO_2$ in the off-gas was measured as mentioned above. At the end of the experiment, the organic matter that accumulated in the reactor tube was collected by squeezing out the attached organic matter using a bottle as a rolling pin. Visual observations revealed that as the biofilms matured, small aggregates would sporadically exit the tube reactor with the effluent. These aggregates are denser than water. Therefore a simple trap consisting of a 1.5 ml Eppendorf tube with the influent line positioned below the effluent line was devised for collecting the aggregate-free liquid phase in a container with sodium azide (final concentration, 70 mg/liter) to inhibit further microbial degradation of carbonaceous compounds.

## 2.4. Results

The CEMS was developed for measuring real-time, whole biofilm $CO_2$ production rates. This device was used to assess the biofilm response to changing environmental conditions

and carbon channeling in biofilms.

### 2.4.1. Calibration.

When the CEMS was tested with gas phases on both sides of the silicone membrane according to methods described by ASTM standards (AST), the gas permeability coefficient was $(3.02 \pm 0.04) \times 10^{-6}$ $cm^3 \cdot mm \cdot s^{-1} \cdot cm^{-2} \cdot cmHg^{-1}$ and corresponded well with values from the manufacturer (same order of magnitude). Milli-Q water with known dissolved $CO_2$ concentrations (between 0 and 4% saturation) was used to test the $CO_2$ transfer across the silicone tube wall to the gas phase. The $CO_2$ measured in the gas phase was highly linear ($R^2 \pm 0.999$) with various dissolved $CO_2$ concentrations. Experimental results for biofilm $CO_2$ production were well within the range tested during the calibration experiments.

### 2.4.2. Effect of temperature on biofilm metabolism

Figure 2.2 shows an actual output from the $CO_2$ analyzer. Popular models for describing the dependence of microbial metabolic activity to temperature were used to verify the relationship of steadystate, gaseous $CO_2$ measurements to variations in temperature. The Arrhenius equation is an exponential function used to model temperature relationships, and the plot of the log of activity ($CO_2$ measurement) against the inverse of the absolute temperature should be a straight line if the activation energy is constant over the range of measurement (Pietikäinen et al., 2005). Indeed, the results showed an $R^2$ value equal to 0.990 and 0.977 for growth on 1 mM citrate and 3 mM glucose, respectively, for *Pseudomonas* sp. strain CT07 *gfp*. Another model for relating temperature to microbial activity is a square root relationship used for microbes growing at suboptimal temperatures, which was the case for the strains used in these experiments. A plot of the square root of the activity against the temperature should give a straight line (Pietikäinen et al.,

2005), which was the case with an $R^2$ value of 0.988 for growth on 1 mM citrate and an $R^2$ value of 0.993 for growth on 3 mM glucose for *Pseudomonas* sp. strain CT07 *gfp*.

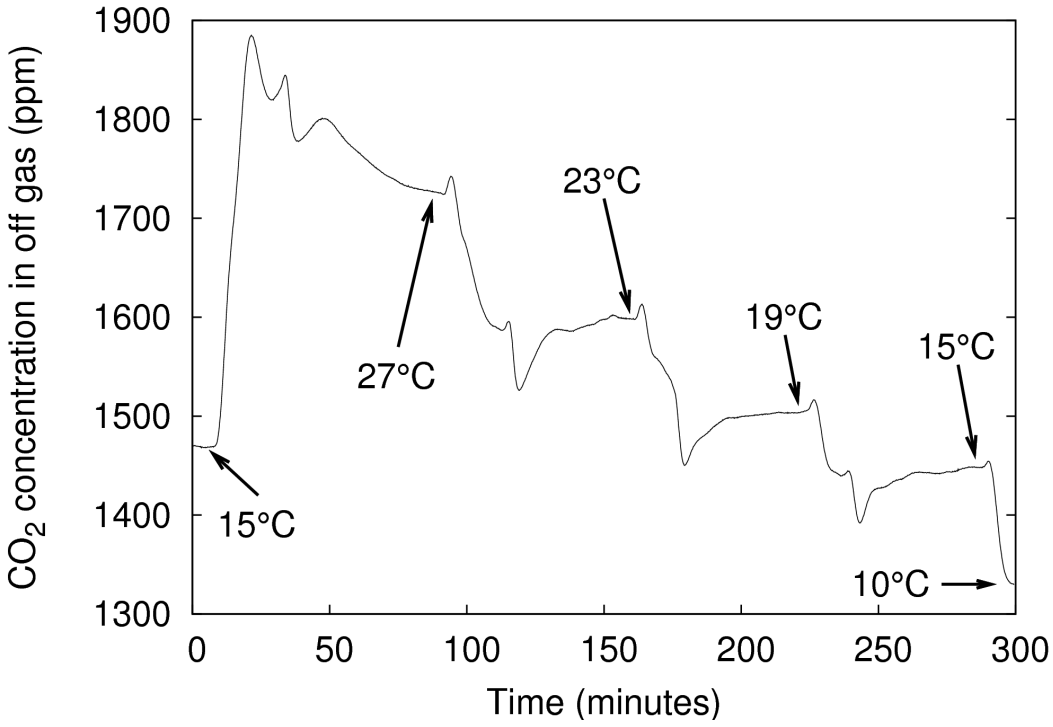


**Fig. 2.2.** Effect of temperature on biofilm metabolism. Output data from the $CO_2$ analyzer showing the response of a *Pseudomonas* sp. strain CT07 *gfp* biofilm and the time to reach new steady-state values with temperature perturbations.

Duplicate experiments provided similar results in terms of both $CO_2$ measurements and times to reach steady state (results not shown).

### 2.4.3. Effect of citrate concentration on biofilm metabolism

The citrate concentrations in the medium were varied at random (Figure 2.3B) while measuring the $CO_2$ in the off-gas. For citrate concentrations between 0.5 mM and 5 mM, the response in $CO_2$ evolution was nearly linear ($R^2 \pm 0.996$) for *Pseudomonas* sp. strain CT07 *gfp*. Similarly, the response in $CO_2$ evolution for *P. aeruginosa* PA01 between 0.5 and 4 mM citrate was also nearly linear, with an $R^2$ value of 0.995. Because of its wider range of

carbon sources, *P. aeruginosa* PA01 was also cultivated on glucose, benzoate, and tryptic soy broth with similar linear responses ($R^2$ values of 0.996, 0.994, and 0.999, respectively).

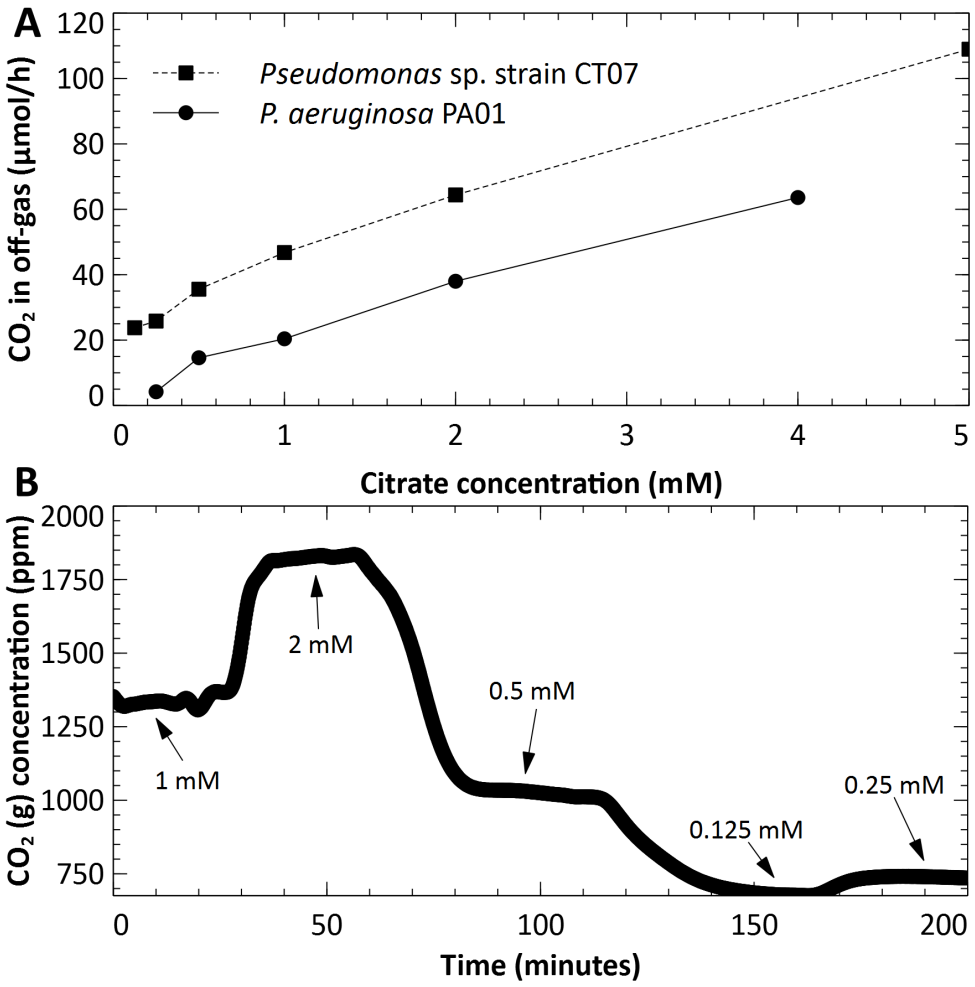


**Fig. 2.3.** $CO_2$ production rates showing biofilm response to changes in influent citrate concentrations. Biofilm metabolic response showing the linear correlation (an $R^2$ value of 0.995 and 0.996 for *P. aeruginosa* PAO1 and *Pseudomonas* sp. strain CT07, respectively) (A) with citrate concentration despite the random order (*Pseudomonas* sp. strain CT07 in this case) (B) in which the concentration was changed, demonstrating the adaptability of biofilms to environmental changes

This metabolic response with various carbon concentrations above the threshold of 0.5 mM (0.3 g/liter in the case of tryptic soy broth) can be explained with the relationship described by Gillooly et al. (2001), presented in Materials and Methods. The last two terms in their equation can be considered constant (reasons mentioned below), which

leaves the metabolic rate directly proportional to the concentration of reactants (citrate). Microbes have the ability to modulate nutrient uptake and enzyme affinities to ensure high metabolic fluxes even under low-nutrient conditions (with the assumption that fluxes will be kept fairly constant under the conditions of our experiments; i.e., second term) (Teixeira De Mattos and Neijssel, 1997). The kinetic energy (third term) of the system is dependent on temperature, which was kept constant during the experiment.

### 2.4.4. Carbon balance

All the carbon exiting the biofilm reactor in the liquid (as suspended materials) and gas phases was compared with the carbon flowing into the reactor over a period of 8 days (Figure 2.4). The carbon balance for replicate experiments closed to within 2 and 4%. For the experiment summarized in Figure 4, carbon that exited the reactor in the liquid phase accounted for 72.4% of the incoming carbon. The cumulative amount of gaseous $CO_2$ leaving the reactor was 24.9% of the inflowing carbon, while 4.1% of the carbon remained attached to the inner surface of the reactor tube. Components that contributed to the liquid phase carbon fraction that exited the reactor included dissolved $CO_2$ cellular carbon (biofilm biomass lost, e.g., sloughing, dispersion, and erosion), unused citrate, and EPS. Calibration experiments using known concentrations of dissolved $CO_2$ and concomitant gas phase measurements showed that at least an amount similar to that of the $CO_2$ in the gas phase exited the reactor in a dissolved form.

Microbial cells in the effluent reached values of $\sim 10^6$ cells $\cdot$ cm$^{-2}$ $\cdot$ h$^{-1}$ (cells produced per biofilm footprint area per unit of time) within 24 h after inoculation and reached pseudo-steady-state values of $\sim 10^7$ cells cm$^{-2}$ $\cdot$ h$^{-1}$ after 3 days. The carbon fraction leaving the reactor as nonaggregated cells was always less than 10%, as determined by direct microscopy, image analysis, and the conversion formula described in Materials and Methods. Carbon leaving the reactor as aggregates accounted for 30% of the inflowing

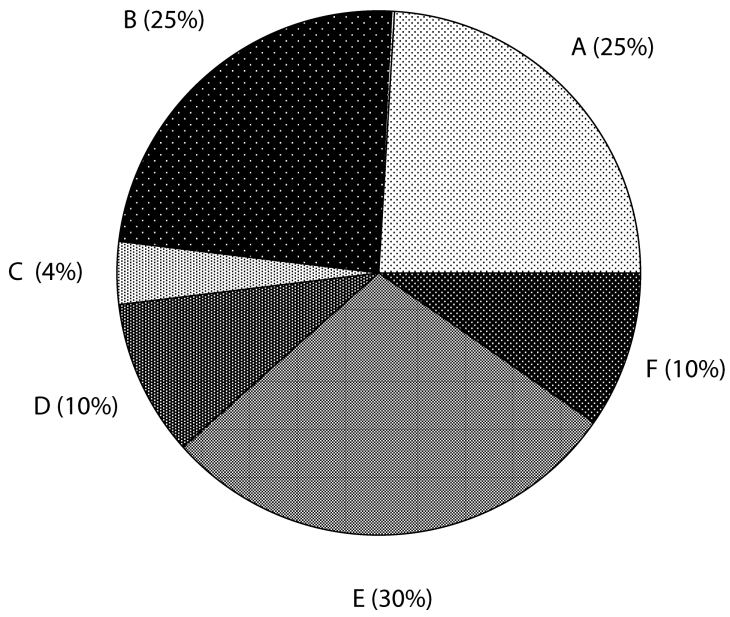


**Fig. 2.4.** Carbon balance for a *Pseudomonas* sp. strain CT07 biofilm over an 8-day cultivation. Shown are cumulative $CO_2$ exiting in gas phase (A), cumulative $CO_2$ exiting in liquid phase (B), carbon remaining behind in the biofilm (C), cumulative carbon exiting as cells (D), cumulative carbon exiting as aggregates (less than 1% of vol) (E), and cumulative unused citrate (F). The carbon balance typically closed within 2 - 4%.

carbon condensed in less than 1% of the exiting volume. The composition of these aggregates in terms of cell numbers and other contributing constituents has not yet been determined. Unused citrate plateaued at 10% of the growth medium value after 3 days.

## 2.5. Discussion

Lewandowski and Beyenal (2003) lamented the divide between the generation of mon-

itoring results and the useful application thereof, due mainly to the inability of mathematical models to accept the monitored parameters even if the monitoring is done with technical excellence. Building the bridge between biofilm monitoring and mathematical models that can successfully implement the data to correlate measured parameters to biofilm function is beyond the scope of this article. However, we hope to demonstrate that simple biofilm monitoring measurements can provide insight into the important biofilm functions of protection (EPS production) and proliferation (releasing progeny into the environment by physiological means and by employing physical means such as erosion, abrasion, and sloughing). Being aware of the phenomenological responses of biofilms may lead to the identification of focus areas for more fundamental research. Kreft (2004) considered the conflict in biofilms for the economical use of limiting resources to channel it toward either a specific growth rate (the rate of biomass increase per time and biomass) or growth yield (biomass formed per amount of resource used), where a high growth yield can be attained only through a decrease in the specific growth rate. In pure culture work, Bester et al. (2005) showed that microbes in a biofilm released high numbers of cells into the environment, even at very early stages of biofilm development. EPS production varies with different physical environmental conditions and available nutrients. Xavier and Foster (2007) simulated competition between microbial strains that differ in their ability to produce EPS. They concluded that polymer production may afford a competitive advantage in mixed-species biofilms under certain conditions by suffocating neighbouring nonpolymer producers and exposing later generations to better oxygen conditions. $CO_2$ production is another important and often neglected sink of carbon in biofilm systems. Liu et al. (2003) described an observed growth yield in biofilms that takes channeling of dissolved organic carbon to $CO_2$ and biomass fractions into account. According to the equation presented by these authors for the observed growth yield it is clear that, given a finite dissolved organic carbon source, an increase in respiration will imply a de-

crease in biomass as the authors indeed show with data from the literature. It has been proposed that under conditions of energy limitation, catabolic reactions are tightly coupled to anabolic reactions (Russell and Cook, 1995) and diversion of substrate carbon into extracellular products is minimized (Harder and Dijkhuizen, 1983). Our studies show that between 40% and 50% of the inflowing carbon is used for respiration; 25% exits during the gas phase, and a similar amount remains dissolved and exits during the liquid phase. Furthermore, around 30% of the carbon leaves as dense aggregates, presumably consisting of cells bound to the EPS. Even if cell density in the aggregates is assumed to be similar to values of the biofilm, it means that roughly 20% of the carbon is converted to EPS and released to the effluent, even though our system may be considered carbon limited (Beyenal et al. (2003) considered 5 mM of glucose to be a carbon-limiting condition in *P. aeruginosa* chemostat cultures). Our focus here is not to elucidate the different EPS fractions; for that, refer to the seminal work by Laspidou and Rittmann (2002) who discussed EPS and soluble microbial products with their various subfractions and address the confusion regarding terminology that originated because EPSs have historically been studied from various backgrounds. In brief, a common theme of EPSs (bound and soluble) and soluble microbial products is that they are both organic materials of microbial origins but do not contain any active cells. These authors also reported EPS values as a percentage of influent carbon for continuously stirred tank and batch reactors. Our data suggest that the measurement of $CO_2$ in the off-gas is a suitable way of determining biofilm metabolic responses to changes in environmental parameters given the linear relationship to dissolved $CO_2$ under the conditions used. For changes in citrate concentration, the metabolic responses of *Pseudomonas* sp. strain CT07 *gfp* and *P. aeruginosa* PA01 *gfp* were nearly linear for values above 0.5 mM, which would suggest a regime of carbon sufficiency for those particular biofilms. For values below 0.5 mM citrate, the response deviated from linearity and can be explained in terms of a threshold

level of nutrients required for maintenance. When the level of available substrate carbon is lower than the value required for maintenance, the microbial cell must use carbon from its reserves (Touratier et al., 1999). The biofilm metabolic response was sensitive even to small changes in temperature. It should be noted that for the measurement of the temperature response, neither the silicone permeability dependence on temperature nor the temperature influence on gas solubility was taken into account. The gas permeability of silicone increases with increasing temperatures according to an Arrhenius-type relationship (Mulder, 1996), while the solubility of $CO_2$ in growth media increases with decreasing temperatures. However, these influences should be negligible over the temperature ranges used in these experiments. With equation 2.6, the overall transfer coefficient for the CEMS, $K_L$, can be determined for known dissolved $CO_2$ concentrations by measuring the $CO_2$ flux in the off-gas. We have not yet determined the $K_L$ because of the requirement of the constant dissolved $CO_2$ concentration, C1, in the derivation of equation 2.6. The requirement for constant $C_1$ could be accomplished by either increasing the dissolved $CO_2$ concentration and assuming that the $CO_2$ loss across the membrane is negligible or by shortening the length of the CEMS to minimize the loss of $CO_2$ along the length of the silicone tube. Once the $K_L$ has been determined, the resulting equation shows a linear relationship between the dissolved $CO_2$ and the $CO_2$ measured in the gas phase. Frahm et al. (2002) simultaneously solved a set of differential equations to relate carbon dioxide transfer rate measurements (measured in the gas phase) in mammalian suspension cultures to the carbon dioxide production rate. The equations included information about pH changes, buffer, and media composition and $CO_2$ transfer from the liquid phase to the gas phase. Weissenbacher et al. (2007) used a similar approach to calculate the carbon dioxide production rate from the carbon dioxide transfer rate measurements in activated sludge systems by correcting for the dissolved $CO_2$ /bicarbonate equilibrium transformations. Although our method is slightly less sophisticated by considering only a clumped

transfer coefficient, it seems that we are still able to predictably relate dissolved $CO_2$ with $CO_2$ measured in the gas phase. In systems considering mass transfer from the gas-to-liquid phase via membranes, liquid and gas flow rates influence the transfer rate. Zhang et al. (2006) determined that in the case of physical absorption (when $CO_2$ does not react with liquid it dissolves into water, and the authors considered $CO_2$ dissolving into water as a physical process), the $CO_2$ flux across the membrane increased with liquid velocity while the gas velocity had no effect on the $CO_2$ flux when the direction of transfer was from gas to liquid. A reason for increased transfer would be an increase in the gradient of the driving force across the membrane. In our system, the liquid phase concentration is assumed to be constant but an increase in the gas flow rate will result in a lower average $CO_2$ concentration on the gas side, which will increase the driving force gradient for an increased transfer rate. Caution is therefore necessary to ensure constant gas flow rates while using the CEMS during the same experiment. In conclusion, the CEMS proved to be a useful tool for nondestructive, real-time monitoring of biofilm metabolic activity. Using this approach, it was shown that biofilms responded rapidly to changes in nutrients and temperature. The nondestructive nature of this approach renders it appropriate to accurately and rapidly assess the influence of other environmental conditions on overall biofilm activity, including antimicrobials, nutrient limitation, and microbial community interactions such as predation, competition for a finite substrate, or cooperation to utilize recalcitrant molecules. This approach should therefore not be limited to pure cultures and defined laboratory media; it also provides a measured parameter ($CO_2$ production as a measure of biofilm activity) with a potential application in mathematical models. In the current research, the CEMS made it possible to determine carbon channeling by biofilm cells, showing that a small fraction ($<5\%$) of the influent carbon is retained in the biofilm, which is a relatively small investment, enabling the biofilm to serve as a catalytic unit to transform carbon from the surrounding environment.

# Chapter 3*

# Metabolic differentiation in biofilms as indicated by $CO_2$ production rates

*This chapter has been published as: Bester, E.; Kroukamp, O.; Wolfaardt, G. M.; Boonzaaier, L. and Liss, S. N. Metabolic differentiation in biofilms as indicated by carbon dioxide production rates. *Applied and Environmental Microbiology*, 2010, **76**, 1189–1197

(The experiments were designed and performed in equal measure by O. Kroukamp and E. Bester. O. Kroukamp developed and described the theoretical model for the quantification of the carbon dioxide evolution rates in consultation with L. Boonzaaier. Data analysis and interpretation were done by O. Kroukamp and E. Bester. Writing was completed in consultation with the co-authors.)

# 3. Metabolic differentiation in biofilms as indicated by $CO_2$ production rates

## 3.1. Abstract

The measurement of carbon dioxide production rates as an indication of metabolic activity was applied to study biofilm development and response of *Pseudomonas* sp. biofilms to an environmental disturbance in the form of a moving air-liquid interface (i.e., shear). A differential response in biofilm cohesiveness was observed after bubble perturbation, and the biofilm layers were operationally defined as either shear-susceptible or non-shear-susceptible. Confocal laser scanning microscopy and image analysis showed a significant reduction in biofilm thickness and biomass after the removal of the shear-susceptible biofilm layer, as well as notable changes in the roughness coefficient and surface-to-biovolume ratio. These changes were accompanied by a 72% reduction of whole-biofilm $CO_2$ production; however, the non-shear-susceptible region of the biofilm responded rapidly after the removal of the overlying cells and extracellular polymeric substances (EPS) along with the associated changes in nutrient and $O_2$ flux, with $CO_2$ production rates returning to preperturbation levels within 24 h. The adaptable nature and the ability of bacteria to respond to environmental conditions were further demonstrated by the outer shear-susceptible region of the biofilm; the average $CO_2$ production rate of

cells from this region increased within 0.25 h from 9.45 $\pm$ 5.40 fmol of $CO_2 \cdot cell^{-1} \cdot h^{-1}$ to 22.6 $\pm$ 7.58 fmol of $CO_2 \cdot cell^{-1} \cdot h^{-1}$ when cells were removed from the biofilm and maintained in suspension without an additional nutrient supply. These results also demonstrate the need for sufficient monitoring of biofilm recovery at the solid substratum if mechanical methods are used for biofouling control.

## 3.2. Introduction

Spatial differences in biofilm cohesiveness have been observed after the application of increased shear forces. Coufort et al. (2007) subjected both aerobic and anaerobic biofilms, cultivated on ethanol or wastewater, to increased shear stress and found that the biofilm layer at the bulk liquid interface was removed by slight increases in shear rates (0.2 Pa), whereas the middle and base biofilm layers were able to resist removal when exposed to up to 2 Pa and 13 Pa, respectively (Coufort et al., 2007). Total organic carbon (TOC) analyses indicated that the sensitive top layer of the biofilm contained approximately 60% of the total biofilm biomass while the remaining two layers each represented approximately 20%. In a follow-up study, biofilms grown under similar conditions exhibited comparable degrees of heterogeneity in the susceptibility of the various biofilm layers to shear and abrasion (Derlon et al., 2008). It was also indicated that the basal biofilm layer contained active microorganisms, as characterized by oxygen uptake rates, but no details were provided on the methodology or time lapse after the removal of the less-cohesive upper biofilm layers.

Spatial differentiation in metabolic activity in biofilms has also been noted. Most experimental strategies to determine biofilm activity have been centered on microscopy in combination with fluorescent reporter genes or probes that target various indicators of physiological activity in the cell. Several fluorescent stains have been applied previously,

such as 5-cyano-2,3-ditolyl tetrazolium chloride (CTC) (Huang et al., 1995) and acridine orange (Wentland et al., 1996) as well as the commercially available Bac-Light viability kit (Korber et al., 1997). Reporter gene expression is another means to evaluate physiological activity in a biofilm. Alkaline phosphatase activity correlated well with oxygen penetration into the upper layers (30 $\mu$m) of 117– to 151–$\mu$m thick biofilms (Werner et al., 2004). Although all of the above approaches have been shown to be effective, most suffer from inherent disadvantages (Stewart and Franklin, 2008), including incomplete penetration of fluorescent stains and the production of artefacts, and, perhaps most significantly, generally allow only end point analysis due to cellular toxicity. Reporter gene technologies may circumvent this problem but require prior genetic manipulation, and it is unknown what, if any, changes in cell physiology may occur as a result of expression of the reporter gene. The need for genetic manipulation further constrains analysis to pure culture studies.

The basis for spatial heterogeneity in biofilm physiological activity is widely accepted, as previously reviewed (Spormann, 2008; Stewart and Franklin, 2008). Limited diffusion of nutrients and oxygen into the biofilm from the bulk liquid and waste products from a multilayered biofilm are among the simplest explanations since the absence of a complete exchange with the environment, in concert with microbial activity, leads to the formation of chemical gradients in the biofilm. The bacteria in the biofilm respond to the gradients, likely by altering gene expression patterns as determined by global regulators. The remarkable recalcitrance of biofilms toward many antimicrobials may in part be due to the insensitivity of dormant cells in the regions of the biofilm where limited diffusion reduces metabolic activity.

The effect of air bubbles on biofilm stability has mostly been studied in a dental context, where biofilm removal is the goal. Gómez-Suárez et al. (2001) utilized a single bubble to investigate the strength of bacterial cell adhesion to various surfaces (Gómez-Suárez et al., 2001). According to the authors, the probability of cell detachment due to the movement

of an air bubble over an attached cell is determined by several factors, namely, collision efficiency, bubble-bacteria attachment efficiency, and the stability of the bubble-bacteria aggregate. For a bubble spanning the entire width of a flow chamber, the collision efficiency is expected to be equal to 1 although the velocity of the bubble may also influence the detachment efficiency since a rapidly moving bubble will result in a thicker liquid film surrounding the bubble, which in turn decreases the collision efficiency. Bacterium-substratum adhesion forces of $\sim 10^{-9}$ N were estimated, which is significantly smaller than the detachment force of a bubble moving over an attached cell (up to $10^{-7}$ N).

Liquid flow in most environments-in nature, industry, and clinical or dental settings - typically shows much variation. It can be expected that microbial biofilms have evolved to manage this variability and even to utilize the resulting differences in flow to optimize activity (e.g., the prevention of excessive biomass accumulation for the maintenance of optimum gradients of nutrients and gases) or to relocate to more favourable environments. Furthermore, increased shear is a recognized strategy to remove unwanted microbial growth from surfaces; therefore, methods to measure the effect of shear on biofilms, including biofilm recovery after partial shear-induced removal, should contribute to our overall understanding of this important form of microbial existence. We developed an approach that measures $CO_2$ production as an indication of biofilm activity in real-time and combined this method with confocal laser scanning microscopy (CLSM) and cell yield measurements to study activity-structure relationships in biofilms. This approach is an extension of the one we described in 2009 (Kroukamp and Wolfaardt, 2009) and enables us to comment on differences in metabolic activity of the whole biofilm versus that of the shear-susceptible biofilm region and to compare biofilm-derived planktonic cells with those growing in batch culture.

## 3.3. Materials and methods

### 3.3.1. Strain and culture conditions.

Pure culture biofilms of *Pseudomonas* sp. CT07 (Bester et al., 2005), labeled with the green fluorescent protein as previously described (Bester et al., 2009), were cultivated in flow cells under continuous flow of a sterile, defined growth medium [final concentrations of 1.51 mM $(NH_4)_2SO_4$, 3.37 mM $Na_2HPO_4$, 2.20 mM $KH_2PO_4$, 179 mM NaCl, 0.1 mM $MgCl_2 \cdot 6H_2O$, 0.01 mM $CaCl_2 \cdot 2H_2O$, and 0.001 mM $FeCl_3$] (Clark and Maaløe, 1967) with 5 mM sodium citrate as the sole carbon source.

### 3.3.2. Continuous-flow culture of biofilms.

#### 3.3.2.1. Experimental setup.

Multichannel flow cells were milled from Plexiglas, as previously described (Wolfaardt et al., 1994), with individual chamber dimensions of 7.22 mm by 3.00 mm by 60.0 mm (width, depth, and length, respectively). A glass coverslip was attached to the flow cell with silicone adhesive and served as the primary attachment surface for microscopic studies. The flow chambers were connected to growth medium reservoirs with silicone tubing (inner diameter, 1.58 mm), and Watson-Marlow 205S peristaltic pumps supplied the growth medium to the biofilm at a constant flow rate ($F_l$) of 37.5 ml $\cdot$ $h^{-1}$ or a linear velocity of 0.47 mm$\cdot$ $s^{-1}$ (Reynolds number of 2.00; shear rate of 3.58 $s^{-1}$).

#### 3.3.2.2. Disinfection and inoculation

The system was disinfected after assembly with a 1 in 10 dilution of a commercial bleach solution in distilled $H_2O$ ($dH_2O$) for 2 h, followed by continuous irrigation with sterile $dH_2O$ for a minimum of 15 h. The $dH_2O$ was displaced with sterile growth medium for 20

min before the flow was stopped, and each chamber was inoculated with 0.2 ml of a *Pseudomonas* sp. CT07::*gfp*-2 preculture using a sterile needle and syringe. The flow of medium was resumed after 30 min. Since the medium dilution rate in the flow chambers (28.47 $h^{-1}$) significantly exceeded the maximum specific planktonic growth rate ($\mu_{\text{max planktonic}}$) of *Pseudomonas* sp. CT07::*gfp*-2 in the 5 mM citrate medium ($\mu_{\text{max planktonic}}$, $0.35 \pm 0.05\ h^{-1}$ for six replicate batch cultures), it was concluded that planktonic cell replication did not contribute to the effluent cell numbers; i.e., microbial cells in the flow cell effluent originated from the attached biofilm.

#### 3.3.2.3. Experimental conditions and perturbation

Biofilms were cultured in multiple flow chambers (n = 9) for 8 days. Various parameters were investigated at 24-h intervals, including biofilm $CO_2$ production and total and viable biofilm-derived cell numbers in the effluent (n = 6). The extent of biofilm formation on the glass coverslip was investigated in three additional flow chambers with CLSM. After 5 days of incubation, a single air bubble was introduced into all of the flow chambers to remove the shear-susceptible fraction of the biofilm. Each bubble was generated by disconnecting the silicone tube from the growth medium reservoir upstream of the peristaltic pump. An air bubble, large enough to fill the entire flow chamber volume, was introduced at a linear flow rate of 0.47 $mm \cdot s^{-1}$, as controlled by the pump head, and allowed to move through the chamber. The flow cell was tilted vertically with the inlet at the top to ensure that the air bubble spanned the entire chamber cross-section and contacted all sides as it traveled through the chamber. The displaced biofilm material (containing the shear-susceptible biofilm region as well as the bulk liquid) was clearly visible as a slimy, milky-white layer ahead of the bubble, which increased in size as the bubble sheared off the attached biomass as it moved through the chamber before the biomass was collected at the outlet for subsequent analyses. After collection, the up- and

downstream tubing were reconnected, and six of the flow chambers were refilled with medium to measure recovery over 2 to 3 days (three flow chambers for $CO_2$ production and effluent cell number enumeration and three flow chambers for CLSM). Cells from the non-shear-susceptible biofilm (i.e., the biomass that resisted shear removal) in the three remaining flow chambers were removed by sonication, and the cell numbers were determined using direct microscopy.

### 3.3.3. Viable and total cell counts

Effluent from two of the six chambers was collected directly from each chamber outlet, after the downstream tubing was disconnected, for serial dilution in sterile saline (0.9% NaCl) and spread-plating onto agar plates containing the 5 mM citrate defined medium to confirm bacterial viability in the effluent. Approximately 1.5 ml of effluent was collected directly from each chamber outlet (n = 6) and preserved for subsequent microscopic enumeration of total cell numbers by the addition of formaldehyde to a final concentration of 2.0% (vol/vol), followed by vortexing and storage at 4°C (Hobbie et al., 1977). Each sample was diluted in sterile saline to achieve a minimum of 20 cells per microscope field after incubation with the fluorescent nucleic acid stain 4',6-diamidino-2-phenylindole (DAPI; final concentration of 5 $\mu g \cdot ml^{-1}$) for a minimum of 20 min in the dark. Five milliliters of the stained, diluted sample was vacuum filtered onto a 0.2-$\mu$m-pore-size black, polycarbonate filter (25-mm diameter; Nuclepore, Whatman) before each filter was mounted onto a glass slide; a coverslip was fixed into place with a drop of Citifluor antifade mounting medium AF2 (catalogue number 17971-25; Electron Microscopy Sciences). Each filter was examined with a 63 $\times$ oil immersion lens (Plan Apochromat 63 $\times$ /1.4) with a Zeiss Axiovert 200M inverted epifluorescent microscope (Zeiss), and 40 to 50 images of microscope fields were captured at random from each filter and used for digital image analysis. The number of cells in each microscope field was determined with image analysis after

a threshold was determined manually with Scion Image for Windows (Scion Corporation and the public-domain NIH Image program [http://rsb.info.nih.gov/nih-image/]), using digital imaging filtering steps as previously described (Massana et al., 1997).

### 3.3.4. Dispersion of shear-susceptible and base biofilm layers

The bubble-displaced content of each flow chamber was collected as described, and the volume was determined (approximately 1.3 ml). This fraction contained liquid medium, single (i.e., nonaggregated) biofilm-derived planktonic cells, and the shear-susceptible portion of the biofilm biomass. In order to enumerate the number of cells in these samples, it was necessary to disperse the cells from the biofilm matrix. Methanol was added to each sample to a final concentration of 1% (vol/vol), followed by sonication in an ultrasonic cleaner (Elma Ultrasonic LC20/H) at 35°C at 35 kHz for 15 min (Lunau et al., 2005). The samples were preserved by the addition of formaldehyde and stored prior to enumeration by direct fluorescent counting as described previously.

The number of cells in the non-shear-susceptible biofilm layer that remained in the flow chambers after the bubble perturbation was also enumerated by direct counting. Three of the emptied flow chambers were filled with 1% methanol, sealed, and sonicated as described previously. After sonication, the content of each chamber was collected in a microcentrifuge tube with repeated up and down pipetting to aid in the removal of biomass from the surfaces. Each chamber was filled with methanol for a second time and sonicated, and the contents were collected to determine the removal efficiency of the first sonication step; analysis of the results indicated that the second sonication step removed 2 orders of magnitude fewer cells than the first, which showed that the first removal step was effective. These samples were preserved in the same manner as the shear-susceptible samples prior to direct fluorescent counting.

### 3.3.5. CLSM and COMSTAT

The extent of biofilm formation in three independent flow chambers was examined daily using a Zeiss CLSM microscope with a 20× Plan Apochromat objective and excitation from a 488-nm argon laser. The fluorescence emitted by the *gfp* protein was detected with a long-pass 505-nm filter. Ten microscope fields (area of 0.002 $cm^2$) were chosen at random along a central transect ranging from the chamber inlet to outlet, and a stack of images was captured in the Z direction with the Zeiss LSM 510 software (version 3.2 SP2) for subsequent image analysis. Each Z image stack was exported from the Zeiss LSM Image Browser (version 4.2.0.121) as a raw series of single images and converted to gray-scale tagged-image file format (TIF) files with the freeware IrfanView (version 4.10) for analysis with the COMSTAT program (http://www.im.dtu.dk/comstat), which runs as a script in MatLab, equipped with the Image Processing Toolbox (Heydorn et al., 2000). Only a selected number of the COMSTAT functions were used for the analysis of the biofilm: the biovolume of each image stack, expressed as the volume of biomass per substratum area ($\mu m^3 \cdot \mu m^{-2}$), the mean thickness of the biofilm ($\mu$m), the maximum thickness of the biofilm ($\mu$m), the biofilm surface-to-volume ratio ($\mu m^2 \cdot \mu m^{-3}$), and the dimensionless roughness coefficient, which is a product of biofilm thickness variability and provides a measure of structural heterogeneity.

### 3.3.6. CMR setup

The $CO_2$ production measurement reactor (CMR) consisted of a 20-ml serum vial equipped with a butyl rubber stopper containing four ports (one port each for inflowing liquid, outflowing liquid, inflowing gas, and outflowing gas), as well as a magnetic stirrer bar. All of the tubing connecting the flow cell, CMR, and the $CO_2$ gas analyzer consisted of Tygon, which has very low gas permeability. Sterile growth medium with or without dissolved $CO_2$ (for $k_l a$ determination) or flow cell effluent (to measure the steady-state biofilm $CO_2$

production rate) was delivered to the CMR at a constant flow rate ($F_l$ = 37.5 ml $\cdot$ $h^{-1}$) provided by a Watson-Marlow peristaltic pump. Air without $CO_2$ (grade TOC of <0.5 ppm of $CO_2$ Linde Canada) was bubbled through the liquid in the CMR at a constant gas flow rate ($F_g$ = 1,530 ml $\cdot$ $h^{-1}$) provided by a Watson-Marlow peristaltic pump. The gas flow rate was determined by volumetric displacement. Off-gas $CO_2$ was measured with an absolute, nondispersive, infrared LI-820 $CO_2$ gas analyzer (Li-Cor Biosciences, NE).

The CMR was situated downstream of the flow chambers (Fig. 3.1), which allowed the real-time, nondestructive measurement of the $CO_2$ produced by the whole biofilm as well as of the contributions of the shear-susceptible biofilm layer, the remaining base biofilm layer after the removal of the shear-susceptible layer, and the biofilm-derived planktonic cells exiting the flow cell in the effluent. The $CO_2$ production and contributions of the different biofilm fractions were measured in the gas phase using two different measuring regimes, namely, open- and closed-loop configurations.

### 3.3.7. Theory for open loop

Measurement of the total amount of $CO_2$ produced by an intact (in situ) biofilm growing in a flow cell was accomplished by using the CMR in an open-loop configuration (clamp 3 was closed, while clamps 1, 2, and 4 remained open, as shown in Fig. 3.1). A $CO_2$ mole balance over the flow cell at steady state (with no accumulation) can be written as follows:

$$\begin{aligned} 0 &= \text{mol of } CO_2 \text{ into flow cell - mol of } CO_2 \text{ out of flow cell} \\ &\quad + \text{mol of } CO_2 \text{ generated within flow cell} \\ &= c_{FC,in} \cdot F_{l,FC,in} - c_{FC,out} \cdot F_{l,FC,out} + \text{CER}_{FC} \\ &= c_{FC,in} \cdot F_{l,FC,in} - c_{A,CMR,in} \cdot F_{l,FC,out} + \text{CER}_{FC} \end{aligned} \tag{3.1}$$

where $F_{l,FC,in} = F_{l,FC,out}$ is the liquid flow rate into and out of the flow cell, respectively (liter $\cdot$ h$^{-1}$), $c_{FC,in}$ is the $CO_2$ concentration in the sterile liquid medium entering the flow cell ($\mu$mol of $CO_2$ $\cdot$ liter$^{-1}$ of liquid medium), $c_{FC,o}$ is the $CO_2$ concentration exiting the flow cell and serves as the feed to the CMR (this assumes that all of the $CO_2$ produced in the flow cell reached the CMR since the connecting Tygon tubing is highly impermeable to $CO_2$ thus recognizing that $c_{FC,out} = c_{A,CMR,in}$), and $CER_{FC}$ is the $CO_2$ production rate ($\mu$mol of $CO_2$ $\cdot$ h$^{-1}$) of all microbial cells within the flow cell (sum of $CO_2$ contributions from all three in situ biofilm fractions, namely, the biofilm-derived planktonic cells and the shear-susceptible and base biofilm layers).

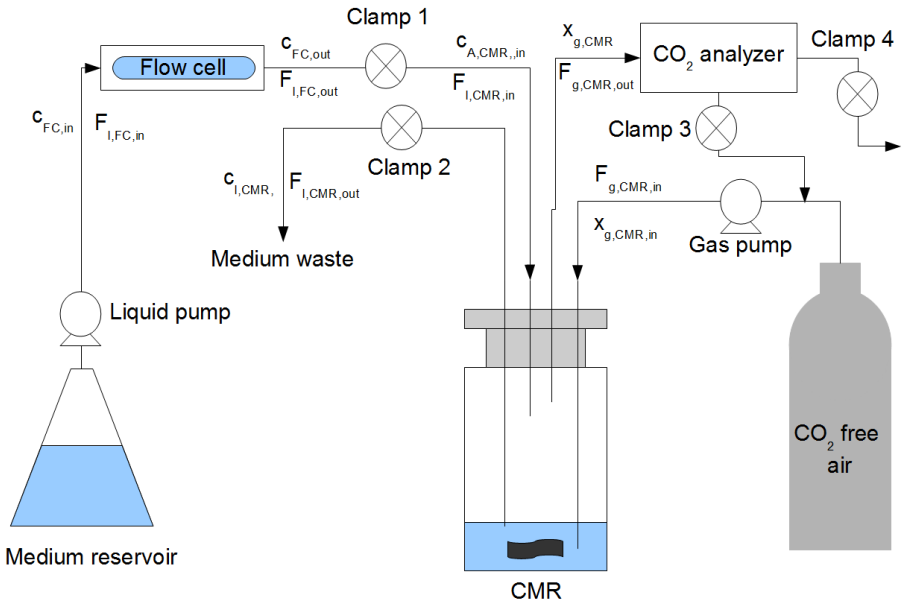


**Fig. 3.1.** A schematic diagram of the experimental setup showing the flow cell and the CMR

For a gas that does not interact with the liquid phase, the gas mole balance across the CMR can be written as:

$$V_l \frac{\partial c_{l,CMR}}{\partial t} = F_{l,CMR,in} \cdot c_{l,CMR,in} - F_{l,CMR,out} \cdot c_{l,CMR} + k_l a \left(c_l^* - c_{l,CMR}\right) V_l + CER_{CMR} \quad (3.2)$$

where $V_l$ is the liquid volume in the CMR (liter); $c_{l,CMR}$, is the dissolved gas concentration in the liquid phase in the CMR ($\mu$mol of gas$\cdot$ liter$^{-1}$ of liquid medium); $F_{l,CMR,in}$ is the liquid flow rate into the CMR (liters of liquid medium $\cdot$h$^{-1}$); $F_{l,CMR,out}$ is the liquid flow rate out of the CMR (liters of liquid medium$\cdot$h$^{-1}$) where $F_{l,CMR,in} = F_{l,CMR,out}$; $k_l a$ is the volumetric transfer coefficient (h$^{-1}$); $c_l^*$ is the concentration of gas in the liquid phase that is in equilibrium with the gas phase ($\mu$mol of gas$\cdot$liter$^{-1}$ liquid medium); and CER$_{CMR}$ is the gas produced in the system ($\mu$mol of $CO_2\cdot$h$^{-1}$).

Dissolved $CO_2$ interacts with water, however, and can convert to bicarbonate, carbonate, and carbonic acid, depending on environmental conditions such as the pH, temperature, and ionic strength of the solution (Schumpe et al., 1982). To accommodate the conversion of dissolved $CO_2$ to the bicarbonate ion under the experimental pH conditions, Bonarius et al. (1995) introduced $c_A$ as a term to include both of the forms of $CO_2$ in the liquid phase, i.e., the sum of the dissolved $CO_2$ ($c_{CO_2}$) and the bicarbonate ion ($c_{HCO_3}$), or $c_A = c_{CO_2} + c_{HCO_3}$ (Bonarius et al., 1995). The equilibrium constant, $K_1$, which relates the equilibrium of dissolved $CO_2$ and the bicarbonate ion

$$K_1 = \frac{c_{HCO_3^-} c_H}{c_{CO_2}}$$

can then be used to find a relationship between $c_A$ and $c_{CO_2}$:

$$c_{CO_2} = \frac{c_A}{1 + 10^{pH} + 10^{-pK_1}} \quad (3.3)$$

It should be noted that only the dissolved form of $CO_2$ can move cross the gas-liquid interface and be transferred to the gas phase (i.e., bicarbonate ions cannot). Therefore, at

steady state and a $CER_{CMR}$ of 0 ($CO_2$ produced by the biofilm-derived planktonic cells in the CMR from the effluent is negligible; see below), substituting equation 3.3 into equation 3.2 (taking the "transfer" of dissolved $CO_2$ to bicarbonate ions due to the pH range of the experiment into account) yields:

$$0 = F_{l,\text{CMR,in}} \cdot c_{l,\text{CMR,in}} - F_{l,\text{CMR,out}} \cdot c_{l,\text{CMR}} + k_l a_{CO_2} \left( \frac{c_A^*}{(1 + 10^{\text{pH}} + 10^{-\text{pK}_1})} - \frac{c_{A,\text{CMR}}}{(1 + 10^{\text{pH}} + 10^{-\text{pK}_1})} \right) V_l \tag{3.4}$$

A gas-phase $CO_2$ balance around the CMR yields:

$$\frac{P}{RT} V_g \frac{\partial x_{g,CMR}}{\partial t} = \frac{P}{RT} F_{g,\text{CMR,in}} \cdot x_{g,\text{CMR,in}} - \frac{P}{RT} F_{g,\text{CMR,out}} \cdot x_{g,\text{CMR}} - k_l a_{CO_2} \left( \frac{c_A^*}{(1 + 10^{\text{pH}} + 10^{-\text{pK}_1})} - \frac{c_{A,\text{CMR}}}{(1 + 10^{\text{pH}} + 10^{-\text{pK}_1})} \right) V_l \tag{3.5}$$

where $V_g$ is the headspace volume (liter), $F_{g,CMR,in}$ is the total gas volumetric flow rate into the CMR (liters of gas·$h^{-1}$),$F_{g,CMR,out}$ is the total gas volumetric flow rate out of the CMR ($F_{g,CMR,in} = F_{g,CMR,out}$), $x_{g,CMR,in}$ is the $CO_2$ concentration of gas flowing into the CMR (ppm; $\mu$l of $CO_2$ ·liter$^{-1}$ of total gas), $x_{g,CMR}$ is the $CO_2$ concentration in the gas phase in the CMR (ppm; $\mu$l of $CO_2$ · liter$^{-1}$ of total gas), $P$ is the pressure in the CMR (kPa), $R$ is the universal gas constant (liter· kPa·$K^{-1}$·$mol^{-1}$), and $T$ is the temperature of the gas in the CMR (in K).

At steady state and with $x_{g,CMR,in} = 0$ ($CO_2$ free air was used for gas flow), equation 3.5

becomes:

$$0 = -\frac{P}{RT} F_{g,\text{CMR,out}} \cdot x_{g,\text{CMR}} - k_l a_{CO_2} \left( \frac{c_A^*}{(1 + 10^{\text{pH}} + 10^{-\text{pK}_1})} - \frac{c_{A,\text{CMR}}}{(1 + 10^{\text{pH}} + 10^{-\text{pK}_1})} \right) V_l \tag{3.6}$$

Substituting equation 3.6 into equation 3.4 yields:

$$0 = F_{l,\text{CMR,in}} \cdot c_{l,\text{CMR,in}} - F_{l,\text{CMR,out}} \cdot c_{l,\text{CMR}} - \frac{P}{RT} F_{g,\text{CMR,out}} \cdot x_{g,\text{CMR}} \tag{3.7}$$

Considering the Henry's law relationship of $CO_2$ concentration in the gas phase in equilibrium with the liquid phase and equation 3.3 yields:

$$c_{CO_2}^* = \frac{\frac{P}{RT} \cdot x_{g,CMR}}{H} = \frac{c_A^*}{(1 + 10^{\text{pH}} + 10^{-\text{pK}_1})} \tag{3.8}$$

where $H$ is the dimensionless Henry's law coefficient (liter of liquid·liter$^{-1}$ of gas). Equation 3.6 and equation 3.8 yield:

$$c_{A,CMR} = \left(1 + 10^{\text{pH}} + 10^{-\text{pK}_1}\right) \left( \frac{P}{RT} \cdot x_{g,CMR} \right) \left( \frac{F_{g,CMR,out}}{k_l a_{CO_2} \cdot V_l} + \frac{1}{H} \right) \tag{3.9}$$

Substituting equation 3.9 into equation 3.7 yields:

$$c_{A,CMR,in} = \left(1 + 10^{\text{pH}} + 10^{-\text{pK}_1}\right) \left( \frac{P}{RT} \cdot x_{g,CMR} \right) \left( \frac{F_{g,CMR,out}}{k_l a_{CO_2} \cdot V_l} + \frac{1}{H} \right) + \frac{P}{RT} \frac{F_{g,\text{CMR,out}}}{F_{l,CMR}} x_{g,\text{CMR}} \tag{3.10}$$

By substituting equation 3.10 into equation 3.1, it is possible to determine the $\text{CER}_{FC}$ ($CO_2$ contribution from all of the biomass fractions in the flow cell). The $CO_2$ contribution of the base layer was determined by solving equation 3.1 after the bubble had removed the

shear-susceptible biofilm layer, and the $CO_2$ contribution of the shear-susceptible layer was calculated as the difference between the total biofilm $CO_2$ production and the base layer. To determine the $CO_2$ contribution of the shear-susceptible biofilm fraction and the planktonic cells (i.e., biofilm-derived planktonic cells as well as planktonic cells harvested during exponential growth in batch culture), the CMR was used in a closed-loop configuration (clamps 1 and 2 were closed after a known volume of effluent was pumped into the CMR, followed by closure of clamp 4; clamp 3 remained open with no flow from the compressed $CO_2$free air tank) (Fig. 3.1).

### 3.3.8. Theory for the closed loop

In the closed-loop (batch) system, the total amount of $CO_2$ at a specific time was considered a combination of the $CO_2$ in the liquid and gas phases (Chai et al., 2008):

$$m_t = c_{A,CMR} V_l + x_{g,CMR} \frac{P}{RT} V_g \tag{3.11}$$

where $m_t$ is the number of the moles of $CO_2$ in the system at time $t$. In the closed loop it is assumed that the $CO_2$ in the liquid phase is in equilibrium with the gas phase, similar to equation 3.8 (Dřímal et al., 2006):

$$\begin{aligned} m_t &= (1 + 10^{\mathrm{pH}} + 10^{-\mathrm{pK_1}}) \frac{\frac{P}{RT} x_{g,CMR}}{H} V_l + x_{g,CMR} \frac{P}{RT} V_g \\ &= x_{g,CMR} \frac{P}{RT} \left( (1 + 10^{\mathrm{pH}} + 10^{-\mathrm{pK_1}}) \frac{V_l}{H} + V_g \right) \end{aligned} \tag{3.12}$$

It can therefore be seen that the total amount of $CO_2$ in the closed vessel can be determined by measuring the $CO_2$ concentration only in the gas phase.

By measuring the total amount of $CO_2$ in the system at different time intervals, it is thus possible to determine a rate of $CO_2$ produced ($\mu$mol of $CO_2 \cdot h^{-1}$) by microbes in the CMR. During short time intervals (<10 min), the increase in total $CO_2$ of the system can

be attributed primarily to respiration and not to a significant increase in cell numbers.

## 3.3.9. Defining the essential parameters for the CMR

### 3.3.9.1. Determining the volumetric transfer coefficient ($k_l a$)

The $k_l a$ ($h^{-1}$) was determined using the static method, as described previously (Blanch and Clark, 1996), which involves solving both the gas and liquid mass balances for the CMR. Steady-state off-gas measurements were obtained for known dissolved gas concentrations ($c_{A,CMR,in}$) in the open-loop system configuration, and the $k_l a$ was calculated by rearranging equation 3.10.

Known concentrations of $CO_2$ were generated by agitating solid-state $CO_2$ pellets (dry ice) in the 5 mM citrate growth medium until saturation. This concentrated dissolved $CO_2$ solution was diluted in sterile growth medium to concentrations that resulted in off-gas readings similar to those obtained from the flow cell effluent. The concentration of dissolved $CO_2$ was determined by measuring the inorganic carbon content with a catalytic combustion, nondispersive infrared total carbon analyzer (TOC-VCSH/CSN; Shimadzu, Kyoto, Japan). Growth medium, without the addition of the dissolved $CO_2$ was used as a blank to determine the off-gas reading for growth medium equilibrated with atmospheric $CO_2$.

### 3.3.9.2. Determining the headspace volume ($V_g$)

Since the CMR system was assembled in the laboratory, it was necessary to determine the headspace ($V_g$, in liters) experimentally. A liquid-free CMR was prepared and flushed with $CO_2$free air until no $CO_2$ could be detected in the off-gas. Precise volumes of growth medium with known dissolved $CO_2$ concentrations, prepared as described above, were injected into the CMR, and the $CO_2$ in the off-gas was measured in the closed-loop system

configuration. Known concentrations of dissolved $CO_2$ allowed the determination of $V_g$ according to equation 3.12. (iii) Calculation of the dimensionless Henry's coefficient ($H$). The dimensionless Henry's coefficient ($c_{gas}/c_{liq}$; liters of gas/liters of liquid) for $CO_2$ was calculated to be 1.12 at 22°C with data from Schumpe et al. (1982) and corrected for the ionic strength of the growth medium (Schumpe et al., 1982). (iv) Open-loop calculations to determine steady-state whole-biofilm $CO_2$ production. Whole-biofilm $CO_2$ production rates were measured at 24-h intervals with the CMR in an open-loop configuration, i.e., continuous, once-through flowthrough of both the liquid and gas phases. Effluent exiting the flow cell entered the CMR at a known flow rate ($F_l$ = 37.5 ml·h$^{-1}$) while being sparged with $CO_2$ -free air as before ($F_g$ = 1,530 ml·h$^{-1}$). Equation 1 was used in conjunction with equation 10 to determine the $CO_2$ production of the in situ whole biofilm. The values for the various parameters were those applied during the $k_la$ determination, except that in this case the $c_{A,CMR,in}$ was calculated from the experimental steady-state gas phase $CO_2$ values captured during measurements by the off-gas analyzer. (v) Closed-loop calculations to determine $CO_2$ production of the shear-susceptible biofilm region and planktonic cells. The closed-loop method was selected as a means to distinguish the $CO_2$ produced by the whole biofilm (originating in the flow cell upstream of the CMR) and that produced by the biofilm-derived planktonic cells swept along by the exiting liquid flow, as well as the shear-susceptible biofilm fraction. The closed-loop method measures the increase in $CO_2$ in the CMR only as a result of respiring suspended cells collected in a known volume of flow cell effluent or bubble-displaced content. In contrast, an open-loop system measures dissolved $CO_2$ in the continuous-flow liquid, thus also measuring $CO_2$ that originated from biofilm cells upstream in the flow cell.

In the closed-loop configuration the liquid flow into and out of the CMR was halted, while continuous stirring of the liquid phase in the CMR was maintained by the magnetic stirrer. The gas was continuously circulated through the system via a peristaltic pump at

flow rate of 1,530 ml·h$^{-1}$. Prior to the closed-loop measurement, the flow cell effluent entered the CMR under open-loop conditions, with the liquid flowing through the CMR at a constant rate and $CO_2$free air being sparged into the liquid. After a steady-state off-gas $CO_2$ reading was obtained, the liquid flow was halted while the liquid continued to be flushed with the $CO_2$free air for 3 to 5 min to drive off the residual dissolved $CO_2$ that originated from the flow cell biofilm. The liquid in the CMR was subsequently sparged with ambient air until steady-state $CO_2$ off-gas readings were reached, after which the gas flow was closed, resulting in a continuous recirculation of gas in the headspace through the system. A linear increase in $CO_2$ measurements was recorded for at least 10 min or until the measurement exceeded the upper limit of the $CO_2$ analyzer (as in the case of the shear-susceptible layer responses, where the detection limit was exceeded after approximately 4.5 min). The $CO_2$ produced in the CMR was calculated by using equation 3.12 with parameters and variables as before and with $V_g$ as the headspace volume (in liters). The calculation involved the arbitrary choice of two $CO_2$ measurements ($x_{g0}$ and $x_{g1}$) at specific time points ($t_0$ and $t_1$).

It was shown that $CO_2$ production by the biofilm-derived effluent cells, when not concentrated, was below the closed-loop detection limit. This confirmed that the effluent cells produced a negligible amount of $CO_2$ relative to the biofilm, so there was no need to take this fraction into account for steady-state open-loop measurements. To measure the $CO_2$ contribution of planktonic cells exiting the flow cell, effluent from three 48- and 72-h-old biofilms was collected on ice for 1.5 h (approximately 160 ml), and the biofilm-derived effluent cells were concentrated by centrifugation at a relative centrifugal force (RCF) of 3,000 (5,000 rpm) for 20 min at 4°C. After the removal of the supernatant, the remaining cell pellets were resuspended in 3.3 ml of sterile growth medium, of which 3 ml was used to determine $CO_2$ production in the closed-loop configuration, and the remainder was used to determine the viable cell numbers after spread plating.

Planktonic batch cultures were incubated until the exponential phase of growth (as monitored by optical density measurements at 600 nm), prior to the harvesting of cells by centrifugation and resuspension as described for the biofilm-derived effluent cells. The viable cell numbers and $CO_2$ production rate for a fixed volume of this suspension were determined in addition to values for an original batch sample and a 1 in 10 dilution of the latter. The centrifugation and resuspension steps taken in preparation of the batch culture samples were found not to influence the $CO_2$ production rate per cell number for the various batch culture samples (correlation of $R^2$ = 0.998 between the amount of $CO_2$ produced per cell number for the various dilutions of exponential phase cells).

### 3.3.10. Statistical analysis

Statistical analysis of replicate measurements (for $CO_2$ production rates, direct cell counts, and biofilm parameters) was performed with analysis of variance (ANOVA) and Tukey's test for comparison of means (P = 0.05).

## 3.4. Results

### 3.4.1. Validation of the experimental system

The steady-state $CO_2$ ($x_g$; $\mu$l of $CO_2$ ·liter$^{-1}$ of air) measured in the off-gas for the different dissolved $CO_2$ concentrations was highly linear ($R^2$ = 0.997) and was within the range of the off-gas measurements taken during the subsequent experimentation. A $k_l a$ value of 21 h$^{-1}$ was calculated for the experimental setup described here. The influence of the gas flow rate on $k_l a$ measurements was also investigated, and lower gas flow rates were found to decrease the $k_l a$ value, which is in agreement with Blanch and Clark (1996).

For known dissolved $CO_2$ concentrations that had off-gas readings in a similar range

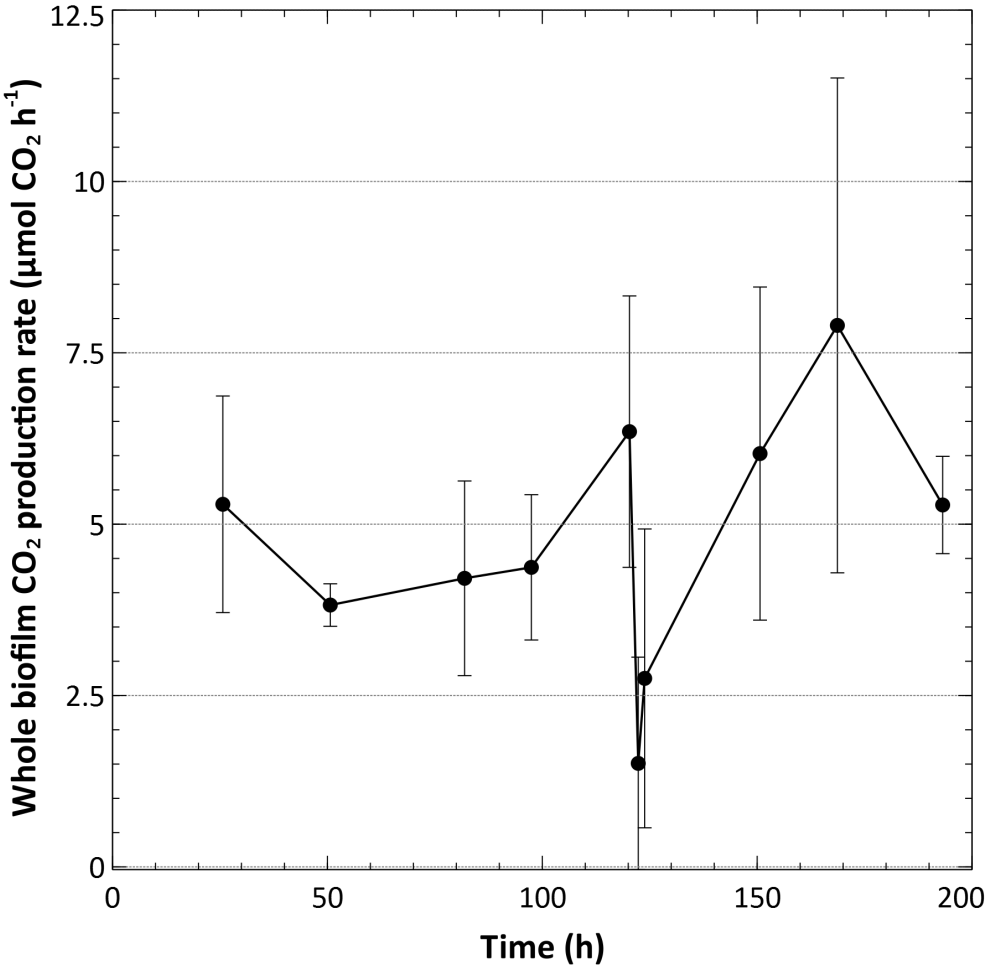


**Fig. 3.2.** The average whole-biofilm $CO_2$ production rate ($\mu$mol of $CO_2$ produced$\cdot h^{-1}$) as measured for six biofilms (24 to 120 h) and three biofilms (122 h and 124 to 192 h) using the open-loop system configuration. Up until 120 h, the average $CO_2$ production for six biofilms was determined. After the steady state measurement of the respiration rate was taken at 120 h, an air bubble was introduced into each flow cell to remove the shear susceptible biofilm region. Three of the biofilms were sacrificed at this stage, and open-loop measurements continued on the three remaining flow cells for a total of 192 h.

to the level of the whole biofilm, the open- and closed-loop configurations yielded results that were within 5% of each other. Both pH and $k_l a$ may have noticeable influences on the determination of dissolved $CO_2$ concentration from off-gas measurements using equation 3.10. In the current experimental system, the effluent pH (6.92) did not differ significantly from that of the sterile growth medium (pH 6.97). A common way to mea-

sure the $CO_2$ volumetric transfer coefficient is to use a linear relationship with the oxygen transfer coefficient, the latter being simpler to measure experimentally (Bloemen et al., 2003). Our results indicate (data not shown) that $kla_{CO2}$ was not constant with varying dissolved $CO_2$ concentrations and that therefore care has to be taken when determining $kla_{CO2}$ for the particular experimental conditions.

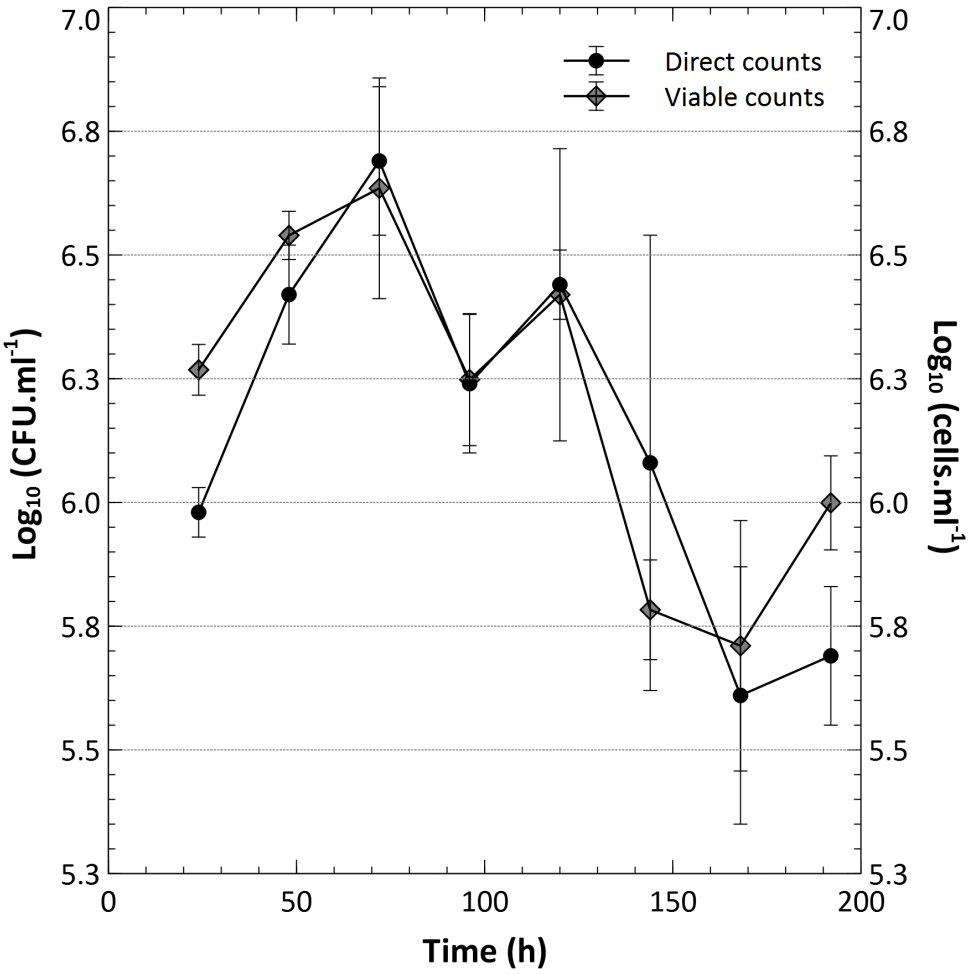


**Fig. 3.3.** The number of cells produced by the biofilms and released into the bulk liquid was enumerated from the flow cell effluent with direct fluorescent counts and plate counts by sampling the effluent at 24-h intervals (n = 6 biofilms from 24 to 120 h, and n = 3 biofilms from 144 to 192 h)

### 3.4.2. Steady-state whole-biofilm $CO_2$ production

Whole-biofilm $CO_2$ production rates were measured every 24 h for the first 120 h at 2 and 4 h after the bubble perturbation and thereafter again at 24-h intervals for the remainder of the experiment (Fig. 3.2) using the open-loop system configuration. Removal of the shear-susceptible region led to a significant reduction ($P < 0.05$) in the rate of $CO_2$ production in the flowcell; only 28% $\pm$ 29% of the predisturbance $CO_2$ production rate was maintained by the remaining non-shear-susceptible base biofilm layer 2 h after the perturbation (122 h of incubation). $CO_2$ production in these base biofilm layers recovered to 51% $\pm$ 41% of the previous steady-state production rate within 4 h after the removal of the shear-susceptible biofilm fraction and to 104% $\pm$ 42% after an additional 24 h. Interestingly, the postdisturbance rate of $CO_2$ evolution stabilized at a higher level than what was observed previously (136% $\pm$ 64% at 48 h after the bubble although this increase was not statistically significant at a P value of 0.05).

### 3.4.3. Biofilm-to-planktonic cell yield

In addition to respirometry, the number of free-floating cells produced and released into the effluent by the biofilms was determined with direct fluorescent counting and image analysis as well as viable cell counts (Fig. 3.3). Direct counting allowed the evaluation of the nature of the detached biomass (single cells versus matrix-encased clumps of cells) and facilitated comparison of the cell numbers in the shear-susceptible and base biofilm regions, respectively.

Microscopic examination of the effluent biomass prior to the introduction of the bubble and during biofilm recovery (24, 48, and 72 h subsequent to the removal of the shear-susceptible biofilm layer) indicated that single cells made up the majority of the biomass released from the biofilm as aggregates of matrix-encased cells were rarely present. The yield of cells from the biofilms initially decreased less than a log-fold (a significant de-

crease for the viable cell counts, but not the direct counts at a P value of $<0.05$) after the introduction of the bubble despite the fact that a significant fraction of the attached biomass was removed, as suggested by the reduction in the rate of $CO_2$ production after the bubble (Fig. 3.2) and shown by a series of representative CLSM micrographs of the biofilm taken over the course of the experiment (Fig. 3.4). Planktonic cell yield from the biofilm recovered to predisturbance levels after 168 to 192 h of incubation (48 and 72 h after the bubble disturbance; statistically there was no significant difference compared to 120 h, with a P value of 0.05).

### 3.4.4. Biofilm architecture

The bubble perturbation removed a large portion of the biofilm biomass at the glass surface; single cells and some aggregates (Fig. 3.4(f)), much smaller than before, were observed attached in isolated regions of the glass along the central transect while more extensive biomass survived the perturbation along the edge of the chamber (Fig. 3.4(g)), likely as a result of reduced shear forces in these areas. Image analysis was not performed at this point due to insufficient amounts of biomass at the area normally viewed (i.e., central transect) of the flow chambers. COMSTAT image analysis of the CLSM-acquired images provided information on biofilm architecture in terms of biofilm biomass, average thickness (Fig. 3.5A), roughness, and the surface area-to-biovolume ratio (Fig. 3.5B). At the magnification applied, CLSM allowed the observation only of the biofilms growing on the glass coverslips (35% of total surface area available for attachment). However, the observed biomass volume and the average biofilm thickness showed a similar trend as the whole-biofilm $CO_2$ production and did not reach a steady state in the first 120 h of cultivation.

Biofilm architecture at the glass surface was also significantly altered after the perturbation; the bubble-mediated removal of the shear-susceptible biofilm region resulted in

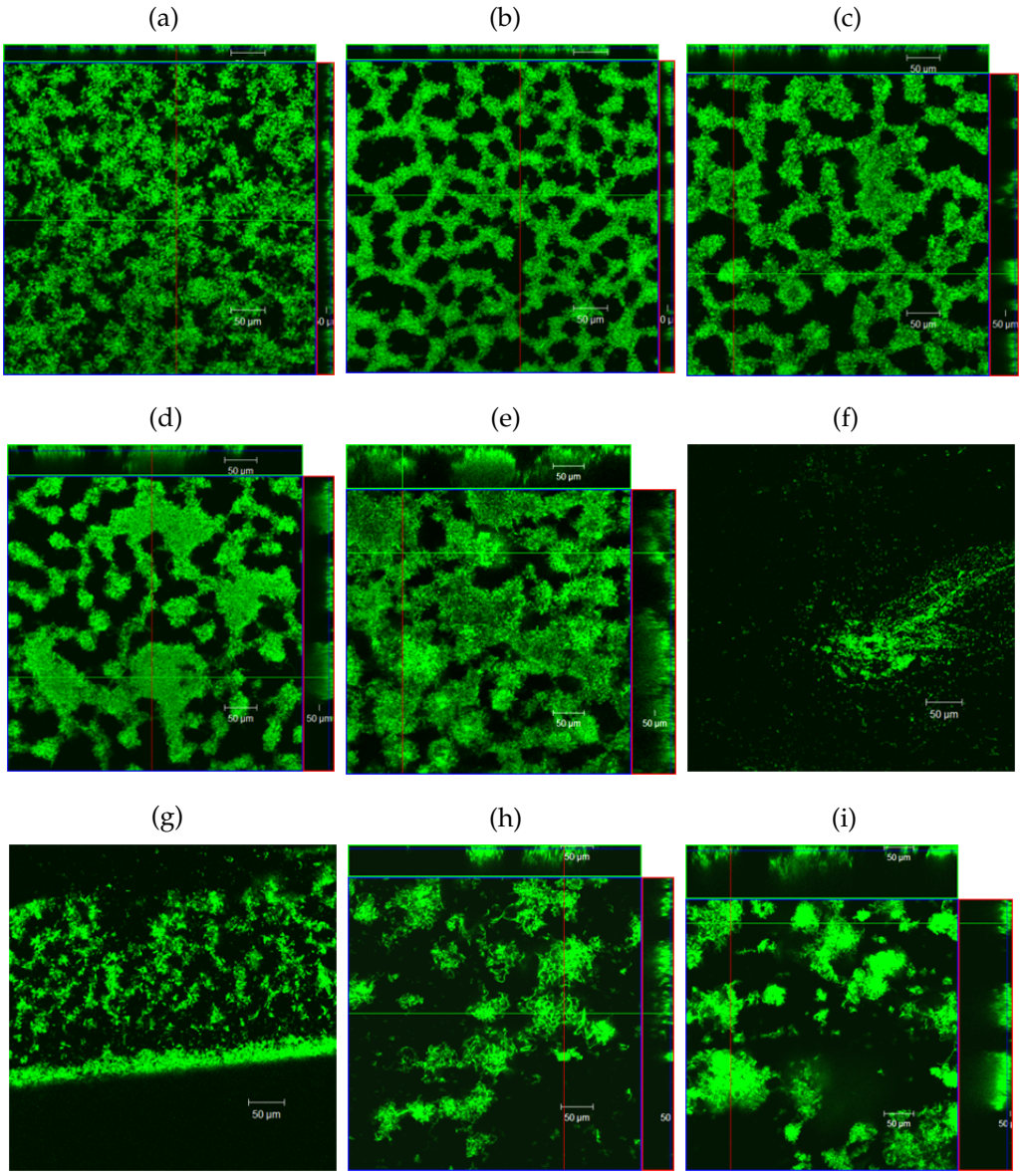


**Fig. 3.4.** Single CLSM micrographs taken at 24-h intervals at random locations of the *gfp*-labeled *Pseudomonas* sp. CT07 biofilms cultivated in conventional flow cells under continuous-flow conditions: 24 h (a), 48 h (b), 72 h (c), 96 h (d), and 120 h (e). (f) The single cells at the glass surface 1 h after the bubble perturbation. The biomass along the edge of the flow cell where the glass coverslip meets the Plexiglas is shown 1 h after the perturbation (g), 24 h after the perturbation (144 h) (h), and 48 h after the perturbation (168 h) (i). Micrographs shown in panels (f) and (g) were not included in the image analysis with COMSTAT

significant changes ($P < 0.05$) in all of the measured biofilm parameters at 144 h (24 h after the perturbation). Analysis of these parameters indicated that the biofilm was rougher

and had a larger surface area-to-volume ratio than the predisturbance biofilm at 120 h and that it consisted of less biomass and exhibited a reduced thickness compared to the predisturbance biofilm at 120 h (Fig. 3.5A and 3.5B). Biofilm biomass and the surface area-to-volume ratio at 144 and 168 h (24 and 48 h after the disturbance) recovered to the levels measured for the 72- and 24-h-old biofilms, respectively, while the mean biofilm thickness recovered to the values observed for a 96-h-old biofilm (P = 0.05). These observations, together with the increased steady-state $CO_2$ production and recovery of biofilm-to-planktonic cell yield, indicated that biofilms remained metabolically active during the first 48 h after the disturbance and that rebuilding of biofilm structure occurred soon after the disturbance.

### 3.4.5. Comparison of $CO_2$ production rates

The average rate of $CO_2$ production per cell was compared between planktonic cells in the exponential phase of growth, biofilm-derived effluent cells, the shear-susceptible biofilm layer (both in situ and in the CMR after removal), and the base biofilm layer (Fig. 3.6). The average cell number of the non-shear-susceptible base biofilm layer at 120 h was 4.84 $\times 10^8 \pm 1.94 \times 10^8$ while that of the shear-susceptible fractions was 6.91 $\times 10^8 \pm 2.47 \times 10^8$. Thus, approximately half of the bacterial cells were removed from the flow cell by the bubble perturbation while only 28% $\pm$ 29% of the pre-disturbance $CO_2$ rate of production was maintained by the remaining base biofilm after the bubble removal. Using the average cell numbers in the respective biofilm layers, it was possible to calculate the steady-state $CO_2$ production rates per cell, as indicated in Fig. 3.6.

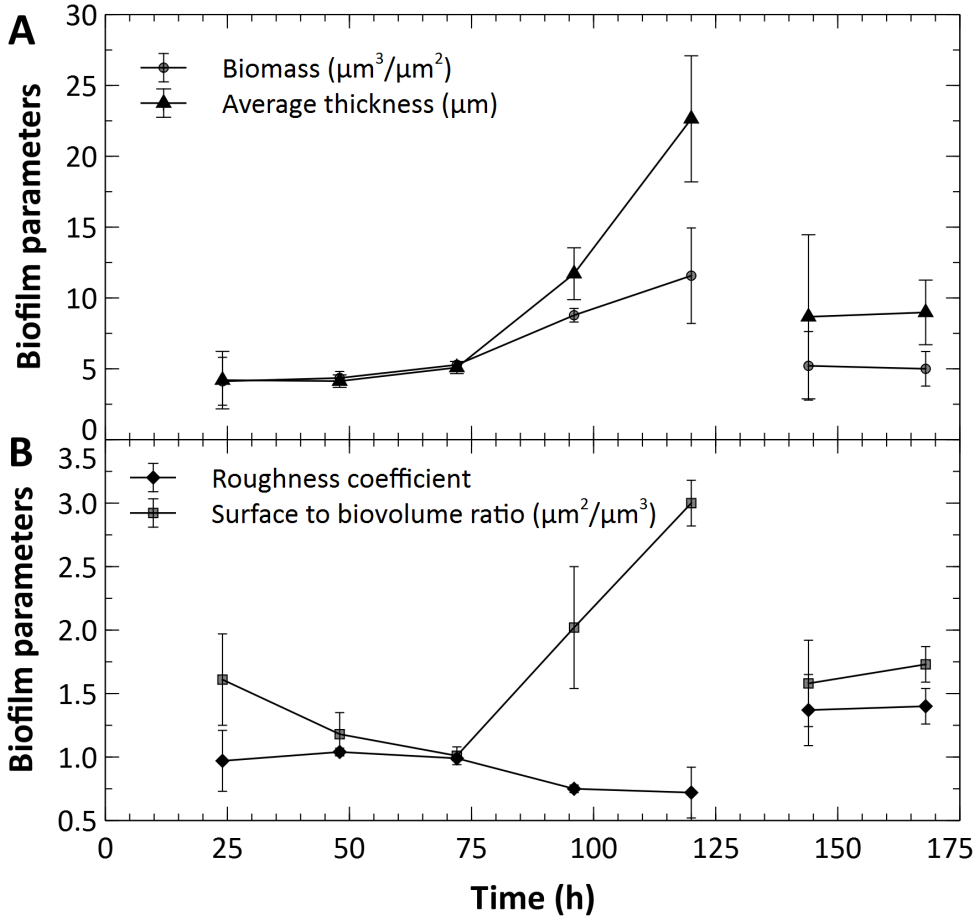


**Fig. 3.5.** COMSTAT image analysis of four biofilm parameters was averaged for three biofilms cultivated under the same conditions, as described previously. The average amount of biofilm biomass at the surface ($\mu m^3 \cdot \mu m^{-2}$) and average biofilm thickness ($\mu m$) are plotted in panel A, and the roughness coefficient and surface area-to-biovolume ratio ($\mu m^2 \cdot \mu m^{-3}$) are plotted in panel (B). The absence of sufficient biofilm biomass at the glass surface after the bubble perturbation at 121 h (Fig 3.4(f)) did not allow the capture of images suitable for analysis, and hence this data point could not be included.

## 3.5. Discussion

The goal of this investigation was not to measure the shear forces generated by the moving air bubble or the extent to which the *Pseudomonas* sp. CT07 biofilms can withstand different shear forces, as has been done previously (Coufort et al., 2007), but, rather, to selectively remove a region of the biofilm to evaluate biofilm metabolic response in

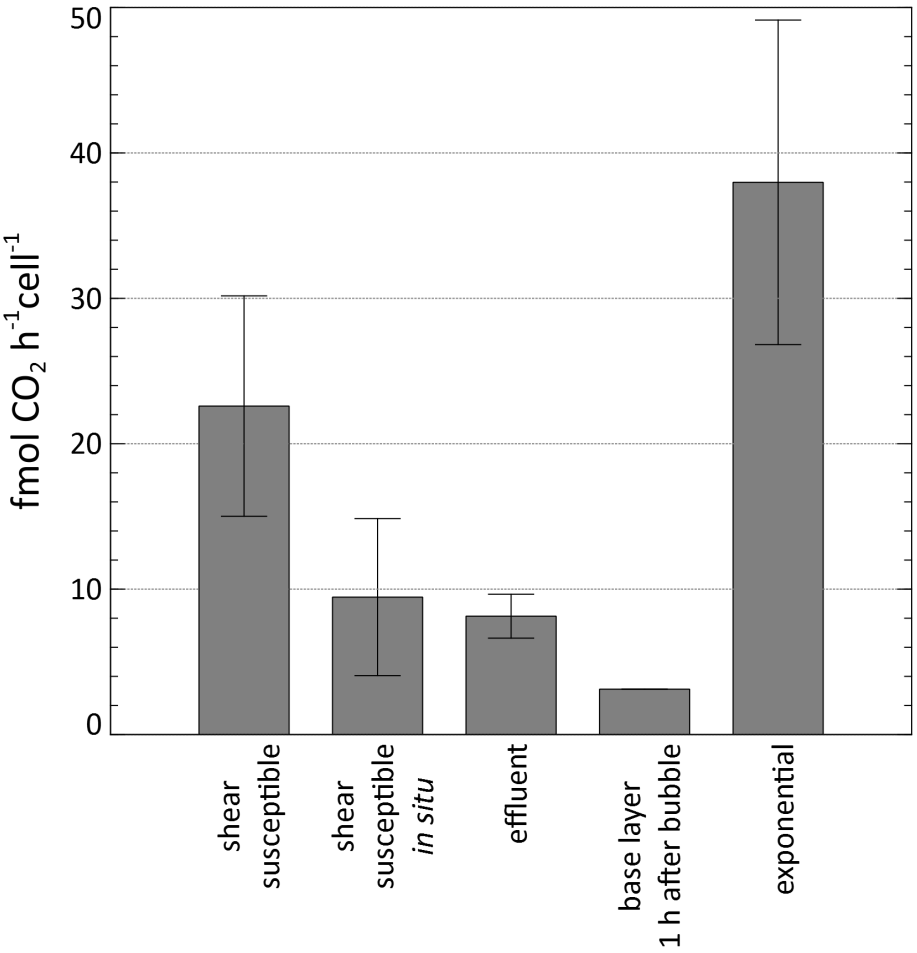


**Fig. 3.6.** The average rate of $CO_2$ production per cell was compared between planktonic cells in the exponential phase of growth, biofilm-derived effluent cells, the shear-susceptible biofilm, and the non-shear-susceptible base biofilm layer. Activity of the shear-susceptible biofilm layer was determined in situ (as part of the biofilm) and as suspended cells after removal from the biofilm.

terms of $CO_2$ production and biofilm-derived planktonic cell yield, as well as biofilm structural adaptation, by utilizing microscopy and image analysis. Other environmental perturbations, such as increased fluid shear, particle abrasion, or an antimicrobial challenge, could instead be utilized to achieve a similar outcome. The choice of an air bubble proved to simplify execution since it facilitated the quick and efficient removal of the shear-susceptible biofilm region for immediate downstream analysis of changes in $CO_2$ production rates, which was an important consideration in order to capture the

expected rapid response in microbial metabolism. This approach yielded reproducible results, as can be seen from the notably similar numbers of cells enumerated from the different shear-susceptible regions after dispersion (no statistically significant difference; P value of 0.05).

The results show that biofilm-derived single cells as well as the cells in the shear-susceptible biofilm layer (in situ) are metabolically less active-as indicated by a lower average $CO_2$ production rate on a per cell basis-than exponentially growing planktonic cells but more active than cells in the base biofilm layer 1 h after exposure to the bulk liquid after the removal of the shear-susceptible layer (Fig. 3.6). The quick increase in the $CO_2$ production rate by the base biofilm layer provides additional support for numerous suggestions that biofilm cells are less active (i.e., dormant, but not dead) for reasons such as diffusion limitation. The results indicate that the shear-vulnerable layer, which in this case contained half of the biofilm cells, produced 72% of the $CO_2$ in the system, which is consistent with previous indications of spatial heterogeneity in biofilm metabolic activity.

Werner et al. (2004) demonstrated stratification of active protein synthesis in *Pseudomonas aeruginosa* biofilms, where most of the activity was located at the bacterial colony-air interfaces, and at the biofilm-liquid interface for biofilms cultivated under continuous-flow conditions (Werner et al., 2004; Mangalappalli-Illathu et al., 2009). Rani et al. (2007) also reported on stratified DNA replication, protein synthesis, and respiratory activity in staphylococcal colonies (Rani et al., 2007). Moreover, these activities were found to be colocated at the biofilm-air interface (upper 31- to 38-$\mu$m layers) and the biofilm-nutritive substratum interface (14- to 16-$\mu$m layers) of 153- to 172-$\mu$m thick colonies. The authors identified four cell physiologies, namely, active aerobic growth, active anaerobic growth, nonactive or dormant but viable cells at the interior of colonies, and dead cells (approximately 10% of the total), and suggested that the dormant cells might regain activity if exposed to oxygen and/or nutrients. The average per cell $CO_2$ production rate of the shear-

susceptible layer, after removal from the biofilm, was found to be significantly higher than the in situ rate (P value of 0.05) (Fig. 3.6). This result demonstrates that biofilms possess a remarkable ability to not only respond rapidly to environmental changes but also retain a powerful metabolic capacity when access to nutrients and oxygen becomes unrestricted. Unlike persister cells that are apparently programmed primarily for survival (Keren et al., 2004b; Harrison et al., 2005a), the primary function of cells from this region is probably to optimize proliferation. It should be pointed out that the term ”persisters” usually refers to cells that can survive high antibiotic concentrations while the disturbance in the present study was shear. In contrast to the small percentage of persisters (less than 1% of the total biofilm population in *Escherichia coli* according to Harrison et al. (2005a)), we found that approximately 50% of the biofilm cells could withstand the applied shear in this case. An increase in shear would likely result in the removal of a greater percentage of biofilm biomass, but this was outside the scope of the current investigation. The increase in $CO_2$ production after the base layer was exposed (Fig. 3.2) indicates that, similar to the cells in the shear-susceptible region that rapidly increase their activity when transferred to a planktonic state, these previously dormant (or less active) cells can speedily respond to re-establish overall biofilm activity. The findings reported here are thus in agreement with previous indications of active microorganisms in the basal biofilm layer (Derlon et al., 2008).

Further applications of this approach may be useful in the study of biofilm form-function relationships. The rapid recovery of metabolic activity after the perturbation suggests that biofilms may, indeed, benefit from shear-related perturbations. The removal of excess biomass may facilitate the maintenance of biofilms with an optimized architecture to ensure maximal utilization of resources, as seen by the increase in biofilm roughness once the biofilm was exposed to the bulk liquid after the removal of the shear-susceptible biofilm layer. The increased roughness measured after the perturbation may facilitate

greater rates of nutrient and oxygen transfer to the biofilm, which is confirmed by the higher subsequent metabolic activity. Considering that relatively few real-world environments are bubble and turbulence free, such adaptation can be expected, even if it is not a requirement for survival. It is not known whether the cell distribution or EPS composition in the biofilm was altered in response to the shear-mediated removal of the susceptible layer, as has been observed for biofilms cultivated under higher flow rates (Pereira et al., 2002), and so we cannot speculate on whether the resulting biofilm could withstand subsequent changes in shear to a greater degree.

Finally, the approach described here overcame a number of the limitations associated with the methods available to measure biofilm metabolic activity, as described by Stewart and Franklin (2008). A notable improvement is that this approach is not dependent on fluorescent stains that are susceptible to incomplete penetration or to the cellular toxicity characteristic of many of these stains. The approach also overcomes the requirement of working with pure cultures that are amenable to genetic manipulation, typical of reporter gene technologies.

# Chapter 4*

# Nature of inoculum has a pronounced effect on biofilm development in flow systems

*This chapter has been published as: Kroukamp, O., Dumitrache, R. G. and Wolfaardt, G. M., Nature of inoculum has a pronounced effect on biofilm development in flow systems, *Applied and Environmental Microbiology*, 2010, **76**, 6025 – 6031
(Writing was completed in consultation with the co-authors.)

# 4. Nature of inoculum has a pronounced effect on biofilm development in flow systems

## 4.1. Abstract

Biofilm formation renders sessile microbial populations growing in continuous flow systems less susceptible to variation in dilution rate than planktonic cells, where dilution rates exceeding an organism's $\mu_{max}$ results in planktonic cell washout. In biofilm-dominated systems, the overall biofilm's $\mu_{max}$ may therefore be more relevant than the organism's $\mu_{max}$ where the biofilm $\mu_{max}$ is considered as a net process dependent on the adsorption rate, growth rate and removal rate of cells within the biofilm. Together with lag (acclimation) time, the overall biofilm's $\mu_{max}$ is important wherever biofilm growth is a dominant form, from clinical setting where the aim is to prevent transition from lag to exponential growth, to industrial bioreactors where the aim is to shorten the lag and rapidly reach maximum activity. The purpose of this study was to measure $CO_2$ production as indicator of biofilm activity to determine the effect of nutrient type and concentration, and origin of the inoculum on the length of the lag phase, biofilm $\mu_{max}$, and steady state metabolic activity of *Pseudomonas aeruginosa* PA01, *Pseudomonas fluorescens* CT07 and a mixed com-

munity. As expected, the different microorganisms have different length in lag phase of biofilm development and biofilm $\mu_{max}$, whereas different nutrient concentrations result in different lengths of lag phase and steady state values but not in different biofilm $\mu_{max}$ rates. The data further showed that inocula from different phenotypic origins give rise to different length in lag time, and that this influence persists for a number of generations after inoculation.

## 4.2. Introduction

Microbial growth in batch cultures has been studied for a long time and the observed phases designated as the lag phase, the acceleration phase, the exponential phase, the retardation phase, the stationary phase and the phase of decline although not each culture displays all of the mentioned phases (Monod, 1949). In contrast to batch cultures and static (no flow) biofilms (e.g. those that form in 96 well plates), the increase of biofilm cells in a flowing environment is a net process that is dependent on the irreversible adsorption rate of cells to the surface, the growth rate of the microorganisms and the removal rate of cells lost to the bulk flow (Mueller et al., 1992). There are numerous benefits for the cells in biofilms e.g. protection against antimicrobials, opportunity for and proliferation by continuous cell dispersion. There is also a possible competitive advantage if cells colonize surfaces at multiple sites and grow in such a manner that the resulting three-dimensional architecture will expose maximum biofilm surface area to surrounding nutrients. The most successful colonizers would therefore be the cells with the ability to adhere to the surface (and stay adhered) and start multiplying at maximum rate. The process of events from being free floating cells to the so-called permanently surface-attached phase involves early steps including reversible attachment and cells undergoing a phenotypic change from a planktonic state to a sessile state with the concomitant changes

in gene expression; these steps contribute to a lag phase that will occur before maximal growth / biofilm development can take place (Rice et al., 2000). Clearly, the ability to progress from the lag phase to a fast growing phase, including the duration of the lag phase, is an important determinant of biofilm function and has an impact in a diverse range of environments-often with implications to infection or contamination control, as well as industrial processes.

At the cell level, an extended lag phase and slower growth creates the risk of being displaced by faster growing micro-colonies as was demonstrated by Klayman et al. (2008) in dual species biofilms. A microorganism's competence in dominating a surface area can therefore be evaluated by comparing the lag phases and maximal growth rates of a biofilm growth curve. Knowing a bacterial population's specific growth rate is a requirement for its cultivation at optimum rates in a chemostat or other continuously-fed bioreactors. A key assumption for this type of cultivation is that wall growth has a negligible effect; which is in stark contrast to systems where surface associated growth dominates. Indeed, while dilution rates exceeding an organism's $\mu_{\max}$ results in cell washout in a conventional chemostat setting, biofilm formation enables microbial populations to persist at dilution rates much higher than the organism's $\mu_{\max}$.

Biofilm growth rates have been measured by various techniques such as fluorescence in situ hybridization (FISH) (Jang et al., 2005; Yang et al., 2008), the incorporation of radioactive substances like $^{3}$H thymidine and $^{32}$P (Freeman and Lock, 1993, 1995), microscopy (Bester et al., 2005; Klayman et al., 2008; Mueller, 1996) , measuring the total increase in biofilm mass (both cells and extracellular polymeric substances) (Richter et al., 2007; Tam et al., 2007), colorimetric XTT assays (Seneviratne et al., 2009) or measurement of amide II bands, as determined by attenuated total reflectance-Fourier transform infrared spectroscopy (Delille et al., 2007). Some of the above mentioned techniques suffer the drawback that the biofilms have to be sacrificed with sampling or otherwise that the measured

increases do not distinguish between live and dead matter in the biofilm (i.e. increases measured might not represent an accurate increase in viable cell numbers).

In this study a carbon dioxide evolution measurement device (CEMS) (Kroukamp and Wolfaardt, 2009) was used to track biofilm development rate in real time. The advantage of using this system is that the measured rates represent the metabolic activity of the active cell mass, and can be done non-destructively for any biofilm forming microorganism. In the past, measurement of oxygen uptake rates have been used for determination of growth rates in batch cultures (Novák et al., 1994) and localized growth rate in biofilms (Zhou et al., 2009). $CO_2$ measurements by a gas chromatograph have been used to determine growth rate in batch systems (Chai et al., 2008) but to our knowledge this is the first time that $CO_2$ measurements have been used to determine whole-biofilm specific growth rates. We applied this technique to compare biofilm $\mu_{max}$ for two well-described Pseudomonads and a mixed microbial community when grown on different nutrients, and to test the premise that the origin of inoculum has an impact on early biofilm development.

## 4.3. Materials and Methods

### 4.3.1. Strains and culture conditions:

An environmental isolate, *Pseudomonas* sp. strain CT07::*gfp*2 (a *P. fluorescens* (Wolfaardt et al., 2008) GenBank Accession No. DQ 777633) was used for the majority of the experiments. *Pseudomonas aeruginosa* PA01 *gfp* was used for comparison and validation of the approach. Plasmid construction and the protocol followed were described by Bester et al. (2009). The two strains were maintained on defined media agar plates with 5 mM citrate as the carbon source. A mixed microbial community was obtained from the drain of a sink in a public washroom. This community was maintained in 3 g/L Tryptic Soy Broth (TSB) (EMD Chemicals) broth at room temperature. In related research (Hota et al., 2009)

it was showed that multidrug resistant *Pseudomonas* biofilms persist in drain sinks; and demonstrated in the case of hospital intensive care units that poor facility design lead to the dissemination of the bacteria from these drain-biofilms during hand washing causing nosocomial infections and fatalities. We further demonstrated that *P. aeruginosa* PA01 effectively integrate into these biofilms (M. Ghadakpour et al., unpublished results) and were therefore interested in the current study to compare biofilm development rates of the communities with that of the test strains. Routine cultivation of the organisms was carried out on a modified AB medium with a final concentration of 1.51 mM $(NH_4)_2SO_4$, 3.37 mM $Na_2HPO_4$, 2.20 mM $KH_2PO_4$, 179 mM NaCl, 0.1 mM $MgCl_2{\cdot}6H_2O$, 0.01 mM $CaCl_2{\cdot}2H_2O$ and 0.001 mM $FeCl_3$ with different concentrations of sodium citrate as the sole carbon source (Clark and Maaløe, 1967). TSB was used as growth medium in various concentrations, as indicated. Pre-cultures from the stationary growth phase (grown overnight) or the exponential growth phase (confirmed with $OD_{600}$ measurements) used for inoculation of the biofilm reactors were incubated either in defined medium with 5 mM citrate or in 3 g/l TSB at 32 $\pm$ 3 °C and shaking at 250 rpm. The biofilm effluent cells used for inoculation were harvested from one week old biofilms grown at room temperature in 50 cm long silicone tube (inside diameter, 0.16 cm) reactors fed with 1mM citrate minimal medium at 15 ml/h. The cell numbers for each inoculation were determined by spread plate counting.

### 4.3.2. Biofilm cultivation:

Biofilms were cultivated in a continuous flow reactor system with growth media being supplied at 15 ml/h by a Watson Marlow 205U peristaltic pump with a corresponding residence time of 12 minutes given the following reactor dimensions (inside diameter, 0.16 cm; outside diameter, 0.24 cm; length 150 cm). The reactor was a $CO_2$ evolution measurement system (CEMS) (Kroukamp and Wolfaardt, 2009) that allows the continuous

online measurement of $CO_2$ in the gaseous phase. It was shown that the $CO_2$ measured in the gas phase has a direct correlation with the dissolved $CO_2$ in the liquid phase (at the physiological $CO_2$ concentrations under investigation) and can therefore be used as a reliable indication of active cell mass in the reactor during the early stages of biofilm development (Kroukamp and Wolfaardt, 2009). In essence, the reactor comprises of a $CO_2$ and $O_2$ permeable silicone tube, housed in an outer shell of gas impermeable Tygon tubing. $CO_2$ produced by the biofilm growing on the inside of the silicone tube cross the silicone tube wall into the annular space between the Tygon and silicone tubes. The annular space is connected to an absolute, non-dispersive, infrared LI-820 $CO_2$ gas analyzer (LI-COR Biosciences, NE), and compressed $CO_2$free air (TOC grade, $CO_2 < 0.5$ ppm, CO $< 0.5$ ppm, $O_2$ 20 – 22 % and THC $< 0.1$ ppm, Linde, Canada) is used as the sweeper gas at rates that varied from 1.5 – 2.3 l/h. Gas flow rates were determined by volumetric displacement. The CEMS were submerged in a water bath that was kept at 27 °C for all experiments. The CEMS was inoculated with 200 $\mu$l pre-culture under no-flow conditions. The cells were allowed to attach to the reactor tube wall for 30 minutes where after growth medium flow was resumed.

### 4.3.3. Growth rate measurements in CEMS:

Considering that during the early stages of biofilm development the environmental conditions in the reactor are not changing (with regards to pH, nutrient concentration and temperature), the $CO_2$ production rate can be used as an indication of active cell numbers at a specific time (in contrast with respiration rates of a fixed number of cells that may vary due to environmental changes). A biofilm growth rate ($\mu_{\text{biofilm}}$) was obtained by determining the slope of the natural logarithm of $CO_2$ production rate plotted against time:

$$\mu_{\text{biofilm}} = \frac{\ln X_{t_2} - \ln X_{t_2}}{t_2 - t_1}$$

where $X_{t2}$ is the $CO_2$ production at time, $t_2$ and $X_{t1}$ is the $CO_2$ production rate at time, $t_1$. Often the biofilm exponential growth phase did not occur as one smooth continuous line (as found in batch cultures), possibly due to sloughing events so different time intervals ($t_2 - t_1$) of 1, 2 and 4 hours were used for comparison purposes. For all subsequent discussion, $\mu_{\text{biofilm}}$ is considered the net growth rate comprising of adsorption, cellular growth and loss of active biomass to the bulk flow via sloughing and erosion processes. The length of the lag phases was determined as the time where the tangent to the maximum slope intersected with the x-axis.

### 4.3.4. Correlating cell numbers to protein concentration and $CO_2$ production

In order to verify the validity of $CO_2$ measurements to quantify biofilm growth rate, protein concentration as an indication of increase in biofilm biomass (e.g. (Ragusa et al., 2004)) were measured in conjunction with the metabolic activity of the biofilm.

#### 4.3.4.1. Cell lysis and protein concentration determination

Cells were lysed in 0.1 N NaOH (final concentration) with incubation at 70 °C for one hour. The solubilised proteins from the lysed cells were measured with the Pierce® BCA total protein determination kit according to the manufacturer's instructions.

#### 4.3.4.2. Protein concentration as a measure of cell numbers

Different volumes of an overnight culture of *P. fluorescens* CT07 was centrifuged at 12 000 *g* for 5 minutes at 4 °C. The supernatant was discarded and the pelleted cells were lysed in 0.1 N NaOH with incubation at 70 °C for one hour and the protein concentration was determined. The protein concentration showed a high correlation with cell numbers ($R^2$ = 0.996).

#### 4.3.4.3. Protein concentration as an indication of cell numbers in biofilms

Twelve silicone tubes of the same dimensions as the inner tube of the CEMS were inoculated with *P. fluorescens* CT07 from cells in the exponential growth phase and grown at room temperature under continuous flow conditions (15 ml/h) with 1 mM citrate growth media. The biofilms growing in these tubes were sacrificed in duplicate for a total of six protein concentration data points by first draining the entire volume of bulk fluid ($\sim$ 3 ml) into a receptacle and adding NaOH (for a final concentration of 0.1 N) to this liquid containing free floating cells and loosely associated biofilm cells. Three millilitre of pre-warmed (60 °C) 0.1 N NaOH was injected into the emptied silicone tube and it was rinsed by pipetting the liquid back and forth to loosen and dissolve the attached biofilm. Subsequently the ends of the silicone tube were sealed off and then incubated (with the the 0.1 N NaOH still inside) at 70 °C, similar to the drained bulk fluid. After one hour of incubation the contents of the silicone tube (removed and dissolved biofilm) was further rinsed and stored as fraction 1 at $-20$ °C until protein concentration could be determined. The rinsing step (with 0.1 N NaOH) was done a second time and after incubation at 70 °C was stored as fraction 2. Two CEMS were inoculated at the same time as the 12 silicone tubes with the same inoculum and grown under the same conditions to compare $CO_2$ production with biofilm cell numbers.

### 4.3.5. Evaluation of the effect of various parameters on early biofilm development

The experimental system and conditions described above were used to compare (i) the two test strains and the mixed community, (ii) the effect of nutrient concentrations, and (iii) the effect of the origin of inoculum on early biofilm development.

## 4.4. Results

### 4.4.1. Correlation of biofilm growth determined by protein and $CO_2$ measurement

The biofilm development as determined by protein measurement was compared with the results obtained by CEMS for $CO_2$ production (Figure 4.1). The duration of the lag phase as determined by $CO_2$ measurements and protein determination were 22 h and 24 h, respectively, while biofilm $\mu_{max}$ were $0.27 \pm 0.01$ and $0.25 \pm 0.04$, respectively.

Protein concentrations for the sample that was collected earlier than the first data point shown were below the detection limit of the assay used. Biofilm growth was measured with the CEMS and compared in terms of lag phase, maximum growth rate and the steady state plateau phase where the increase in $CO_2$ production rate has levelled off.

### 4.4.2. Different microorganisms have different length in lag phase and maximum biofilm growth rates

As expected, under identical growth conditions (27 °C with a growth medium of 1 mM citrate minimal medium), different organisms exhibited a difference in lag phase. As shown in Figure 4.2, *P. aeruginosa* PA01 had a shorter lag phase than *P. fluorescens* CT07, which

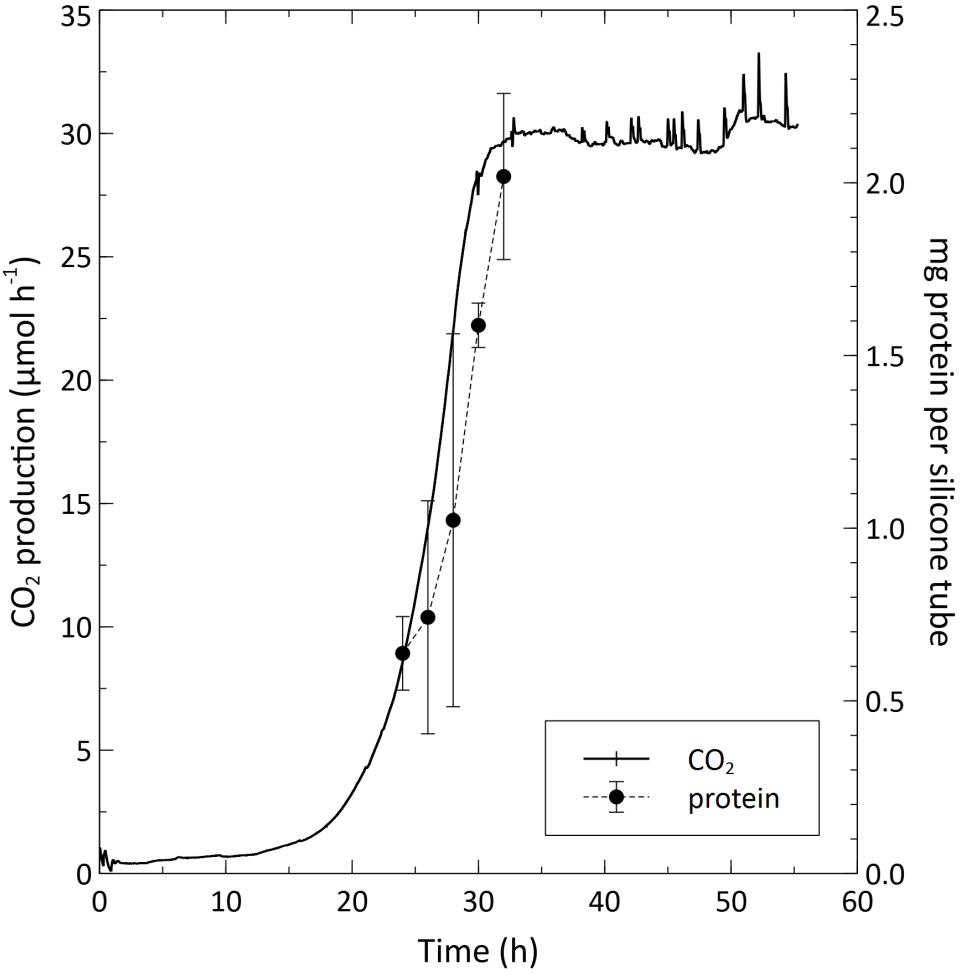


**Fig. 4.1.** Comparison of *P. fluorescens* CT07 biofilm growth during the exponential phase as determined by protein and $CO_2$ measurements.

indicates an enhanced ability to irreversibly attach to the surface and convert to a biofilm phenotype despite the fact that *P. aeruginosa* PA01 was growing at suboptimal temperatures while it was within the optimum temperature range for *P. fluorescens* CT07 (25 – 30 °C as reported in literature). The maximum biofilm growth rates also differed between *P. aeruginosa* PA01 and *P. fluorescens* CT07. PA01 had an average maximum biofilm growth rate of 0.37 $\pm$ 0.01 $h^{-1}$ while CT07 had an average maximum growth rate of 0.26 $\pm$ 0.03 $h^{-1}$ (both growth rates taken with $t_2 - t_1 = 2$ h) which differs significantly from one another ($P < 0.05$). The same average steady state values were obtained for the two *Pseu-*

*domonas* species with relatively small extent in sloughing events noticed even ∼50 h after inoculation.

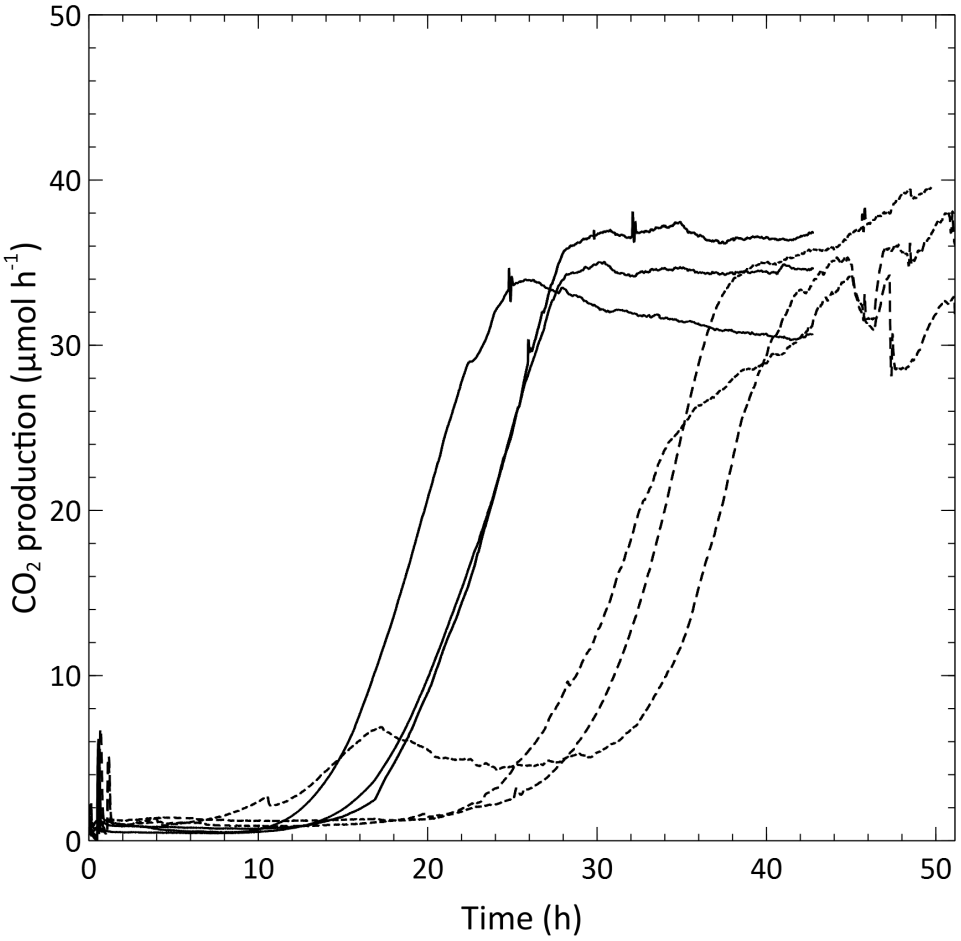


**Fig. 4.2.** Growth curves of *P. aeruginosa* PA01 (—) and *P. fluorescens* CT07 (- -) biofilms inoculated from citrate medium overnight pre-cultures and grown on 1mM citrate.

When the behaviour of the mixed culture and *P. fluorescens* CT07 grown on 1.5g/L TSB at 27 °C was compared, the mixed culture had a much shorter lag phase than CT07 (Figure 4.3). Interestingly, the comparison with growth in TSB showed similar maximum growth rates ($0.39 \pm 0.05$ $h^{-1}$ and $0.39 \pm 0.04$ $h^{-1}$ for mixed cultures and *P. fluorescens* CT07, respectively) and steady state values. However, the sloughing events occurring between 40 and 50 hours of incubation were much more pronounced than in the biofilms

grown on 1 mM citrate minimal medium.

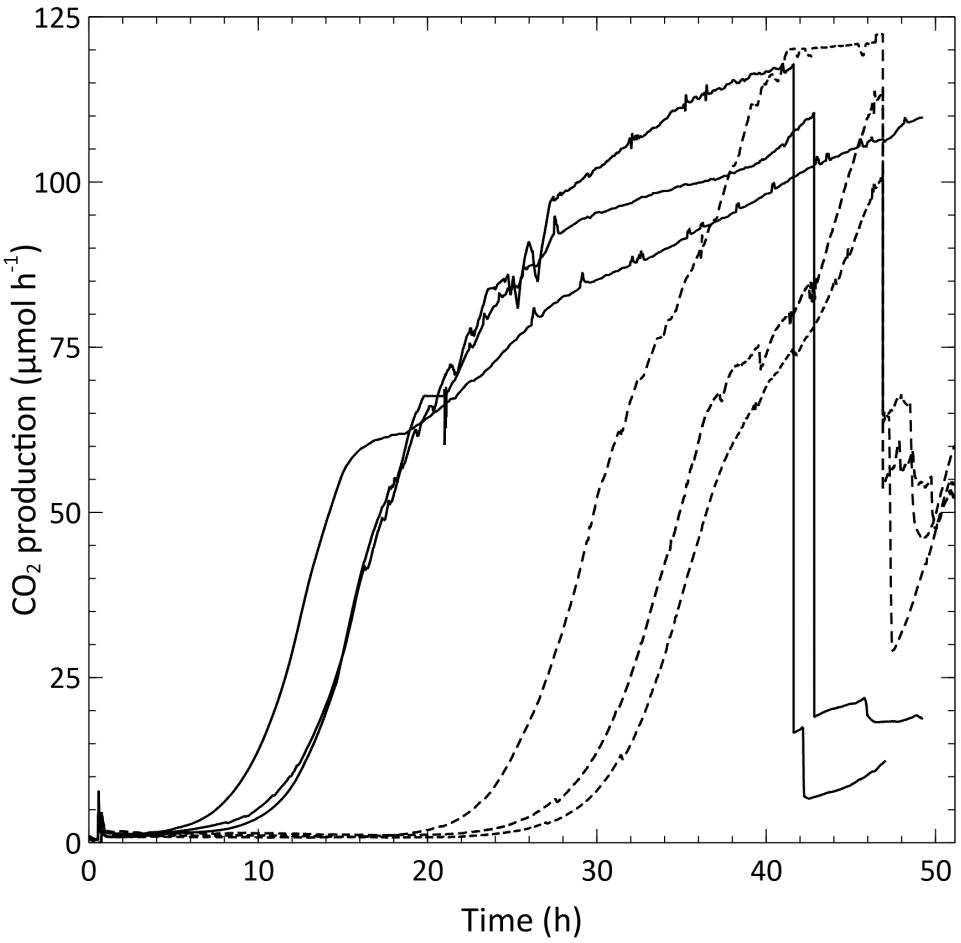


**Fig. 4.3.** Growth curves of mixed culture (—) and *P. fluorescens* CT07 (- -) biofilms inoculated from TSB medium overnight pre-cultures and grown on 1.5g/L TSB.

### 4.4.3. Different nutrient concentrations result in different lengths of lag phase and steady state values but not in differences in maximum growth rates

When *P. fluorescens* CT07 was grown in minimal growth medium with 1, 2 and 4 mM citrate as the sole carbon source, the average lag phases decreased with increasing citrate

concentration. The average maximum growth rates increased with citrate concentration ($0.26 \pm 0.03\ h^{-1}$, $0.26 \pm 0.03\ h^{-1}$ and $0.31 \pm 0.01\ h^{-1}$ for 1, 2 and 4 mM citrate respectively) but these changes were not significantly different. The steady state values and intensity of sloughing events increased with increasing citrate concentration.

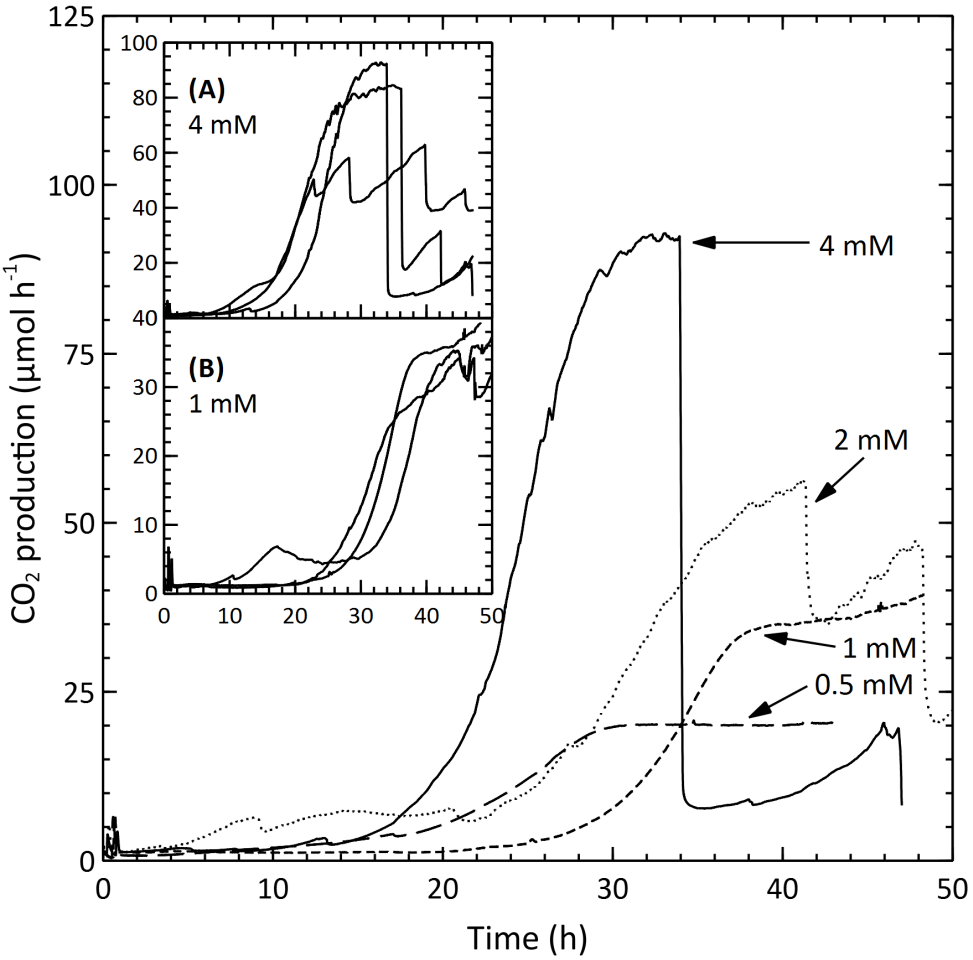


**Fig. 4.4.** Growth curves of *P. fluorescens* CT07 biofilms inoculated from citrate medium overnight pre-cultures and grown on different concentrations of citrate media. Notice that steady state values and the severity of sloughing increase with increasing citrate concentration. Inset (A) shows replicate runs of biofilms grown on 4 mM citrate and inset (B) shows replicate runs of biofilms grown on 1 mM citrate to illustrate the differences and reproducibility.

Remarkable recovery was observed after these sloughing events (Figure 4.4). *P. fluorescens* CT07 grown on 0.75 and 1.5 g/L TSB showed similar trends with lag phases

decreasing with increasing TSB concentration, similar maximum growth rates ($0.39 \pm 0.04\ h^{-1}$ and $0.34 \pm 0.03\ h^{-1}$ for 0.75 and 1.5 g/L TSB respectively) and increasing steady state values and sloughing with increasing TSB concentration (data not shown).

### 4.4.4. Different origins of inoculum result in different lag phases, but not in different maximum growth rates

When biofilm effluent cells were used as inoculum, the average lag phase was considerably shorter than the case where overnight cultures (from batch) were used as inoculum (Figure 4.5). The maximum growth rate was not significantly different when the slopes were calculated over a period of 2 hours ($0.31 \pm 0.01\ h^{-1}$ for effluent inoculum and $0.26 \pm 0.03\ h^{-1}$ for overnight inoculum) but it was significantly different ($P < 0.05$) when the slopes were calculated over 4 hours ($0.30 \pm 0.01\ h^{-1}$ for effluent inoculum and $0.24 \pm 0.02\ h^{-1}$ for overnight inoculum). The steady states stabilized at similar values.

When batch-grown exponential phase cells were used as inoculum and compared to inocula from overnight cultures, similar values in lag phase, maximum growth rates and steady state values were obtained. An interesting observation that was repeatedly made is the fact that the growth of biofilms inoculated from exponentially growing cells exhibited almost identical behaviour for replicate runs (Figure 4.6).

To further evaluate the effect that the origin-of-inoculum may have on subsequent biofilm development, *P. fluorescens* CT07 biofilms were grown with 1.5 g/L TSB as growth medium but one set of pre-cultures were grown in 3 g/L TSB while the other set of pre-cultures were grown in 5 mM citrate minimal medium. The average lag phase for the biofilms originating from TSB pre-culture was significantly shorter than that of the citrate pre-culture biofilms (Figure 4.7). The maximum growth rates were almost the same ($0.37 \pm 0.04\ h^{-1}$ and $0.39 \pm 0.04\ h^{-1}$) for the TSB pre-culture and the citrate pre-culture respectively while the biofilms from the TSB pre-culture reached much higher steady state

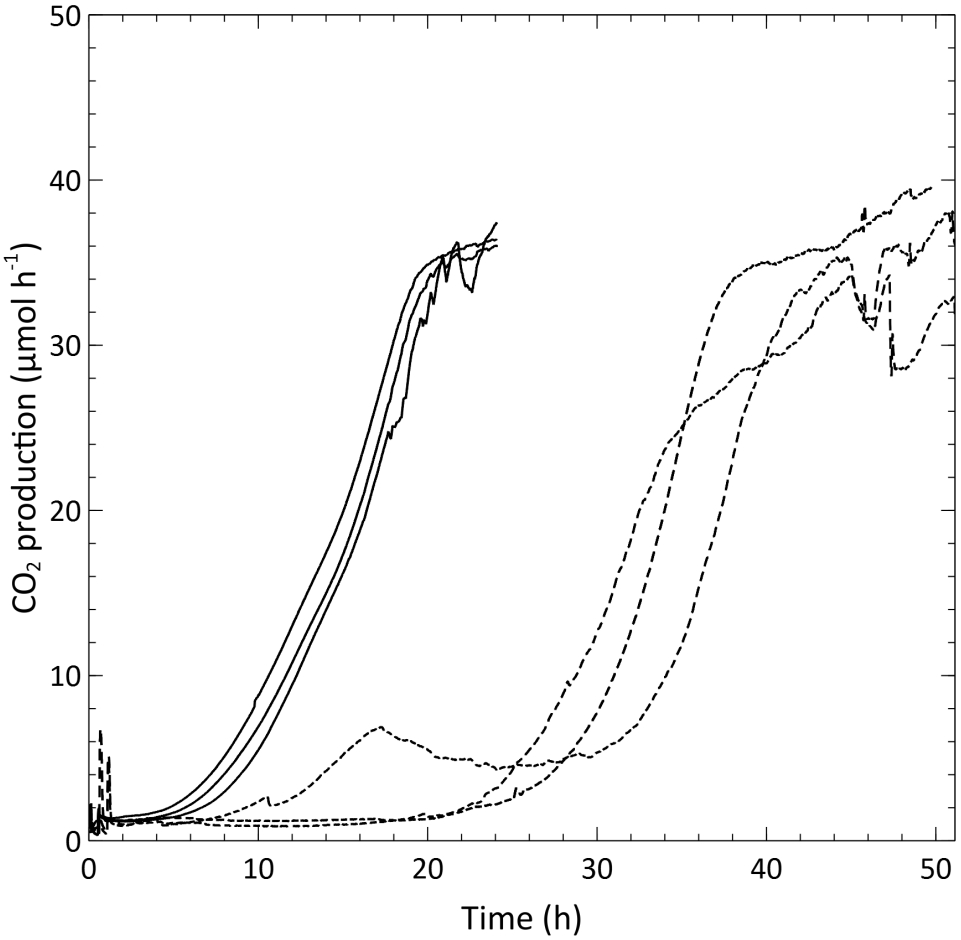


**Fig. 4.5.** Growth curves for *P. fluorescens* CT07 biofilms grown on 1 mM citrate. Graphs with solid lines (—) were inoculated from biofilm effluent while the graphs with dashed lines (- -) were inoculated from overnight pre-cultures.

values than the biofilms from the citrate pre-cultures.

## 4.5. Discussion

Measuring biofilm development with CEMS allowed determination of the length of the lag phase, maximum biofilm growth rate and steady state values with predictability as well as the monitoring of dynamic behaviour such as biofilm sloughing events and recovery. A shorter lag phase and higher maximal growth rate are both indicators of the

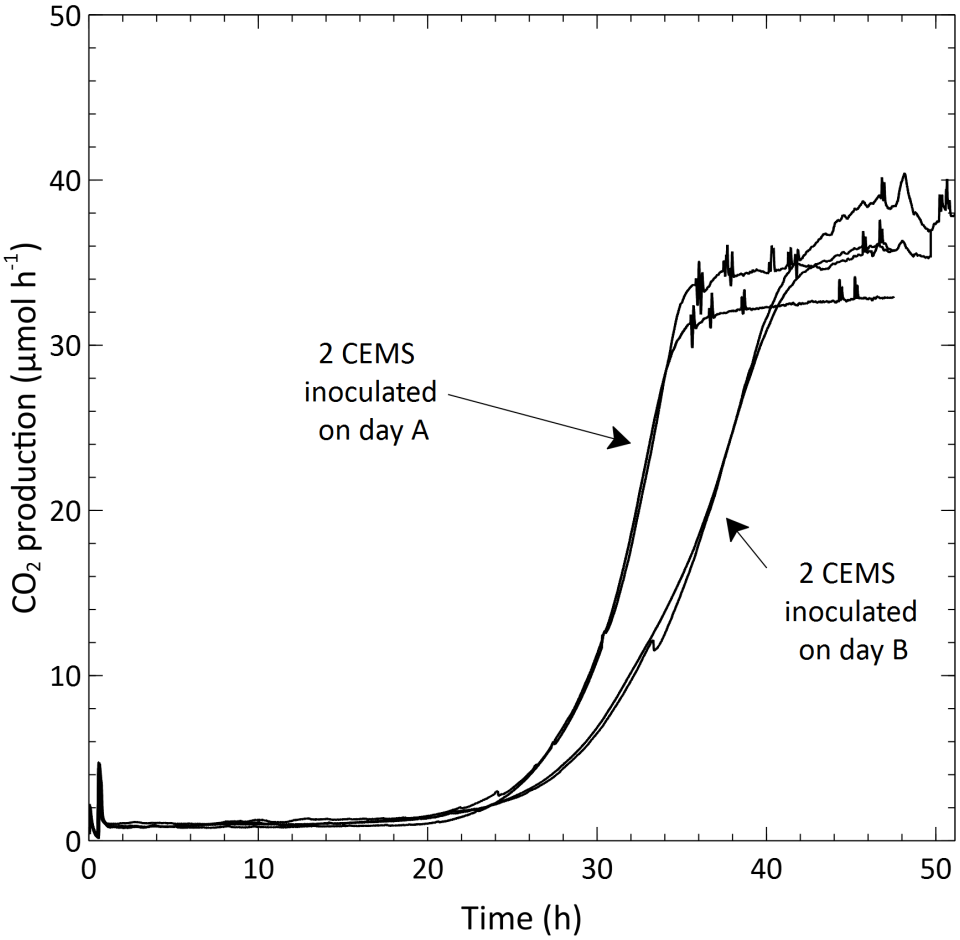


**Fig. 4.6.** Growth curves for *P. fluorescens* CT07 biofilms inoculated from exponentially growing cells and grown on 1 mM citrate. Notice the almost identical growth behaviour for replicate runs inoculated from the same inoculum on each respective day.

competitive advantage that an inoculum may have to colonize a new surface. The process that takes place when free floating cells leave the bulk liquid to settle permanently on a surface encompasses the steps of reversible attachment and irreversible attachment (Mueller et al., 1992; Rice et al., 2000) coupled with a cascade of different gene expressions for conversion from a planktonic to a biofilm phenotype. All these steps contribute to a lag phase before attached cells can start to reproduce maximally. Not all cells that attach irreversibly start to multiply at maximum rates. Rice et al. (2000) observed that the first cells to attach irreversibly, what they referred to as the primary biofilm cells, and their

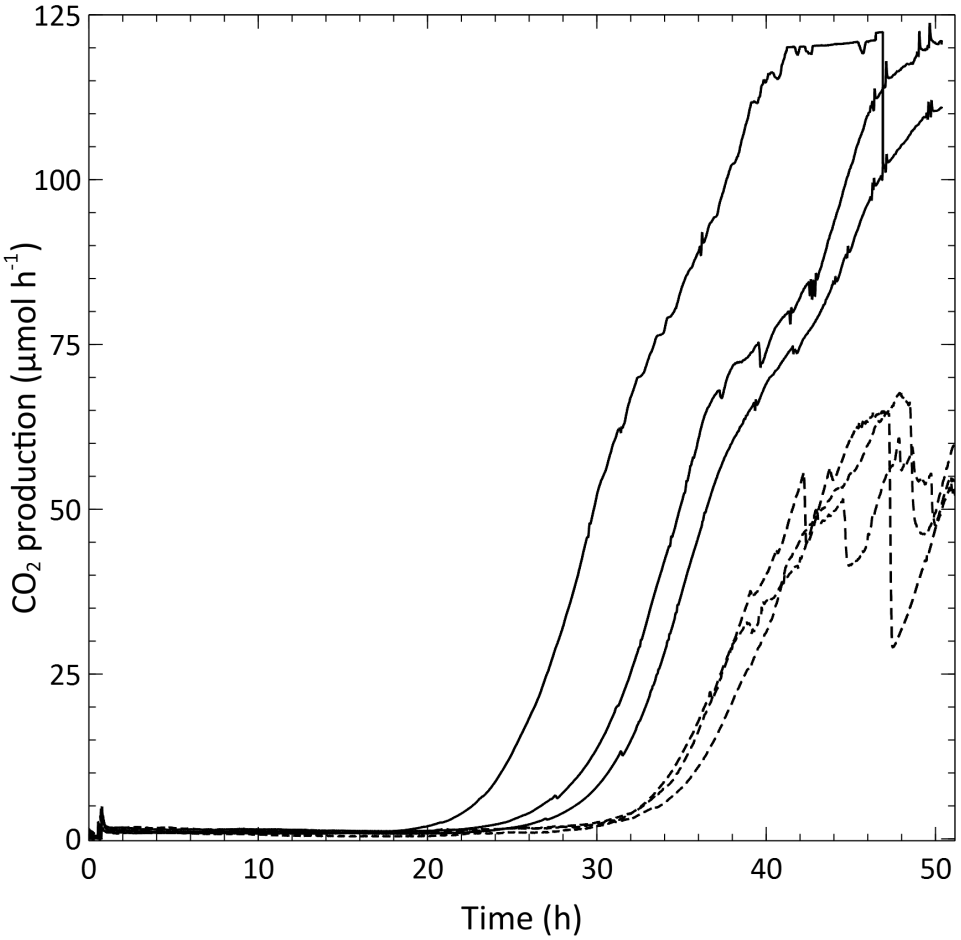


**Fig. 4.7.** Growth curves for *P. fluorescens* CT07 biofilms grown on 1.5 g/L TSB with pre-cultures from 3 g/L TSB medium (—) and 5 mM citrate minimal medium (- -).

progeny-the secondary biofilm cells, behaved markedly different in that the latter replicated at a much faster rate and emigrated more readily than the primary biofilm cells. Klayman et al. (2008) also observed a base layer of cells uniformly colonizing the surface with a zero net accumulation of cells when they co-inoculated two *P. aeruginosa* PA01 strains labelled with different fluorescent proteins into glass capillary flow cells.

A major benefit of faster growing cells is that they can displace non-growing attached cells (Klayman et al., 2008), while the development of a three dimensional structure by these fast growers that protrude into the bulk liquid may result in faster metabolism be-

cause of improved exposure to nutrients and oxygen as was the case where stalk formers displayed lowered metabolic activity than the cap formers of mushroom type micro-colonies in *P. aeruginosa* biofilms (Pamp et al., 2009). It appears probable that higher steady state metabolic values are an indication of the stability of the biofilm structure i.e. ability of the biofilm cells to remain overall active at maximum rate. Our results suggest that higher nutrient concentrations lead to more biofilm biomass accumulation and a higher overall activity by the accumulated biomass. However, the larger biomass was also prone to more sloughing, which is likely a form of self regulation in order to prevent stagnation due to the development of excessively large inactive zones in the biofilm. It is assumed here that the significant fluctuation in net metabolic activity as measured by $CO_2$ production rates has a direct relationship with sloughing of the biofilm biomass; the basis for this assumption is material balances done in our previous studies that showed that up to 10% of the total carbon input to *P. fluorescens* CT07 in a similar system over an 8-day period were released as aggregates - presumably following sloughing events (compared to 4% that remained as biofilm biomass) (Kroukamp and Wolfaardt, 2009). Furthermore, using a large area photometer to measure biofilm biomass, Bester et al. (2005) showed highly variable values of biofilm biomass by this strain after the first sloughing event, the timing of which correlates with the results presented here. Different nutrient sources result in different biofilm architectures. For instance, *P. aeruginosa* developed three dimensional micro-colonies and mushroom type shapes in 10% TSB (Klayman et al., 2008) whereas flat densely packed biofilms formed in 0.1mM citrate minimal media (Heydorn et al., 2002). In a similar way *P. fluorescen*s CT07 displayed different biofilm morphologies when grown in 10% TBS (Wolfaardt et al., 2008) or 1 mM citrate minimal media (Bester et al., 2010). It is conceivable that a three dimensional architecture with more pronounced protrusion forming at higher nutrient concentrations would be more readily prone to sloughing. *P. aeruginosa* and *P. fluorescens* form biofilms under almost any condition that

allows growth (O'Toole and Kolter, 1998) and it is therefore doubtful that settlement on a surface is primarily a safety mechanism for protection from harsh environments by these organisms. Biofilms can, however, act as agents of continuous proliferation by sending offspring (as single cells or clumped is small aggregated clusters) into the environment. Bester et al. (2009) reported that *Pseudomonas* biofilms yielded a considerable amount of cells to the effluent as early as 6 hours after inoculation and one of their major conclusions was that biofilm formation is a mechanism for proliferation in addition to the role in survival as typically mentioned in the literature. Interestingly, for the experimental system used, the planktonic population contribute only $\sim$1% of the total $CO_2$ (Unpublished data). Telgmann et al. (2004) concluded that sloughing and erosion should not be seen as disturbance events but rather an integral part of biofilm development.

In a batch culture, repeatable growth behaviour is obtained when a particular microorganism is grown under similar environmental conditions (nutrient composition, temperature etc.) i.e. the environment dictates the outcome of the growth curve, similarly to the maxim that "men resemble the times more than they resemble their fathers". The latter would suggest that the decade when people are born (influencing the prevailing political, economical and cultural status of an era) and therefore their environment has a more pronounced influence on the generalized behaviour of a generation than the people who raised them. Considering microorganisms, this would be true for batch cultures but results presented in this study indicate that this seems not to be the case with early biofilm formation (specifically with regards to lag phase and maximum specific growth rate) in *P. fluorescens* CT07. Rice et al. (2000) pointed to a critical need for understanding the nature of the inoculum used to generate the initial biofilm. Our results show that the environment where the cells originate from prior to incorporation into a biofilm has a dramatic effect on the behaviour (and potentially the architecture) of the ensuing biofilm. When the inoculum originated from biofilm effluent, the cells were able to adapt

much quicker to a biofilm lifestyle which is in agreement with observations by Rollet et al. (2009) who tested the biofilm forming capabilities of cells from different origins i.e. sessile cells, cells detached from biofilm and batch grown cells. Their observation that the cells detached from a biofilm (effluent cells in our context) exhibit a "greater capacity to form biofilms", led to the postulation that there exists a transitional phenotype (detached cells) between sessile and planktonic states. This observation provides support to the statement by Rice et al. (Rice et al., 2000) that the biofilm phenotype might already be expressed when the cells approach a new surface, which would account for the decreased time of lag phase. Bester et al. (2009) commented on the large number of freely swimming single cells in close association with micro-colonies of *P. fluorescens* CT07 biofilms grown on citrate minimal medium. These freely swimming cells that appear to be minimally influenced by the much higher flow rates in the bulk liquid phase could be the origin of the mainly non-aggregated cells encountered in the effluent of both *P. fluorescens* CT07 and *P. aeruginosa* PA01 biofilms (Bester et al., 2009). This observation could indeed suggest that planktonic cells closely associated with the surface (or micro-colonies in biofilms) have a biofilm phenotypic advantage to settle on new surfaces. On the other hand it could be that these surface associated planktonic cells are starved for nutrients which may influence their attachment behaviour. Mueller (1996) showed that starved *P. fluorescens* cells increased their ability to adsorb to a surface fourfold compared to non-starving cells. Effluent cells could also be in the form of small aggregates (Stewart, 1993) with extracellular polymeric substances (EPS) aiding in surface attachment. The data show that although cells from different phenotypic origins do not constantly give rise to different biofilm specific growth rates, the lag phases differ markedly; considering the fact that the primary colonizers go through a number of cell divisions before there is a measurable change in overall biofilm activity, it appears that pre-culture conditions may exert an influence on the resulting biofilm for a number of generations after inoculation. Pre-cultures grown

in citrate medium showed extended lag phases and lower steady state values compared to biofilms originating from pre-cultures grown in TSB medium. Such difference in lag phase alludes not only to the adaptation period but also to the resulting biofilm architecture. Kraigsley and Finkel (2009) demonstrated a heritable ability of cells from older biofilms to outcompete younger cells in the presence of a pre-existing biofilm.

For the different nutrient compositions and concentrations tested, no significant difference in specific growth rate could be found, which is in agreement with work from Ellis et al. (2000) although higher concentrations led to higher biomass build-up and also more severe sloughing events. In the current work the ability of CEMS to use $CO_2$ measurements as a way to determine biofilm growth curves was demonstrated in real-time and in a non-destructive manner. Growth rates determined were comparable to values found in literature (Klayman et al., 2008) and with good repeatability. When the observed differences in lag time are considered, together with the fact that biofilm growth in flow systems is a net process that balances irreversible attachment, cellular division and loss of cells to the bulk phase via sloughing and erosion followed by colonization of new surfaces, it appears that the origin of the inoculum may have a profound effect on biofilm function. The approach described here should be applicable to efforts to model biofilm kinetics in bioreactors, and provide a method to evaluate the effect of genetic modifications and external factors such as chemical treatment on biofilm function.

# Chapter 5

# Real-time monitoring of biofilm metabolic activity during antimicrobial exposure

# 5. Real-time monitoring of biofilm metabolic activity during antimicrobial exposure

## 5.1. Introduction

Several pathogens associated with chronic infections are capable of biofilm formation. Possible reasons for increased antimicrobial resistance of biofilms was already discussed in Chapter 1. In this chapter the applicability of CEMS to be used as a tool to test antimicrobial susceptibility in biofilms will be demonstrated.

### 5.1.1. Background

Cystic fibrosis (CF) is the most prevalent lethal genetic disease (Döring et al., 2000; Reid et al., 2008) where chronic bacterial infections lead to excessive inflammatory responses which is ultimately responsible for most of the mortality (Chmiel and Davis, 2003). CF patients were thought to be infected with only a limited variety of organisms mainly *P. aeruginosa*, *Burkholderia cepacia* complex, *Staphylococcus aureus* and *Haemophilus influenzae* but recent studies showed that the diversity is much higher than previously recognized, many of the species being obligate anaerobes (Tunney et al., 2008) and that a high pro-

portion of all the bacterial species detected are indeed active (Rogers et al., 2005). Under anaerobic $CO_2$-rich conditions, Nozawa et al. (2007) showed that *P. aeruginosa* display an aggressive swarming phenotype while Filiatrault et al. (2006) demonstrated in genetic studies that anaerobic metabolism influences virulence in *P. aeruginosa*.

*P. aeruginosa* is the main infectious agent during the later stages of CF (Coutinho et al., 2008) resulting in highly viscous mucus (Boucher, 2007; Donlan, 2002) which again leads to the establishments of steep oxygen gradients (Webb, 2006). It appears probable that the biofilm lifestyle, and even more so when sessile growth is coupled with anaerobic conditions, influences the antimicrobial resistance of resident microorganisms. As mentioned previously, microorganisms growing in biofilms are up to a 1000 times more resistant to antibiotics than their planktonic counterparts. Microorganisms are also more resistant to tobramycin under anaerobic conditions (both when grown as biofilms and planktonically) (Borriello et al., 2004; Field et al., 2005; Hill et al., 2005) compared to aerobic conditions.

It would therefore make sense to have system that has the ability to monitor biofilm response to antibiotics both under aerobic and anaerobic conditions. The most common method to report the resistance of a microorganism to an antibiotic in the planktonic phase is the minimum inhibitory concentration (MIC) which is the minimum concentration of the antibiotic that will inhibit visible growth (Andrews, 2001). Other antimicrobial susceptibility testing methods such as colorimetric assays using the tetrazolium salt 2,3-bis[2-methyloxy-4-nitro-5-sulfophenyl]- 2H-tetrazolium-5-carboxanilide (XTT) are also available (Tunney et al., 2004) although not that widely used. Similar to MIC, the concept of minimum biofilm eradication concentration (MBEC)[1] was developed to quantitatively report the susceptibility of biofilm microorganisms against antibiotics (Ceri et al., 2001). The quantification of surviving biofilm cells (viable cells) after antibiotic treatment is based on

[1]the MBEC assay system uses the Calgary Biofilm Device (Ceri et al., 1999) which is distributed by Innovotech

enumeration by heterotrophic plate counts after the removal of surface associated cells by vortexing and sonication. Although the MBEC assay is widely used in biofilm studies (particulary due to its high throughput capacity (Harrison et al., 2005b)) inherent biases exist such as the uncertainty about the extent of cell removal from the surfaces before enumeration and the effect of sonication on antibiotically treated cells.

The CEMS provides a way to monitor the metabolic activity of biofilm cells non-destructively, in real-time together with biofilm viability after exposure to antimicrobials. A further advantage is that the development of antimicrobial resistance can be tested by repeatedly treating the same biofilm with a variety of doses and exposure times.

## 5.2. Materials and Methods

### 5.2.1. Aerobic and anaerobic growth of biofilms

Aerobic biofilms were grown in CEMS and analyses performed as described in Chapters 2 (general setup) and 4 (calculation of $\mu_{\text{max biofilm}}$ values). The biofilms were grown at either 27°C or 37°C and the NaCl concentration was reduced to 13 mM while sodium nitrate[2] (5.0 mM) was added as an electron acceptor. For anaerobic growth, cysteine as a reducing agent (0.5 g/L) and resazurin as redox indicator (0.002 g/L) were added and the growth medium was purged with nitrogen until it became clear[3]. Nitrogen was used as the sweeper gas instead of compressed $CO_2$-free air.

[2]necessary for growth under anaerobic conditions

[3]resazurin is the most widely used redox indicator as a visible assessment for strict anaerobic (not only oxygen free but also highly reducing) conditions (Fukushima et al., 2003). Under aerobic conditions resazurin is blue, under microaerophilic conditions it is pink and under strict anaerobic conditions it is clear (Karakashev et al., 2003)

### 5.2.2. Exposure of biofilms to tobramycin

Tobramycin was added to the growth medium to various concentrations of up to 100 mg/L (a concentration of more than 10 mg/L is toxic to humans (Schulz and Schmoldt, 1997)) and the biofilms were exposed for different time periods.

## 5.3. Results

The biofilm development rates under aerobic conditions had a much shorter lag phase than under anaerobic conditions although the $\mu_{\text{max biofilm}}$ values were similar (0.44 $h^{-1}$ and 0.40 $h^{-1}$ respectively); the steady state metabolic rate was higher when grown anaerobically (Figure 5.1).

For the aerobic system, 50 mg/L tobramycin[4] in growth medium was administered to the three day old biofilms for 4 hours after which the flow of antibiotic-free growth medium was resumed. Metabolism increased sharply following tobramycin addition to a maximum value and started decreasing for a number of hours after the tobramycin exposure stopped. However, recovery to pre-exposure steady state metabolic values occurred within 24 hours after treatment. The tobramycin exposure on a subsequent day seemed to affect the biofilm more severely ($CO_2$ production values decreasing below steady state sooner and reaching lower minimum metabolic rate values and taking longer to reach pre-treatment steady state values) (Figure 5.2). However, the same antibiotic treatment on day 3 displayed similar responses than the treatment on day 1 (data not shown).

The addition of tobramycin to the anaerobic system was accompanied by the characteristic metabolic response of increased $CO_2$ production, followed by a much longer (double the time compared to aerobic conditions) recovery phase until pre-exposure steady state values were established (Figure 5.3).

[4] initial experiments using 10 mg/L tobramycin showed no deviation from pre-treatment steady state $CO_2$ production rates

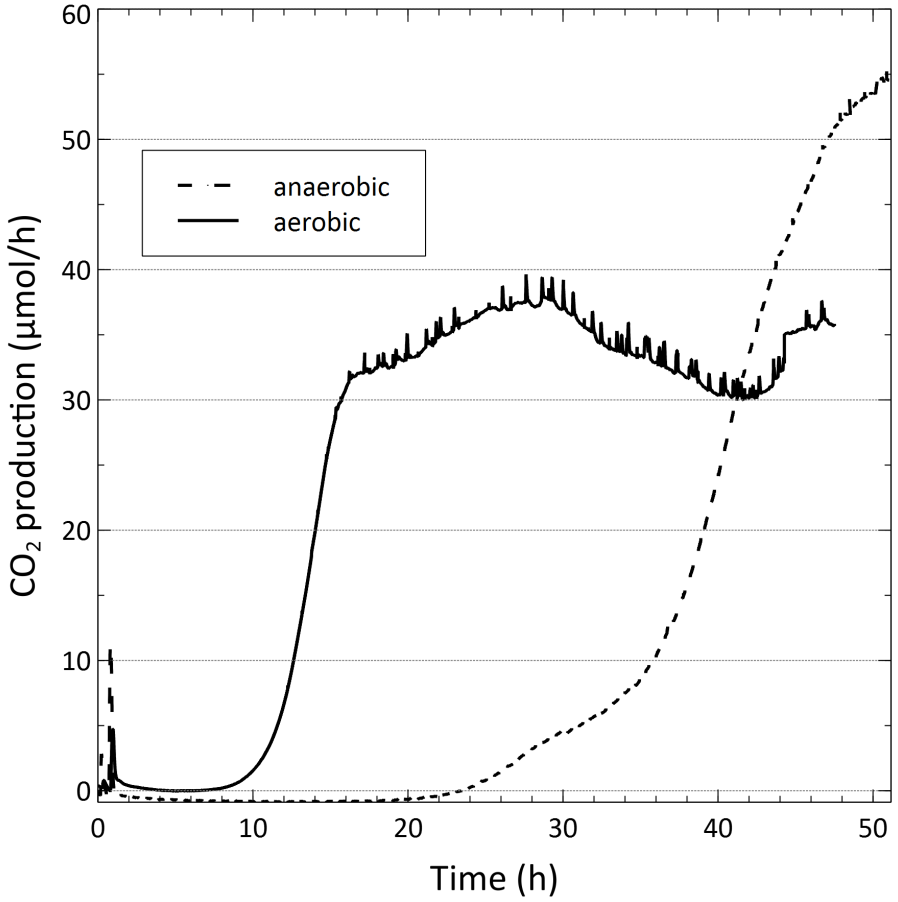


**Fig. 5.1.** Development rate of *P. aeruginosa* PA01 biofilms grown at 37°C under aerobic (—) and anaerobic ( - - ) conditions

Biofilm metabolism was reduced to a greater extent by tobramycin treatment at 37°C as when compared to treatment at 27°C where metabolism hardly fell below normal steady state values even at higher tobramycin concentrations (100 mg/L) (data not shown).

## 5.4. Discussion

### 5.4.1. Biofilm metabolic response to tobramycin exposure

Recognizing that in vitro studies cannot mimic the complexities of any host response (Hassett et al., 2002; Anderson et al., 2008; Moreau-Marquis et al., 2008), it is pointed out

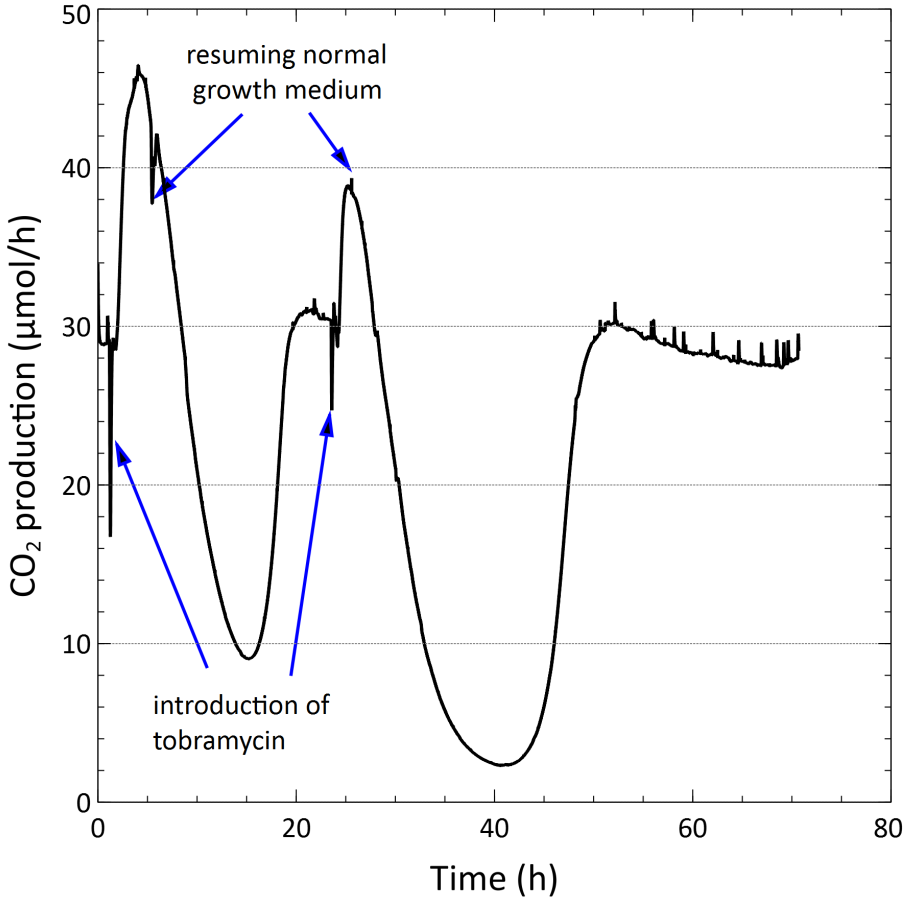


**Fig. 5.2.** Three day old aerobic *P. aeruginosa* PA01 biofilm growing at steady state at 37°C exposed to 50 mg/L tobramycin on subsequent days for a duration of 4 hours each after which the supply of antibiotic-free growth media was resumed

that it was not the intention to use the CEMS as a model for studying antibiotic response of lung infections. Rather the objective was to evaluate the utility of CEMS to reveal clues to the metabolic response of microorganisms under a variety of environmental conditions.

Among the reasons for antimicrobial resistance mentioned in Chapter 1, slow growth will be discussed in more detail. The killing of bacteria by antibiotics is often growth-dependent (Gilbert et al., 1990) as most antibiotics target some type of macromolecular synthesis (Stewart, 2002). Therefore, bacteria in non-growing zones of biofilms are less susceptible than when all the biofilm cells grow at a uniform rate (Xu et al., 2000). With these concepts in mind, Borriello et al. (2006) argued that in *P. aeruginosa* biofiolms, oxygen

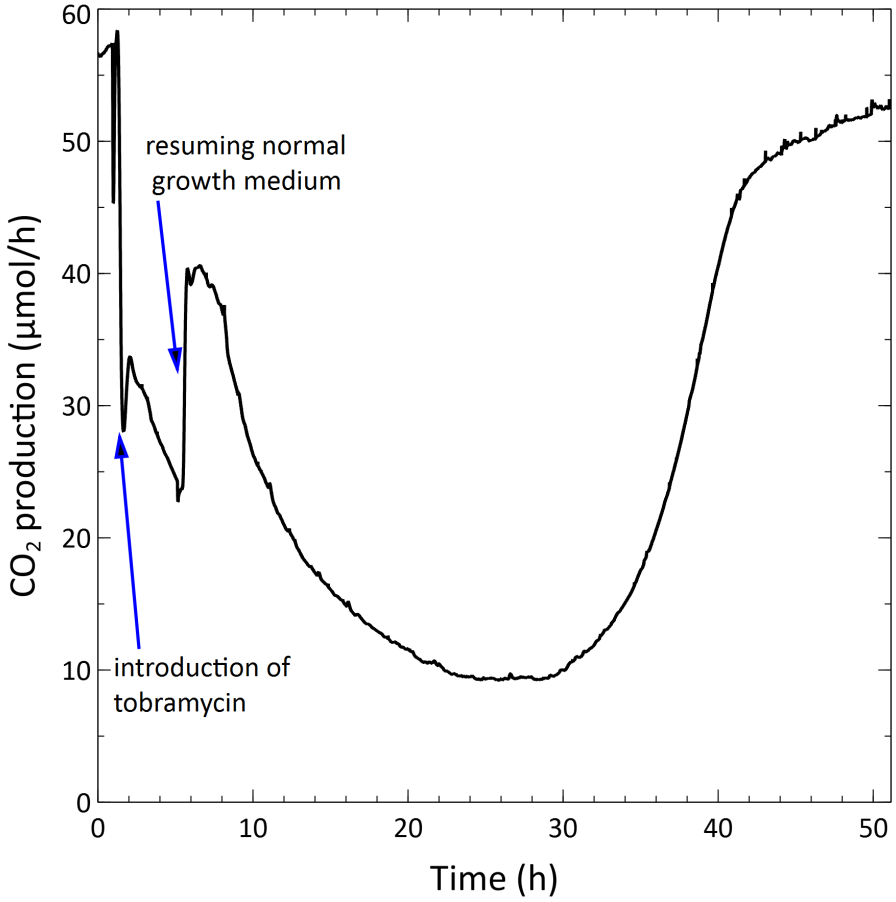


**Fig. 5.3.** Three day old anaerobic *P. aeruginosa* PA01 biofilm growing at steady state at 37°C exposed to 50 mg/L tobramycin for a duration of 4 hours after which the supply of antibiotic-free growth media was resumed

limitation leads to anoxic regions in the biofilm, in anoxic regions the metabolic activity slows down or stops and that the metabolically inactive bacteria are less susceptible to antimicrobial killing. Nutrient limitations have been cited as the causative agent in other antimicrobial studies (e.g. (Spoering and Lewis, 2001)) that found no significant difference in resistance to killing between stationary phase planktonic and biofilm cells. Anderl et al. (2003) came to similar conclusions after showing that zones of slower growth exist within the biofilm and was less affected by the antibiotics (that penetrated thoughout the whole biofilm) than the faster growing zones.

Contrastingly, faster growing cells may also have some advantages when exposed to

antibiotics. Damper and Epstein (1981) showed that the amount of antibiotic accumulated within cells can be given by

$$\int_0^t JAdt = \int_0^t JA_0 e^{\mu t} dt = \frac{JA_0(e^{\mu t} - 1)}{\mu} \tag{5.1}$$

where $J$ is the flux of antibiotic into the cell, $A_0$ and $V_0$ is the surface area and volume of the bacteria at time = 0. With the cell volume at time $t$ equalling $V_0 e^{\mu t}$, the concentration of antibiotic inside the cell $C$ can be given by

$$C = \frac{JA_0(e^{\mu t} - 1)}{\mu V_0 e^{\mu t}} \tag{5.2}$$

When time becomes sufficiently large that $e^{\mu t} \gg 1$, the intracellular antibiotic concentration is inversely proportional to the growth rate. Pamp et al. (2008) showed that slow growing biofilm cells were killed by the antimicrobial peptide, colistin, while the faster growing cells were able to adapt by upregulating unspecific adaptation mechanisms. Growth rate may also play a role in the activity of multidrug efflux pumps. *P. aeruginosa* possesses a number of multidrug efflux pumps where some are more highly expressed in the biofilm phenotype (Zhang and Mah, 2008) while for other families of efflux pumps there is no upregulation during biofilm development (Kievit et al., 2001). Therefore a possible explanation for the increased metabolism after tobramycin exposure as shown in Figures 5.2 and 5.3 may be the increased activity of certain ATP-dependent multidrug efflux pumps (Scatamburlo Moreira et al., 2004).

### 5.4.2. How to interpret antimicrobial results from CEMS

In the CEMS, overall metabolic activity rather than direct cell growth is measured (although it could be assumed that a fraction of the metabolic activity will be diverted into

cellular proliferation to account for the steady state metabolic rate to maintain the biofilm structure and cell numbers in the effluent while continuous sloughing events are taking place). So while a transient increase in $CO_2$ production does not necessarily depict a concomitant increase in cell numbers, diminished $CO_2$ production will be an indication of lower overall metabolic activity eventually leading to slower growth.

CEMS has the advantage that both short and longterm responses to antimicrobials can be monitored in real-time. Transient responses may provide insight into the changes in intermediate metabolic behaviour until a new steady steady state is reached, while changes in stable condition values after antimicrobial treatment (also in combination with other antimicrobials (Tré-Hardy et al., 2008) or biofilm affecting compounds like chelators[5] (Moreau-Marquis et al., 2009) or quorum sensing inhibitors that have been shown to enhance antimicrobial activity (Hentzer et al., 2003; Høiby et al., 2010) of antibiotics) could be interpreted as killing or injuring or arresting development.

Our results show different transient antimicrobial responses under aerobic and anaerobic conditions. It seems that the anaerobic biofilms were more severely affected in $CO_2$ production (both in magnitude and duration) although they had a higher steady state $CO_2$ production and comparable biofilm development rate.

For the purpose of future discussions it might be useful to specifically define what exactly is meant by biofilm antimicrobial resistance or increased resistance. Does it solely mean the total eradication of all biofilm cells or might it be useful to include a "vulnerability" or "ability to recover" component with the purpose to devise treatment or dosing regimes? From the results presented here it is evident that anaerobically grown biofilm cells are more vulnerable to tobramycin treatment although the majority of literature points to the conclusion that oxygen limited biofilms are more resistant to antibiotic treatment. Grobe et al. (2002) came to the conclusion that it is more effective to treat

[5]FDA-approved iron chelators have been shown to eliminate *P. aeruginosa* biofilms on cystic fibrosis cells when used in conjunction with tobramycin

*P. aeruginosa* biofilms with higher concentrations of antimicrobials for shorter periods of time than treatment with lower doses over longer periods of time. Furthermore, the device in which the antimicrobial susceptibility is tested has a pronounced influence on the results. When we compared flow (CEMS) with non-flow (Calgary device) systems[6], the biofilm cells in flow systems were able to withstand antibiotic concentrations at much higher concentrations and duration of treatment (results not shown). It might therefore be necessary to report minimum biofilm eradication concentrations (MBEC) in non-flow and flow systems.

Ongoing studies include determining the MBEC in flow systems, the influence of slow growth (starvation conditions) on antibiotic susceptibility, the influence of metabolic product buildup (comparing flow with non-flow systems) and biofilm suppressors (for example chelators, quorum sensing disruptors, NO as biofilm disperser etc.) in combination with antibiotics.

[6]Slow growth in biofilms may be the result of either nutrient limitation or metabolic product buildup. Metabolic product accumulation typically occurs in batch systems such as the MBEC testing methods in the Calgary Device.

# Chapter 6

# Summary

# 6. Summary

Using $CO_2$ evolution measured in the gas phase as a method to monitor biofilm metabolism is a way to track global (whole biofilm) response quantitatively, non-destructively and in realtime. Current methods that monitor biofilm metabolism suffer from certain drawbacks including the toxicity of reporter molecules, the restrictions imposed by the need of genetically manipulated organisms (incorporated reporter gene constructs), lack of realtime quantitation in various microscopic techniques, substrate specificity of microorganisms or analysis capabilities and restrictions on growth conditions like aerobic or anaerobic reactor configurations.

Although $CO_2$ measurement in the gas phase is not a cure-all method to determine biofilm metabolism it has certain inherent advantages. Apart from the convenience to quantitatively track the $CO_2$ production in realtime, the relatively cheap, simple system had added benefits such as the quantitative, realtime nature of the method that made it possible to monitor dynamic biofilm response and calculate rates of change in biofilm metabolism under various growth conditions. Both the CEMS and CMR are amenable to test metabolic responses to changes in environmental conditions like different nutrients (Kroukamp et al., 2010) or starvation conditions (Bester et al., 2010), different temperatures, antimicrobial attacks or to study growth behaviour (for instance the difference in biofilm development profiles when *P. aeruginosa* growth on glucose or citrate as sole carbon source is compared when taken into account that this organism forms stalks

and mushroom type structures (Pamp et al., 2009) when grown on glucose but dense carpet like growth when grown on citrate (Heydorn et al., 2002)). The measurement of the metabolic response in the gas phase prohibits sensor fouling so experiments can be tracked for long periods of time while the non-destructive nature of the approach allows the same biofilm to be challenged with many different growth conditions thus making it possible to study biofilm adaptation behaviour.

An example of a situation where adaptation is particularly important, is the instance of what happens when a biofilm is repeatedly exposed to different concentrations and durations of antimicrobials. For such a scenario a CEMS tracking of biofilm metabolism has particular advantages over the highly popular Calgary device (Ceri et al., 1999). Although a CEMS system does not nearly possess the high throughput capabilities of the Calgary device, we were able to show that *P. aeruginosa* biofilms displayed different adaptation behaviour at different temperatures (at 27 °C the biofilms were less responsive to tobramycin as when compared to biofilms treated at 37 °C and that tobramycin concentrations much higher than physiologically tolerable by humans were not able to eradicate established biofilms even after 3 hours of exposure) and that the antimicrobial metabolic response was markedly different between aerobic and anaerobic conditions. The ease of switching between aerobic and anaerobic conditions and exposing the biofilms to antibiotics in situ seems a more appropriate method than recently published papers where anaerobically grown biofilms had to be removed (often by scraping, which has the risk of leaving resister cells behind) from the attachment surface and exposed to air for viability studies (Kim et al., 2009) especially if it is taken into account that anaerobic conditions often affects the mechanism of antibiotic action (Worlitzsch et al., 2002; Field et al., 2005; Hassett et al., 2009). In the same vein of antimicrobial treatment, various antibiotic surfaces (whether inherently so or treated) can be tested in evaluating growth of different organisms (pure culture or multi species).

Furthermore, with the CEMS it was possible to do a carbon balance over the reactor allowing the gathering of information regarding carbon channeling into the different fractions of the biofilm (cells, EPS, $CO_2$). This study revealed that under our experimental conditions, only a small fraction of influent carbon was sequestered to remain in the biofilm as cells and EPS while roughly 50 % was excreted as $CO_2$ giving a strong indication of the catalytic capacity of biofilms and underlining their usefulness in treatment systems where the breakdown of organic compounds are needed such as wastewater treatment systems and soil remediation. Modification of the CEMS or CMR may be necessary to be used as a routine online monitoring system of biofilms in industrial applications. To date it has proved useful as a laboratory tool to gain insight in the fundamental behaviour of biofilms. In the mass balance study with the CEMS it was seen that a percentage of the biofilm leaves the reactor as dense aggregates (cells attached to each other and EPS) and that the source of these aggregates (most probably the outer layer of the biofilm) possesses the ability to respond very quickly to more nutrient rich conditions possibly allowing the cells thus sloughed to adapt quickly to new downstream conditions as revealed by the CMR study).

Another area of application where the CEMS will be extremely useful is in the area of microbial cellulose utilization and subsequent conversion to biofuels. The combined ability of CEMS to operate under anaerobic conditions and the ability to perform a carbon balance, uniquely positions it to track metabolism and substrate capture of two of the most popular organisms earmarked for consolidated bioprocessing systems (Lynd et al., 2002); *Thermoanaerobacterium saccharolyticum* and *Clostridium thermocellum*.

The challenge that biofilms pose to researchers is that these structures have to be viewed constantly on 2 different planes, similar to wearing bifocals and having to focus near and far not to lose track of the fact that the average behaviour of a biofilm is in fact dependent on the behaviour of numerous small pockets of different cells. The combined effect of

all the individual components will certainly give rise to emergent properties similar to any complex system. Given this dichotomous nature of the challenge to study biofilms it might be prudent to combine a local investigation method (like microscopy) with a global method like $CO_2$ determination. Such a system has already been conceived in the form of a layered reactor where a flowcell will have one of its walls comprised of a silicone membrane making it possible to study the biofilm in situ microscopically while at the same time recording online metabolic data. This combinatory tool could then truly be considered as an example of a "bifocal" investigating method allowing the study of one biofilm both locally (with microscope) and globally (with $CO_2$ measurements).

# 7. Bibliography

F. Aboka, H. Yang, L. De Jonge, R. Kerste, W. Van Winden, W. Van Gulik, R. Hoogendijk, A. Oudshoorn, and J. Heijnen. Characterization of an experimental miniature bioreactor for cellular perturbation studies. *Biotechnol. Bioeng.*, 95(6):1032–1042, 2006.

D. G. Allison. The biofilm matrix. *Biofouling*, 19:139–150, 2003.

J. N. Anderl, J. Zahller, F. Roe, and P. S. Stewart. Role of nutrient limitation and stationary-phase existence in *Klebsiella pneumoniae* biofilm resistance to ampicillin and ciprofloxacin. *Antimicrob. Agents Chemother.*, 47(4):1251–1256, Apr 2003.

G. G. Anderson, S. Moreau-Marquis, B. A. Stanton, and G. A. O'Toole. In vitro analysis of tobramycin-treated *Pseudomonas aeruginosa* biofilms on cystic fibrosis-derived airway epithelial cells. *Infect. Immun.*, 76(4):1423–1433, Apr 2008.

J. M. Andrews. Determination of minimum inhibitory concentrations. *J. Antimicrob. Chemother.*, 48 Suppl 1:5–16, Jul 2001.

H. Anwar, M. Dasgupta, K. Lam, and J. W. Costerton. Tobramycin resistance of mucoid *Pseudomonas aeruginosa* biofilm grown under iron limitation. *J. Antimicrob. Chemother.*, 24(5):647–655, Nov 1989.

*ASTM F 2476 – 05 Standard Test Method for the Determination of Carbon Dioxide Gas Trans-*

*mission Rate ($CO_2$TR) Through Barrier Materials Using An Infrared Detector*. ASTM International.

M. Augustin, T. Ali-Vehmas, and F. Atroshi. Assessment of enzymatic cleaning agents and disinfectants against bacterial biofilms. *J. Pharm. Pharm. Sci.*, 7(1):55–64, 2004.

N. Bagge, O. Ciofu, L. T. Skovgaard, and N. Høiby. Rapid development in vitro and in vivo of resistance to ceftazidime in biofilm-growing *Pseudomonas aeruginosa* due to chromosomal $\beta$-lactamase. *APMIS*, 108(9):589–600, Sep 2000.

D. Banerjee and D. Stableforth. The treatment of respiratory *Pseudomonas* infection in cystic fibrosis: what drug and which way? *Drugs*, 60(5):1053–1064, Nov 2000.

E. Bester, G. Wolfaardt, L. Joubert, K. Garny, and S. Saftic. Planktonic-cell yield of a pseudomonad biofilm. *Appl. Environ. Microbiol.*, 71(12):7792–7798, 2005.

E. Bester, E. A. Edwards, and G. M. Wolfaardt. Planktonic cell yield is linked to biofilm development. *Can. J. Microbiol.*, 55(10):1195–1206, Oct 2009.

E. Bester, O. Kroukamp, G. M. Wolfaardt, L. Boonzaaier, and S. N. Liss. Metabolic differentiation in biofilms as indicated by carbon dioxide production rates. *Appl. Environ. Microbiol.*, 76(4):1189–1197, Feb 2010.

H. Beyenal, S. N. Chen, and Z. Lewandowski. The double substrate growth kinetics of *Pseudomonas aeruginosa*. *Enzyme Microb. Technol.*, 32(1):92–98, 2003.

T. Bjarnsholt, K. Kirketerp-Møller, P. Jensen, K. Madsen, R. Phipps, K. Krogfelt, N. Høiby, and M. Givskov. Why chronic wounds will not heal: A novel hypothesis. *Wound Repair Regen.*, 16(1):2–10, 2008.

H. Blanch and D. Clark. *Biochemical Engineering*. Marcel Dekker Inc, New York, 1996.

H. Bloemen, L. Wu, W. Van Gulik, J. Heijnen, and M. Verhaegen. Reconstruction of the $O_2$ uptake rate and $CO_2$ evolution rate on a time scale of seconds. *AIChE J.*, 49(7): 1895–1908, 2003.

B. R. Boles, M. Thoendel, and P. K. Singh. Self-generated diversity produces "insurance effects" in biofilm communities. *Proc. Natl. Acad. Sci. U. S. A.*, 101(47):16630–16635, Nov 2004.

H. P. J. Bonarius, C. D. de Gooijer, J. Tramper, and G. Schmid. Determination of the respiration quotient in mammalian-cell culture in bicarbonate buffered media. *Biotechnol. Bioeng.*, 45(6):524–535, March 1995.

G. Borriello, E. Werner, F. Roe, A. M. Kim, G. D. Ehrlich, and P. S. Stewart. Oxygen limitation contributes to antibiotic tolerance of *Pseudomonas aeruginosa* in biofilms. *Antimicrob. Agents Chemother.*, 48(7):2659–2664, 2004.

G. Borriello, L. Richards, G. D. Ehrlich, and P. S. Stewart. Arginine or nitrate enhances antibiotic susceptibility of *Pseudomonas aeruginosa* in biofilm. *Antimicrob. Agents Chemother.*, 50(1):382–38, 2006.

R. C. Boucher. Airway surface dehydration in cystic fibrosis: pathogenesis and therapy. *Annu. Rev. Med.*, 58:157–70, 2007.

M. Brown, D. Allison, and P. Gilbert. Resistance of bacterial biofilms to antibiotics: A growth-rate related effect? *J. Antimicrob. Chemother.*, 22(6):777–780, 1988.

Y. Cai, X.-H. Yu, R. Wang, M.-M. An, and B.-B. Liang. Effects of iron depletion on antimicrobial activities against planktonic and biofilm *Pseudomonas aeruginosa*. *J. Pharm. Pharmacol.*, 61(9):1257–1262, 2009.

D. Caldwell, D. Brannan, M. Morris, and M. Betlach. Quantitation of microbial growth on surfaces. *Microb. Ecol.*, 7(1):1–11, 1981.

C. R. Carere, R. Sparling, N. Cicek, and D. B. Levin. Third generation biofuels via direct cellulose fermentation. *Int J Mol Sci*, 9(7):1342–1360, Jun 2008.

H. Ceri, M. E. Olson, C. Stremick, R. R. Read, D. Morck, and A. Buret. The Calgary biofilm device: new technology for rapid determination of antibiotic susceptibilities of bacterial biofilms. *J. Clin. Microbiol.*, 37(6):1771–1776, Jun 1999.

H. Ceri, M. Olson, D. Morck, D. Storey, R. Read, A. Buret, and B. Olson. The MBEC assay system: multiple equivalent biofilms for antibiotic and biocide susceptibility testing. *Methods Enzymol.*, 337:377–385, 2001.

X.-S. Chai, C. Dong, and Y. Deng. In situ determination of bacterial growth by multiple headspace extraction gas chromatography. *Anal. Chem.*, 80(20):7820–7825, 2008.

J. F. Chmiel and P. B. Davis. State of the art: Why do the lungs of patients with cystic fibrosis become infected and why can't they clear the infection? *Respir. Res.*, 12:1–12, 2003.

D. J. Clark and O. Maaløe. DNA replication and the division cycle in *Escherichia coli*. *J. Mol. Biol.*, 23:99–112, 1967.

J. Costerton, Z. Lewandowski, D. Caldwell, D. Korber, and H. Lappin-Scott. Microbial biofilms. *Annu. Rev. Microbiol.*, 49:711–745, 1995.

P. Côté, J.-L. Bersillon, and A. Huyard. Bubble-free aeration using membranes: Mass transfer analysis. *J. Membr. Sci.*, 47(1-2):91–106, 1989.

C. Coufort, N. Derlon, J. Ochoa-Chaves, A. Liné, and E. Paul. Cohesion and detachment in biofilm systems for different electron acceptor and donors. *Water Sci Technol*, 55: 421–428, 2007. ISSN 0273-1223.

H. D. M. Coutinho, V. S. Falcão-Silva, and G. F. Gonçalves. Pulmonary bacterial pathogens in cystic fibrosis patients and antibiotic therapy: a tool for the health workers. *Int Arch Med*, 1(1):24, 2008.

S. K. Dahod. Dissolved carbon dioxide measurement and its correlation with operating parameters in fermentation processes. *Biotechnol. Prog.*, 9(6):655–660, 1993.

P. D. Damper and W. Epstein. Role of the membrane potential in bacterial resistance to aminoglycoside antibiotics. *Antimicrob. Agents Chemother.*, 20(6):803–808, Dec 1981.

D. Davies. Understanding biofilm resistance to antibacterial agents. *Nat. Rev. Drug Discov.*, 2(2):114–122, Feb 2003.

A. Delille, F. Quilès, and F. Humbert. In situ monitoring of the nascent *Pseudomonas fluorescens* biofilm response to variations in the dissolved organic carbon level in low-nutrient water by attenuated total reflectance-Fourier transform infrared spectroscopy. *Appl. Environ. Microbiol.*, 73(18):5782–5788, Sep 2007.

N. Derlon, A. Massé, R. Escudié, N. Bernet, and E. Paul. Stratification in the cohesion of biofilms grown under various environmental conditions. *Water Res.*, 42(8-9):2102–2110, 2008.

V. Dindore, D. Brilman, P. Feron, and G. Versteeg. $CO_2$ absorption at elevated pressures using a hollow fiber membrane contactor. *J. Membr. Sci.*, 235(1-2):99–109, 2004.

R. M. Donlan. Biofilms: microbial life on surfaces. *Emerg Infect Dis*, 8(9):881–890, Sep 2002.

G. Döring, S. P. Conway, H. G. Heijerman, M. E. Hodson, N. Høiby, A. Smyth, and D. J. Touw. Antibiotic therapy against *Pseudomonas aeruginosa* in cystic fibrosis: a European consensus. *Eur. Respir. J.*, 16(4):749–767, Oct 2000.

P. Dřímal, J. Hrnčiřík, and J. Hoffmann. Assessing aerobic biodegradability of plastics in aqueous environment by GC-analyzing composition of equilibrium gaseous phase. *J. Polym. Environ.*, 14(3):309–316, 2006.

J. Elkins, D. Hassett, P. Stewart, H. Schweizer, and T. McDermott. Protective role of catalase in *Pseudomonas aeruginosa* biofilm resistance to hydrogen peroxide. *Appl. Environ. Microbiol.*, 65(10):4594–4600, 1999.

B. Ellis, P. Butterfield, W. Jones, G. McFeters, and A. Camper. Effects of carbon source, carbon concentration, and chlorination on growth related parameters of heterotrophic biofilm bacteria. *Microb. Ecol.*, 38:330–347, 2000.

M. Eschbach, K. Schreiber, K. Trunk, J. Buer, D. Jahn, and M. Schobert. Long-term anaerobic survival of the opportunistic pathogen *Pseudomonas aeruginosa* via pyruvate fermentation. *J. Bacteriol.*, 186(14):4596–4604, 2004.

T. R. Field, A. White, J. S. Elborn, and M. M. Tunney. Effect of oxygen limitation on the in vitro antimicrobial susceptibility of clinical isolates of *Pseudomonas aeruginosa* grown planktonically and as biofilms. *Eur. J. Clin. Microbiol. Infect. Dis.*, 24:677–687, 2005.

M. J. Filiatrault, K. F. Picardo, H. Ngai, L. Passador, and B. H. Iglewski. Identification of *Pseudomonas aeruginosa* genes involved in virulence and anaerobic growth. *Infect. Immun.*, 74:4237–4245, 2006.

H. C. Flemming. Role and levels of real-time monitoring for successful anti-fouling strategies–an overview. *Water Sci Technol*, 47(5):1–8, 2003.

M. Fletcher. Measurement of glucose utilization by *Pseudomonas fluorescens* that are free-living and that are attached to surfaces. *Appl. Environ. Microbiol.*, 52(4):672–676, Oct 1986.

B. Frahm, H.-C. Blank, P. Cornand, W. Oelßner, U. Guth, P. Lane, A. Munack, K. Johannsen, and R. Pörtner. Determination of dissolved $CO_2$ concentration and $CO_2$ production rate of mammalian cell suspension culture based on off-gas measurement. *J. Biotechnol.*, 99(2):133–148, Oct 2002.

C. Freeman and M. Lock. [$^3$H]thymidine incorporation as a measure of bacterial growth within intact river biofilms. *Sci. Total Environ.*, 138(1-3):161–167, 1993.

C. Freeman and M. Lock. Isotope dilution analysis and rates of $^{32}$P incorporation into phospholipid as a measure of microbial growth rates in biofilms. *Water Res.*, 29(3): 789–792, 1995.

R. Fukushima, P. Weimer, and D. Kunz. Use of photocatalytic reduction to hasten preparation of culture media for saccharolytic *Clostridium* species. *Brazilian Journal of Microbiology*, 34(1):22–26, 2003.

C. A. Fux, J. W. Costerton, P. S. Stewart, and P. Stoodley. Survival strategies of infectious biofilms. *Trends Microbiol*, 13(1):34–40, Jan 2005.

G. G. Geesey, R. Mutch, J. W. Costerton, and R. B. Green. Sessile bacteria: An important component of the microbial population in small mountain streams. *Limnol. Oceanogr.*, 23(6):1214–1223, 1978.

P. Gilbert, P. Collier, and M. Brown. Influence of growth rate on susceptibility to antimicrobial agents: Biofilms, cell cycle, dormancy, and stringent response. *Antimicrob. Agents Chemother.*, 34(10):1865–1868, 1990.

J. Gillooly, J. Brown, G. West, V. Savage, and E. Charnov. Effects of size and temperature on metabolic rate. *Science*, 293(5538):2248–2251, 2001.

C. Gómez-Suárez, H. J. Busscher, and H. C. van der Mei. Analysis of bacterial detachment from substratum surfaces by the passage of air-liquid interfaces. *Appl. Environ. Microbiol.*, 67(6):2531–2537, Jun 2001.

S. Govender, V. Pillay, and B. Odhav. Nutrient manipulation as a basis for enzyme production in a gradostat bioreactor. *Enzyme Microb. Technol.*, 46:603–609, 2010.

K. Grobe, J. Zahller, and P. Stewart. Role of dose concentration in biocide efficacy against *Pseudomonas aeruginosa* biofilms. *J. Ind. Microbiol. Biotechnol.*, 29(1):10–15, 2002.

R. Gross, B. Hauer, K. Otto, and A. Schmid. Microbial biofilms: new catalysts for maximizing productivity of long-term biotransformations. *Biotechnol. Bioeng.*, 98(6):1123–1134, Dec 2007.

C. Haisch and R. Niessner. Visualisation of transient processes in biofilms by optical coherence tomography. *Water Res.*, 41(11):2467–2472, 2007.

S. K. Hansen, J. A. J. Haagensen, M. Gjermansen, T. M. Jørgensen, T. Tolker-Nielsen, and S. Molin. Characterization of a *Pseudomonas putida* rough variant evolved in a mixed-species biofilm with *Acinetobacter* sp. strain C6$^{\nabla}$. *J. Bacteriol.*, 189(13):4932–4943, 2007a.

S. K. Hansen, P. B. Rainey, J. A. J. Haagensen, and S. Molin. Evolution of species interactions in a biofilm community. *Nature*, 445(7127):533–536, Feb 2007b.

W. Harder and L. Dijkhuizen. Physiological responses to nutrient limitation. *Annu. Rev. Microbiol.*, 37:1–23, 1983.

J. Harrison. *Multimetal resistance and tolerance in microbial biofilms*. PhD thesis, University of Calgary (Canada), 2008.

J. J. Harrison, R. J. Turner, and H. Ceri. Persister cells, the biofilm matrix and tolerance

to metal cations in biofilm and planktonic *Pseudomonas aeruginosa*. *Environ. Microbiol.*, 7(7):981–994, Jul 2005a.

J. J. Harrison, R. J. Turner, and H. Ceri. High-throughput metal susceptibility testing of microbial biofilms. *BMC Microbiol.*, 5:53, 2005b.

D. J. Hassett, J. Cuppoletti, B. Trapnell, S. V. Lymar, J. J. Rowe, S. S. Yoon, G. M. Hilliard, K. Parvatiyar, M. C. Kamani, D. J. Wozniak, S. H. Hwang, T. R. McDermott, and U. A. Ochsner. Anaerobic metabolism and quorum sensing by *Pseudomonas aeruginosa* biofilms in chronically infected cystic fibrosis airways: rethinking antibiotic treatment strategies and drug targets. *Adv Drug Deliv Rev*, 54(11):1425–1443, Dec 2002.

D. J. Hassett, M. D. Sutton, M. J. Schurr, A. B. Herr, C. C. Caldwell, and J. O. Matu. *Pseudomonas aeruginosa* hypoxic or anaerobic biofilm infections within cystic fibrosis airways. *Trends Microbiol.*, 17(3):130–138, Mar 2009.

P. Hatzinger, P. Palmer, R. Smith, C. Peñarrieta, and T. Yoshinari. Applicability of tetrazolium salts for the measurement of respiratory activity and viability of groundwater bacteria. *J. Microbiol. Methods*, 52(1):47–58, 2003.

M. Hausner and S. Wuertz. High rates of conjugation in bacterial biofilms as determined by quantitative in situ analysis. *Appl. Environ. Microbiol.*, 65(8):3710–3713, Aug 1999.

M. Hentzer, G. Teitzel, G. Balzer, A. Heydorn, S. Molin, M. Givskov, and M. Parsek. Alginate overproduction affects *Pseudomonas aeruginosa* biofilm structure and function. *J. Bacteriol.*, 183:5395–5401, 2001.

M. Hentzer, H. Wu, J. Andersen, K. Riedel, T. Rasmussen, N. Bagge, N. Kumar, M. Schembri, Z. Song, P. Kristoffersen, M. Manefield, J. Costerton, S. Molin, L. Eberl, P. Steinberg, S. Kjelleberg, N. Høiby, and M. Givskov. Attenuation of *Pseudomonas aeruginosa* virulence by quorum sensing inhibitors. *EMBO J.*, 22(15):3803–3815, 2003.

A. Heydorn, A. T. Nielsen, M. Hentzer, C. Sternberg, M. Givskov, B. K. Ersbøll, and S. Molin. Quantification of biofilm structures by the novel computer program COMSTAT. *Microbiology-UK*, 146:2395–2407, 2000.

A. Heydorn, B. Ersbøll, J. Kato, M. Hentzer, M. R. Parsek, T. Tolker-Nielsen, M. Givskov, and S. Molin. Statistical analysis of *Pseudomonas aeruginosa* biofilm development: impact of mutations in genes involved in twitching motility, cell-to-cell signaling, and stationary-phase sigma factor expression. *Appl. Environ. Microbiol.*, 68(4):2008–2017, Apr 2002.

D. Hill, B. Rose, A. Pajkos, M. Robinson, P. Bye, S. Bell, M. Elkins, B. Thompson, C. Macleod, S. D. Aaron, and C. Harbour. Antibiotic susceptabilities of *Pseudomonas aeruginosa* isolates derived from patients with cystic fibrosis under aerobic, anaerobic, and biofilm conditions. *J. Clin. Microbiol.*, 43(10):5085–5090, Oct 2005.

J. E. Hobbie, R. J. Daley, and S. Jasper. Use of nuclepore filters for counting bacteria by fluorescence microscopy. *Appl. Environ. Microbiol.*, 33(5):1225–1228, May 1977.

E. Hoffman. *Membrane separations technology : single-stage, multistage, and differential permeation*. Gulf Professional Publishing, Amsterdam, 2003.

N. Høiby, T. Bjarnsholt, M. Givskov, S. Molin, and O. Ciofu. Antibiotic resistance of bacterial biofilms. *Int. J. Antimicrob. Agents*, 35(4):322–332, 2010.

S. Hota, Z. Hirji, K. Stockton, C. Lemieux, H. Dedier, G. Wolfaardt, and M. A. Gardam. Outbreak of multidrug-resistant *Pseudomonas aeruginosa* colonization and infection secondary to imperfect intensive care unit room design. *Infect. Control Hosp. Epidemiol.*, 30 (1):25–33, Jan 2009.

C. Huang, F. Yu, G. McFeters, and P. Stewart. Nonuniform spatial patterns of respiratory

activity within biofilms during disinfection. *Appl. Environ. Microbiol.*, 61(6):2252–2256, 1995.

K. Ismail, K. Winkley, D. Stahl, T. Chalder, and M. Edmonds. A cohort study of people with diabetes and their first foot ulcer: The role of depression on mortality. *Diabetes Care*, 30(6):1473–1479, 2007.

G. A. James, E. Swogger, R. Wolcott, E. deLancey Pulcini, P. Secor, J. Sestrich, J. W. Costerton, and P. S. Stewart. Biofilms in chronic wounds. *Wound Repair Regen.*, 16(1):37–44, 2008.

A. Jang, S. Okabe, Y. Watanabe, I. Kim, and P. Bishop. Measurement of growth rate of ammonia oxidizing bacteria in partially submerged rotating biological contactor by fluorescent in situ hybridization (FISH). *Journal of Environmental Engineering and Science*, 4 (5):413–420, 2005.

P. Janknecht and L. F. Melo. Online biofilm monitoring. *Reviews in Environmental Science and Bio/Technology*, 2:269–283, 2003.

K. K. Jefferson. What drives bacteria to produce a biofilm? *FEMS Microbiol. Lett.*, 236: 163–173, 2004.

D. Jenkins and A. Krishnan. Surface limitations for gas transport through a silicone film. In *ASAE Annual International Meeting 2004*, pages 3973–3984, University of Hawaii, 2004.

R. P. Jones and P. F. Greenfield. Effect of carbon dioxide on yeast growth and fermentation. *Enzyme Microb. Technol.*, 4(4):210–223, 1982.

J. W. N. M. Kappelhof, H. S. Vrouwenvelder, M. Schaap, J. C. Kruithof, D. Van Der Kooij, and J. C. Schippers. An in situ biofouling monitor for membrane systems. *Water Science and Technology: Water Supply*, 3(5-6):205–210, 2003.

D. Karakashev, D. Galabova, and I. Simeonov. A simple and rapid test for differentiation of aerobic from anaerobic bacteria. *World Journal of Microbiology and Biotechnology*, 19(3): 233–238, 2003.

I. Keren, N. Kaldalu, A. Spoering, Y. Wang, and K. Lewis. Persister cells and tolerance to antimicrobials. *FEMS Microbiol. Lett.*, 230(1):13–18, Jan 2004a.

I. Keren, D. Shah, A. Spoering, N. Kaldalu, and K. Lewis. Specialized persister cells and the mechanism of multidrug tolerance in *Escherichia coli*. *J. Bacteriol.*, 186(24):8172–8180, Dec 2004b.

T. R. D. Kievit, M. D. Parkins, R. J. Gillis, R. Srikumar, H. Ceri, K. Poole, B. H. Iglewski, and D. G. Storey. Multidrug efflux pumps: expression patterns and contribution to antibiotic resistance in *Pseudomonas aeruginosa* biofilms. *Antimicrob. Agents Chemother.*, 45(6):1761–1770, Jun 2001.

E.-J. Kim, W. Sabra, and A.-P. Zeng. Iron deficiency leads to inhibition of oxygen transfer and enhanced formation of virulence factors in cultures of *Pseudomonas aeruginosa* PA01. *Microbiology*, 149(Pt 9):2627–2634, Sep 2003.

J. Kim, J.-S. Hahn, M. J. Franklin, P. S. Stewart, and J. Yoon. Tolerance of dormant and active cells in *Pseudomonas aeruginosa* PA01 biofilm to antimicrobial agents. *J. Antimicrob. Chemother.*, 63(1):129–135, January 2009.

J. Klahre and H.-C. Flemming. Monitoring of biofouling in papermill process waters. *Water Res.*, 34(14):3657–3665, 2000.

B. Klayman, I. Klapper, P. Stewart, and A. Camper. Measurements of accumulation and displacement at the single cell cluster level in *Pseudomonas aeruginosa* biofilms. *Environ. Microbiol.*, 10(9):2344–2354, 2008.

D. R. Korber, A. Choi, G. M. Wolfaardt, S. C. Ingham, and D. E. Caldwell. Substratum topography influences susceptibility of *Salmonella enteritidis* biofilms to trisodium phosphate. *Appl. Environ. Microbiol.*, 63(9):3352–3358, Sep 1997.

A. Kraigsley and S. Finkel. Adaptive evolution in single species bacterial biofilms: Research letter. *FEMS Microbiol. Lett.*, 293(1):135–140, 2009.

J.-U. Kreft. Conflicts of interest in biofilms. *Biofilms*, 1:265–276, 2004.

O. Kroukamp and G. Wolfaardt. $CO_2$ production as an indicator of biofilm metabolism. *Appl. Environ. Microbiol.*, 75(13):4391–4397, 2009.

O. Kroukamp, R. G. Dumitrache, and G. M. Wolfaardt. Nature of inoculum has a pronounced effect on biofilm development in flow systems. *Appl. Environ. Microbiol.*, 76 (18):6025–6031, 2010.

A. Kumar, J. Dewulf, and H. Van Langenhove. Membrane-based biological waste gas treatment. *Chemical Engineering Journal*, 136(2-3):82–91, 2008.

C. S. Laspidou and B. E. Rittmann. A unified theory for extracellular polymeric substances, soluble microbial products, and active and inert biomass. *Water Res.*, 36:2711–2720, 2002.

J. Lawrence, D. Korber, G. Wolfaardt, and D. Caldwell. Behavioural strategies of surface colonizing bacteria. In *Advances in Microbial Ecology*, volume 14, pages 1–75, 1995.

H. Lee, D. Han, S. Lee, J. Yoo, S. Baek, and E. Lee. On-line monitoring and quantitative analysis of biofouling in low-velocity cooling water system. *Korean J. Chem. Eng.*, 15(1): 71–77, 1998.

J.-H. Lee, Y. Seo, T.-S. Lim, P. Bishop, and I. Papautsky. MEMS needle-type sensor array

for in situ measurements of dissolved oxygen and redox potential. *Environ. Sci. Technol.*, 41(22):7857–7863, 2007.

A. Lenz, K. Williamson, B. Pitts, P. Stewart, and M. Franklin. Localized gene expression in *Pseudomonas aeruginosa* biofilms. *Appl. Environ. Microbiol.*, 74(14):4463–4471, 2008.

Z. Lewandowski and H. Beyenal. Biofilm monitoring: a perfect solution in search of a problem. *Water Sci Technol*, 47(5):9–18, 2003.

Z. Lewandowski, H. Beyenal, and D. Stookey. Reproducibility of biofilm processes and the meaning of steady state in biofilm reactors. *Water Sci Technol*, 49(11-12):359–364, 2004.

Y. Liu, Y.-M. Lin, S.-F. Yang, and J.-H. Tay. A balanced model for biofilms developed at different growth and detachment forces. *Process Biochemistry*, 38(12):1761–1765, 2003.

M. Ludensky. An automated system for biocide testing on biofilms. *J. Ind. Microbiol. Biotechnol.*, 20(2):109–115, 1998.

M. Lunau, A. Lemke, K. Walther, W. Martens-Habbena, and M. Simon. An improved method for counting bacteria from sediments and turbid environments by epifluorescence microscopy. *Environ. Microbiol.*, 7(7):961–968, Jul 2005.

L. R. Lynd, P. J. Weimer, W. H. van Zyl, and I. S. Pretorius. Microbial cellulose utilization: fundamentals and biotechnology. *Microbiol. Mol. Biol. Rev.*, 66(3):506–577, Sep 2002.

T.-F. Mah, B. Pitts, B. Pellock, G. C. Walker, P. S. Stewart, and G. A. O'Toole. A genetic basis for *Pseudomonas aeruginosa* biofilm antibiotic resistance. *Nature*, 426(6964):306–310, Nov 2003.

A. Mangalappalli-Illathu, J. Lawrence, and D. Korber. Cells in shearable and nonshearable regions of *Salmonella enterica* serovar enteritidis biofilms are morphologically and physiologically distinct. *Can. J. Microbiol.*, 55(8):955–966, 2009.

C. Marques, V. Salisbury, J. Greenman, K. Bowker, and S. Nelson. Discrepancy between viable counts and light output as viability measurements, following ciprofloxacin challenge of self-bioluminescent *Pseudomonas aeruginosa* biofilms. *J. Antimicrob. Chemother.*, 56(4):665–671, 2005.

K. Marshall, R. Stout, and R. Mitchell. Selective sorption of bacteria from seawater. *Can. J. Microbiol.*, 17(11):1413–1416, 1971.

R. Massana, J. M. Gasol, P. K. Bjørnsen, N. Blackburn, A. Hagström, S. Hietanen, B. H. Hygum, J. Kuparinen, and C. Pedrós-Alió. Measurement of bacterial size via image analysis of epifluorescence preparations: description of an inexpensive system and solutions to some of the most common problems. *Scientia Marina*, 61(3):397–407, September 1997.

R. Maurício, C. Dias, and F. Santana. Monitoring biofilm thickness using a non-destructive, on-line, electrical capacitance technique. *Environmental Monitoring and Assessment*, 119(1-3):599–607, 2006.

M. Mavroudi, S. Kaldis, and G. Sakellaropoulos. A study of mass transfer resistance in membrane gas-liquid contacting processes. *J. Membr. Sci.*, 272(1-2):103–115, 2006.

T. B. May, D. Shinabarger, R. Maharaj, J. Kato, L. Chu, J. D. DeVault, S. Roychoudhury, N. A. Zielinski, A. Berry, and R. K. Rothmel. Alginate synthesis by *Pseudomonas aeruginosa*: a key pathogenic factor in chronic pulmonary infections of cystic fibrosis patients. *Clin. Microbiol. Rev.*, 4(2):191–206, Apr 1991.

E. McAdam and S. Judd. A review of membrane bioreactor potential for nitrate removal from drinking water. *Desalination*, 196(1-3):135–148, 2006.

G. McFeters, F. Yu, B. Pyle, and P. Stewart. Physiological methods to study biofilm disinfection. *J. Ind. Microbiol.*, 15(4):333–338, 1995.

A. McKay, A. Peters, and J. Wimpenny. Determining specific growth rates in different regions of *Salmonella typhimurium* colonies. *Lett. Appl. Microbiol.*, 24(1):74–76, 1997.

J. Merritt, J. Kreth, F. Qi, R. Sullivan, and W. Shi. Non-disruptive, real-time analyses of the metabolic status and viability of *Streptococcus mutans* cells in response to antimicrobial treatments. *J. Microbiol. Methods*, 61(2):161–170, May 2005.

K. Milferstedt, M.-N. Pons, and E. Morgenroth. Optical method for long-term and large-scale monitoring of spatial biofilm development. *Biotechnol. Bioeng.*, 94(4):773–782, Jul 2006.

A. Mollica and P. Cristiani. On-line biofilm monitoring by "BIOX" electrochemical probe. *Water Science and Technology*, 47(5):45–49, 2003.

R. D. Monds and G. A. O'Toole. The developmental model of microbial biofilms: ten years of a paradigm up for review. *Trends Microbiol.*, 17(2):73–87, Feb 2009.

J. Monod. The growth of bacterial cultures. *Annu. Rev. Microbiol.*, 3:371–394, 1949.

S. Moreau-Marquis, B. A. Stanton, and G. A. O'Toole. *Pseudomonas aeruginosa* biofilm formation in the cystic fibrosis airway. *Pulm. Pharmacol. Ther.*, 21(4):595–599, Aug 2008.

S. Moreau-Marquis, G. A. O'Toole, and B. A. Stanton. Tobramycin and FDA-approved iron chelators eliminate *Pseudomonas aeruginosa* biofilms on cystic fibrosis cells. *Am. J. Respir. Cell Mol. Biol.*, 41(3):305–313, Sep 2009.

S. Mudliar, B. Giri, K. Padoley, D. Satpute, R. Dixit, P. Bhatt, R. Pandey, A. Juwarkar, and A. Vaidya. Bioreactors for treatment of VOCs and odours - a review. *J Environ Manage*, 91(5):1039–1054, May 2010.

R. Mueller. Bacterial transport and colonization in low nutrient environments. *Water Res.*, 30(11):2681–2690, 1996.

R. Mueller, W. Characklis, W. Jones, and J. Sears. Characterization of initial events in bacterial surface colonization by two *Pseudomonas* species using image analysis. *Biotechnol. Bioeng.*, 39(11):1161–1170, 1992.

M. Mulder. *Basic principles of membrane technology*. Kluwer Academic, Dordrecht, 2nd edition, 1996.

L. Novák, L. Larrea, and J. Wanner. Estimation of maximum specific growth rate of heterotrophic and autotrophic biomass: A combined technique of mathematical modelling and batch cultivations. *Water Science and Technology*, 30(11):171–180, 1994.

T. Nozawa, T. Tanikawa, H. Hasegawa, C. Takahashi, Y. Ando, M. Matsushita, Y. Nakagawa, and T. Matsuyama. Rhamnolipid-dependent spreading growth of *Pseudomonas aeruginosa* on a high-agar medium: marked enhancement under $co_2$-rich anaerobic conditions. *Microbiol. Immunol.*, 51(8):703–712, 2007.

M. E. Olson, H. Ceri, D. W. Morck, A. G. Buret, and R. R. Read. Biofilm bacteria: formation and comparative susceptibility to antibiotics. *Can. J. Vet. Res.*, 66(2):86–92, Apr 2002.

G. A. O'Toole and R. Kolter. Flagellar and twitching motility are necessary for *Pseudomonas aeruginosa* biofilm development. *Mol. Microbiol.*, 30:295–304, 1998.

S. Pamp, M. Gjermansen, H. Johansen, and T. Tolker-Nielsen. Tolerance to the antimicrobial peptide colistin in *Pseudomonas aeruginosa* biofilms is linked to metabolically active

cells, and depends on the *pmr* and *mexAB-oprM* genes. *Mol. Microbiol.*, 68(1):223–240, 2008.

S. J. Pamp, C. Sternberg, and T. Tolker-Nielsen. Insight into the microbial multicellular lifestyle via flow-cell technology and confocal microscopy. *Cytometry A*, 75(2):90–103, Feb 2009.

M. R. Parsek and P. K. Singh. Bacterial biofilms: an emerging link to disease pathogenesis. *Annu. Rev. Microbiol.*, 57:677–701, 2003.

M. Pereira, M. Kuehn, S. Wuertz, T. Neu, and L. Melo. Effect of flow regime on the architecture of a *Pseudomonas fluorescens* biofilm. *Biotechnol. Bioeng.*, 78(2):164–171, 2002.

C. Picioreanu, M. V. Loosdrecht, and J. Heijnen. Modelling and predicting biofilm structure. In D. Allison, P. Gilbert, H. Lappin-Scott, and M. Wilson, editors, *Community structure and co-operation in biofilms*, pages 129–166, Cambridge, 2000. Cambridge University Press.

J. Pietikäinen, M. Pettersson, and E. Bååth. Comparison of temperature effects on soil respiration and bacterial and fungal growth rates. *FEMS Microbiol. Ecol.*, 52(1):49–58, 2005.

T. Posch, M. Loferer-Krößbacher, G. Gao, A. Alfreider, J. Pernthaler, and R. Psenner. Precision of bacterioplankton biomass determination: a comparison of two fluorescent dyes, and of allometric and linear volume-to-carbon conversion factors. *Aquatic Microbial Ecology*, 25(1):55–63, August 2001.

N. Qureshi, B. A. Annous, T. C. Ezeji, P. Karcher, and I. S. Maddox. Biofilm reactors for industrial bioconversion processes: employing potential of enhanced reaction rates. *Microb Cell Fact*, 4:24, Aug 2005.

S. R. Ragusa, D. McNevin, S. Qasem, and C. Mitchell. Indicators of biofilm development and activity in constructed wetlands microcosms. *Water Res.*, 38(12):2865–2873, 2004.

S. A. Rani, B. Pitts, H. Beyenal, R. A. Veluchamy, Z. Lewandowski, W. M. Davison, K. Buckingham-Meyer, and P. S. Stewart. Spatial patterns of DNA replication, protein synthesis, and oxygen concentration within bacterial biofilms reveal diverse physiological states. *J. Bacteriol.*, 189(11):4223–4233, Jun 2007.

D. W. Reid, G. J. Anderson, and I. L. Lamont. Cystic fibrosis: ironing out the problem of infection? *Am J Physiol Lung Cell Mol Physiol*, 295(1):L23–L24, Jul 2008.

A. Rice, M. Hamilton, and A. Camper. Apparent surface associated lag time in growth of primary biofilm cells. *Microb. Ecol.*, 41:8–15, 2000.

J. Richards and C. Melander. Small molecule approaches toward the non-microbicidal modulation of bacterial biofilm growth and maintenance. *Anti-Infective Agents in Medicinal Chemistry*, 8(4):295–314, 2009.

L. Richter, C. Stepper, A. Mak, A. Reinthaler, R. Heer, M. Kast, H. Brückl, and P. Ertl. Development of a microfluidic biochip for online monitoring of fungal biofilm dynamics. *Lab on a Chip - Miniaturisation for Chemistry and Biology*, 7(12):1723–1731, 2007.

V. Riis, H. Lorbeer, and W. Babel. Extraction of microorganisms from soil: Evaluation of the efficiency by counting methods and activity measurements. *Soil Biology and Biochemistry*, 30(12):1573–1581, 1998.

W. Robb. Thin silicone membranes–their permeation properties and some applications. *Ann. N. Y. Acad. Sci.*, 146(1):119–137, 1968.

M. E. Roberts and P. S. Stewart. Modeling antibiotic tolerance in biofilms by accounting for nutrient limitation. *Antimicrob. Agents Chemother.*, 48(1):48–52, Jan 2004.

G. B. Rogers, M. P. Carroll, D. J. Serisier, P. M. Hockey, V. Kehagia, G. R. Jones, and K. D. Bruce. Bacterial activity in cystic fibrosis lung infections. *Respir. Res.*, 6:49, 2005.

C. Rollet, L. Gal, and J. Guzzo. Biofilm-detached cells, a transition from a sessile to a planktonic phenotype: a comparative study of adhesion and physiological characteristics in *Pseudomonas aeruginosa*. *FEMS Microbiol. Lett.*, 290(2):135–142, Jan 2009.

B. Rosche, X. Z. Li, B. Hauer, A. Schmid, and K. Buehler. Microbial biofilms: a concept for industrial catalysis? *Trends Biotechnol.*, 27(11):636–643, Nov 2009.

J. B. Russell and G. M. Cook. Energetics of bacterial growth: balance of anabolic and catabolic reactions. *Microbiol. Rev.*, 59:48–62, 1995.

K. Sauer, A. K. Camper, G. D. Ehrlich, J. W. Costerton, and D. G. Davies. *Pseudomonas aeruginosa* displays multiple phenotypes during development as a biofilm. *J. Bacteriol.*, 184(4):1140–1154, 2002.

M. Scatamburlo Moreira, E. De Souza, and C. De Moraes. Multidrug efflux systems in gram-negative bacteria. *Brazilian Journal of Microbiology*, 35(1-2):19–28, 2004.

T. Schmid, U. Panne, J. Adams, and R. Niessner. Investigation of biocide efficacy by photoacoustic biofilm monitoring. *Water Res.*, 38(5):1189–1196, 2004.

M. Schulz and A. Schmoldt. Therapeutic and toxic blood concentrations of more than 500 drugs. *Pharmazie*, 52(12):895–911, Dec 1997.

A. Schumpe, G. Quicker, and W.-D. Deckwer. Gas solubilities in microbial culture media. In A. Fiechter, editor, *Reaction Engineering*, volume 24 of *Advances in Biochemical Engineering/Biotechnology*, pages 1–38, Berlin, 1982. Springer-Verlag.

C. Seneviratne, W. Silva, L. Jin, Y. Samaranayake, and L. Samaranayake. Architectural analysis, viability assessment and growth kinetics of *Candida albicans* and *Candida glabrata* biofilms. *Arch. Oral Biol.*, 54(11):1052–1060, 2009.

J. Seymour, S. Codd, E. Gjersing, and P. Stewart. Magnetic resonance microscopy of biofilm structure and impact on transport in a capillary bioreactor. *J. Magn. Reson.*, 167(2):322–327, 2004.

J. A. Shapiro. Thinking about bacterial populations as multicellular organisms. *Annu. Rev. Microbiol.*, 52:81–104, 1998.

P.-C. Shih and C.-T. Huang. Effects of quorum-sensing deficiency on *Pseudomonas aeruginosa* biofilm formation and antibiotic resistance. *J. Antimicrob. Chemother.*, 49(2):309–314, Feb 2002.

M. Simões, M. Pereira, and M. Vieira. Validation of respirometry as a short-term method to assess the efficacy of biocides. *Biofouling*, 21(1):9–17, 2005.

K. Sirkar. Other new membrane processes. In W. W. Ho and K. Sirkar, editors, *Membrane Handbook*, pages 885–912, NY, 1992. Van Nostrand Reinhold.

K. Smith and I. S. Hunter. Efficacy of common hospital biocides with biofilms of multidrug resistant clinical isolates. *J. Med. Microbiol.*, 57(Pt 8):966–973, Aug 2008.

E. Spaeth and S.K.Friedlander. The diffusion of oxygen, carbon dioxide, and inert gas in flowing blood. *Biophys. J.*, 7:827–851, 1967.

A. L. Spoering and K. Lewis. Biofilms and planktonic cells of *Pseudomonas aeruginosa* have similar resistance to killing by antimicrobials. *J. Bacteriol.*, 183(23):6746–6751, Dec 2001.

A. M. Spormann. Physiology of microbes in biofilms. In T. Romeo, editor, *Bacterial biofilms*, pages 17–36, Berlin, Germany., 2008. Springer.

C. Sternberg, B. B. Christensen, T. Johansen, A. T. Nielsen, J. B. Andersen, M. Givskov, and S. Molin. Distribution of bacterial growth activity in flow-chamber biofilms. *Appl. Environ. Microbiol.*, 65(9):4108–4117, Sep 1999.

P. Stewart. A model of biofilm detachment. *Biotechnol. Bioeng.*, 41(1):111–117, 1993.

P. Stewart, R. Murga, R. Srinivasan, and D. De Beer. Biofilm structural heterogeneity visualized by three microscopic methods. *Water Res.*, 29(8):2006–2009, 1995.

P. S. Stewart. Mechanisms of antibiotic resistance in bacterial biofilms. *Int. J. Med. Microbiol.*, 292(2):107–113, Jul 2002.

P. S. Stewart. Diffusion in biofilms. *J. Bacteriol.*, 185(5):1485–1491, Mar 2003.

P. S. Stewart and M. J. Franklin. Physiological heterogeneity in biofilms. *Nat. Rev. Microbiol.*, 6(3):199–210, Mar 2008.

P. S. Stewart, T. Griebe, R. Srinivasan, C. I. Chen, F. P. Yu, D. deBeer, and G. A. McFeters. Comparison of respiratory activity and culturability during monochloramine disinfection of binary population biofilms. *Appl. Environ. Microbiol.*, 60(5):1690–1692, May 1994.

P. Stoodley, K. Sauer, D. G. Davies, and J. Costerton. Biofilms as complex differentiated communities. *Annu. Rev. Microbiol.*, 56:187–209, 2002.

N. Sufya, D. G. Allison, and P. Gilbert. Clonal variation in maximum specific growth rate and susceptibility towards antimicrobials. *J. Appl. Microbiol.*, 95(6):1261–1267, 2003.

S.-P. Sun, C. Nàcher, B. Merkey, Q. Zhou, S.-Q. Xia, D.-H. Yang, J.-H. Sun, and B. Smets. Effective biological nitrogen removal treatment processes for domestic wastewaters with low C/N ratios: A review. *Environ. Eng. Sci.*, 27(2):111–126, 2010.

B. Szomolay, I. Klapper, J. Dockery, and P. S. Stewart. Adaptive responses to antimicrobial agents in biofilms. *Environ. Microbiol.*, 7(8):1186–1191, Aug 2005.

K. Tam, N. Kinsinger, P. Ayala, F. Qi, W. Shi, and N. V. Myung. Real-time monitoring of *Streptococcus mutans* biofilm formation using a quartz crystal microbalance. *Caries Res.*, 41(6):474–483, 2007.

A. Tamachkiarow and H.-C. Flemming. On-line monitoring of biofilm formation in a brewery water pipeline system with a fibre optical device. *Water Science and Technology*, 47(5):19–24, 2003.

Y. Tanji, T. Nishihara, and K. Miyanaga. Monitoring of biofilm in cooling water system by measuring lactic acid consumption rate. *Biochemical Engineering Journal*, 35(1):81–86, July 2007.

M. Teixeira De Mattos and O. Neijssel. Bioenergetic consequences of microbial adaptation to low-nutrient environments. *J. Biotechnol.*, 59(1-2):117–126, 1997.

U. Telgmann, H. Horn, and E. Morgenroth. Influence of growth history on sloughing and erosion from biofilms. *Water Res.*, 38(17):3671–3684, Oct 2004.

Tolker-Nielsen and Molin. Spatial organization of microbial biofilm communities. *Microb. Ecol.*, 40(2):75–84, Aug 2000.

F. Touratier, L. Legendre, and A. Vézina. Model of bacterial growth influenced by substrate C : N ratio and concentration. *Aquatic Microbial Ecology*, 19(2):105–118, 1999.

A. Trampuz and A. F. Widmer. Hand hygiene: a frequently missed lifesaving opportunity during patient care. *Mayo Clin. Proc.*, 79(1):109–116, Jan 2004.

M. Tré-Hardy, F. Vanderbist, H. Traore, and M. Devleeschouwer. In vitro activity of antibiotic combinations against *Pseudomonas aeruginosa* biofilm and planktonic cultures. *Int. J. Antimicrob. Agents*, 31(4):329–336, 2008.

M. M. Tunney, G. Ramage, T. R. Field, T. F. Moriarty, and D. G. Storey. Rapid colorimetric assay for antimicrobial susceptibility testing of *Pseudomonas aeruginosa*. *Antimicrob. Agents Chemother.*, 48(5):1879–1881, May 2004.

M. M. Tunney, T. R. Field, T. F. Moriarty, S. Patrick, G. Doering, M. S. Muhlebach, M. C. Wolfgang, R. Boucher, D. F. Gilpin, A. McDowell, and J. S. Elborn. Detection of anaerobic bacteria in high numbers in sputum from patients with cystic fibrosis. *Am. J. Respir. Crit. Care Med.*, 177(9):995–1001, May 2008.

H. Vanhooren, D. Demey, I. Vannijvel, and P. Vanrolleghem. Monitoring and modelling an industrial trickling filter using on-line off-gas analysis and respirometry. *Water Sci Technol*, 41(12):139–148, 2000.

D. Visser, G. Van Zuylen, J. Van Dam, A. Oudshoorn, M. Eman, C. Ras, W. Van Gulik, J. Frank, G. Van Dedem, and J. Heijnen. Rapid sampling for analysis of in vivo kinetics using the BioScope: A system for continuous-pulse experiments. *Biotechnol. Bioeng.*, 79 (6):674–681, 2002.

M. C. Walters, F. Roe, A. Bugnicourt, M. J. Franklin, and P. S. Stewart. Contributions of antibiotic penetration, oxygen limitation, and low metabolic activity to tolerance of *Pseudomonas aeruginosa* biofilms to ciprofloxacin and tobramycin. *Antimicrob. Agents Chemother.*, 47(1):317–323, Jan 2003.

Z.-W. Wang and S. Chen. Potential of biofilm-based biofuel production. *Appl. Microbiol. Biotechnol.*, 83(1):1–18, May 2009.

S. Wäsche, H. Horn, and D. Hempel. Mass transfer phenomena in biofilm systems. *Water Science and Technology*, 41(4-5):357–360, 2000.

J. S. Webb. Differentiation and dispersal in biofilms. In S. Kjelleberg and M. Givskov, edi-

tors, *Bacterial Biofilm Formation and Adaptation*, pages 164–174. Horizon Scientific Press., 2006.

N. Weissenbacher, K. Lenz, S. N. Mahnik, B. Wett, and M. Fuerhacker. Determination of activated sludge biological activity using model corrected $CO_2$ off-gas data. *Water Res.*, 41(7):1587–1595, Apr 2007.

E. Wentland, P. Stewart, C. Huang, and G. McFeters. Spatial variations in growth rate within *Klebsiella pneumoniae* colonies and biofilm. *Biotechnology Progress*, 12(3):316–321, 1996.

E. Werner, F. Roe, A. Bugnicourt, M. J. Franklin, A. Heydorn, S. Molin, B. Pitts, and P. S. Stewart. Stratified growth in *Pseudomonas aeruginosa* biofilms. *Appl. Environ. Microbiol.*, 70(10):6188–6196, 2004.

M. Whiteley, M. G. Bangera, R. E. Bumgarner, M. R. Parsek, G. M. Teitzel, S. Lory, and E. P. Greenberg. Gene expression in *Pseudomonas aeruginosa* biofilms. *Nature*, 413(6858): 860–864, 2001.

J. Wimpenny, W. Manz, and U. Szewzyk. Heterogeneity in biofilms. *FEMS Microbiol. Rev.*, 24:661–671, 2000.

G. Wolf, J. G. Crespo, and M. A. Reis. Optical and spectroscopic methods for biofilm examination and monitoring. *Re/Views in Environmental Science & Bio/Technology*, 1:227–251, 2002.

G. M. Wolfaardt, J. R. Lawrence, R. D. Robarts, S. J. Caldwell, and D. E. Caldwell. Multicellular organization in a degradative biofilm community. *Appl Environ Microb*, 60: 434–446, 1994.

G. M. Wolfaardt, M. J. Hendry, T. Birkham, A. Bressel, M. N. Gardner, A. J. Sousa, D. R. Korber, and M. Pilaski. Microbial response to environmental gradients in a ceramic-based diffusion system. *Biotechnol. Bioeng.*, 100(1):141–149, May 2008.

D. Worlitzsch, R. Tarran, M. Ulrich, U. Schwab, A. Cekici, K. C. Meyer, P. Birrer, G. Bellon, J. Berger, T. Weiss, K. Botzenhart, J. R. Yankaskas, S. Randell, R. C. Boucher, and G. Döring. Effects of reduced mucus oxygen concentration in airway *Pseudomonas* infections of cystic fibrosis patients. *J. Clin. Invest.*, 109(3):317–325, 2002.

J. B. Xavier and K. R. Foster. Cooperation and conflict in microbial biofilms. *Proc. Natl. Acad. Sci. U. S. A.*, 104(3):876–881, Jan 2007.

K. D. Xu, P. S. Stewart, F. Xia, C. T. Huang, and G. A. McFeters. Spatial physiological heterogeneity in *Pseudomonas aeruginosa* biofilm is determined by oxygen availability. *Appl. Environ. Microbiol.*, 64(10):4035–4039, Oct 1998.

K. D. Xu, G. A. McFeters, and P. S. Stewart. Biofilm resistance to antimicrobial agents. *Microbiology*, 146 ( Pt 3):547–549, Mar 2000.

L. Yang, J. Haagensen, L. Jelsbak, H. Johansen, C. Sternberg, N. Høiby, and S. Molin. In situ growth rates and biofilm development of *Pseudomonas aeruginosa* populations in chronic lung infections. *J. Bacteriol.*, 190(8):2767–2776, 2008.

H. Yasuda. Units of gas permeability constants. *J. Appl. Polym. Sci.*, 19:2529–2536, 1975.

A.-P. Zeng. Effect of $CO_2$ absorption on the measurement of $CO_2$ evolution rate in aerobic and anaerobic continuous cultures. *Appl. Microbiol. Biotechnol.*, 42(5):688–691, 1995.

H.-Y. Zhang, R. Wang, D. Liang, and J. Tay. Modeling and experimental study of $CO_2$ absorption in a hollow fiber membrane contactor. *J. Membr. Sci.*, 279(1-2):301–310, 2006.

H.-Y. Zhang, R. Wang, D. Liang, and J. Tay. Theoretical and experimental studies of membrane wetting in the membrane gas-liquid contacting process for $CO_2$ absorption. *J. Membr. Sci.*, 308(1-2):162–170, 2008.

L. Zhang and T.-F. Mah. Involvement of a novel efflux system in biofilm-specific resistance to antibiotics. *J. Bacteriol.*, 190(13):4447–4452, Jul 2008.

X.-H. Zhou, Q. Yu-Qin, S. Han-Chang, Y. Tong, H. Miao, and C. Qiang. A new approach to quantify spatial distribution of biofilm kinetic parameters by in situ determination of oxygen uptake rate (OUR). *Environ. Sci. Technol.*, 43(3):757–763, 2009.

# A. Appendix to Chapter 2

Derivation of equation 2.6 (A.8 below). Mass balance for annular (gas) side of CEMS (side 2).

$$0 = Q_2 C_2|_z - Q_2 C_2|_{z+dz} + J\pi J_0 dz \tag{A.1}$$

where $Q_2$ is the volumetric flow rate of the gas, $z$ is the beginning of the infinite slice and $z + dz$ is the end of the infinite slice, $d_o$ is the outer diameter of the silicone tube and $J$ is the flux from the liquid phase through the membrane into the annular space.

$$J = \frac{1}{\frac{\sigma_1}{k_1} + \frac{\Delta l}{D} + \frac{\sigma_2}{k_2}} (\sigma_1 C_1 - \sigma_2 C_2)$$

We want to differentiate with respect to $C_2$ so

$$J = \frac{1}{\frac{\sigma_1}{k_1 \sigma_2} + \frac{\Delta l}{D\sigma_2} + \frac{1}{k_2}} \left( \frac{\sigma_1}{\sigma_2} C_1 - C_2 \right)$$

where

$$\frac{\sigma_1}{\sigma_2} = \frac{\frac{c_m(\text{eq})}{C_1(\text{eq})}}{\frac{c_m(\text{eq})}{C_2(\text{eq})}} = \frac{C_2(\text{eq})}{C_1(\text{eq})} = H$$

where $H$ is a Henry's law constant relating equilibrium values

$$0 = \frac{Q_2 C_2|_z - Q_2 C_2|_{z+dz}}{dz} + \pi d_0 K_z \left(HC_1 - C_2\right) \tag{A.2}$$

$$0 = -Q_2 \frac{dC_2}{dz} + \pi d_0 K_z \left(HC_1 - C_2\right) \tag{A.3}$$

$$\frac{dC_2}{(HC_1 - C_2)} = \frac{\pi d_0 K_z}{Q_2} dz \tag{A.4}$$

At $z = 0, C_2 = 0$, and at $z$ = L, $C_2 = C_{2\text{out}}$

$$\int_0^{C_{2\text{out}}} \frac{dC_2}{(HC_1 - C_2)} = \int_0^L \frac{\pi d_0 K_z}{Q_2} dz \tag{A.5}$$

this yields

$$-\ln\left(\frac{HC_1 - C_2}{HC_1}\right) = \frac{\pi d_0 K_L}{Q_2} L \tag{A.6}$$

or

$$\left(\frac{HC_1 - C_2}{HC_1}\right) = e^{-\frac{\pi d_0 K_L}{Q_2} L} \tag{A.7}$$

$$HC_1 - C_2 = HC_1 e^{-\frac{\pi d_0 K_L}{Q_2} L}$$

$$C_2 = HC_1 - HC_1 e^{-\frac{\pi d_0 K_L}{Q_2} L}$$

$$J_{ave} = \frac{(C_2 Q_2)_{z=L}}{A}$$

$$J_{ave} = \frac{Q_2 \left( HC_1 - HC_1 e^{-\frac{\pi d_0 K_L}{Q_2} L} \right)}{\pi L d_0} \tag{A.8}$$